C.P. No. 1333

C.P. No. 1333

PROCUREMENT EXECUTIVE, MINISTRY OF DEFENCE

AERONAUTICAL RESEARCH COUNCIL

CURRENT PAPERS

Interference Problems on Wing-Fuselage Combinations Part III Symmetrical Swept Wing at Zero Incidence attached to a Cylindrical Fuselage

by

J. Weber and M. G. Joyce

Aerodynamics Dept., R.A.E., Farnborough

LONDON: HER MAJESTY'S STATIONERY OFFICE

1975

PRICE £2-60 NET

UDC 533.695.12 : 533.693.1 : 533.6.048.2 : 533.6.011.32

*CP No.1333

December 1973

INTERFERENCE PROBLEMS ON WING-FUSELAGE COMBINATIONS PART III SYMMETRICAL SWEPT WING AT ZERO INCIDENCE ATTACHED TO A CYLINDRICAL FUSELAGE

by

J. Weber

M. Gaynor Joyce

SUMMARY

The interference effect on the incompressible displacement flow past a swept wing attached to a cylindrical fuselage in midwing position is studied. It is shown how this varies with the angle of sweep, with the section shape and with the ratio R/c between the body radius and the wing chord.

To reduce the amount of computation only wings of constant chord and constant section shape are considered. For these wings the results can easily be derived from the velocity field past a single kinked swept source line in the presence of a fuselage. The streamwise velocity component induced in the plane through the source line and the axis of the fuselage and the streamwise and circumferential velocity components induced on the surface of the fuselage have been determined numerically and the values are tabulated. It is shown by comparison with results from other methods that, by means of these tables, good estimates of the interference velocity can be derived also for tapered wings.

*Replaces RAE Technical Report 73189 - ARC 35 413

CONTENTS

1 INTRODUCTION

In a previous Report[1] the interference has been studied between a fuselage and an unswept non-lifting wing of finite thickness. Here we deal with swept wings, considering again an infinite cylindrical fuselage of circular cross section with the axis parallel to the main stream, and a wing of constant chord and infinite span with the same symmetrical section across the span. The fuselage is again attached in midwing position, and viscous and compressibility effects are again neglected.

The fuselage affects the flow near the wing-body junction in a way similar to an infinite reflection plate normal to the wing plane but the flow is influenced also by the finite curvature of the body. The aim of the present Report is to examine this second effect by determining the difference between the pressure distribution on a wing-fuselage combination and that on the wing when it is attached to an infinite reflection plate; this latter distribution is the same as that on the isolated swept wing with its centre section at the wing-body junction.

The flow past the wing-fuselage combination is again represented by source distributions in the plane of the wing and on the surface of the fuselage. Within the accuracy of a first-order theory, the strength of the source distribution on the nett wing is the same as for the isolated wing. The source distribution in that part of the wing plane which is inside the fuselage can be chosen arbitrarily; the choice affects of course the strength of the source distribution on the fuselage. The requirements for the latter can be satisfied more easily when we choose the source distribution in the wing plane such that it takes account of the local reflection effect. This can be achieved in several ways, so we choose a source distribution which simplifies the computation of the induced velocity field. We use inside the fuselage the image (produced by a plane reflection) of that part of the wing source distribution outside the fuselage which has a spanwise width equal to the body radius. For the special case of wings of constant chord and constant section shape, this means that the source distribution in the wing plane is equivalent to a chordwise distribution of swept source lines of constant strength which are piecewise straight but have three kinks, namely at the wing-body junctions and at the axis of the fuselage, as sketched in Fig.1.

The task is again to determine the strength of the source distribution on the fuselage, which cancels the normal velocity induced by the source distribution in the plane of the wing, and then to determine the resulting velocity field.

We examine the interference effect for configurations with different values of the ratio between fuselage diameter and wing chord and for wings of different section shape. To reduce the amount of computation we determine first, in section 2, the flow field past a single swept source line in the presence of a fuselage. We have computed the resulting streamwise velocity component in the wing plane and on the fuselage and also the circumferential velocity component on the fuselage. The results for three angles of sweep, $\phi = 30^{o}$, 45^{o}, 60^{o}, are tabulated.

In section 3 we use the results for the single source line to determine the interference effects for various wing-fuselage combinations, according to first-order theory. Some second-order effects are also studied.

In practice, the wing of a wing-fuselage combination differs of course from the configurations mentioned so far, in that the wing is of finite span and in that the thickness distribution may vary across the span. We expect however that the results derived from infinitely long source lines will allow us to obtain a fair estimate of the interference velocity for a general wing shape. This assumption is based on the fact that, with many configurations, the fuselage has a noticeable effect on the displacement flow in only a fairly narrow area near the wing-body junction (measured in terms of the wing span). The interference velocity is of a magnitude which is usually appreciably smaller than the perturbation velocity of the isolated wing so that a crude estimate is often sufficient. The flow field past a wing attached to an infinite reflection plate can be evaluated, to first or higher order accuracy, by existing computer programs (see for example, J.A. Ledger[2] and C.C.L. Sells[3]). We therefore consider only the interference velocity and not the total pressure distribution on the wing-fuselage configurations.

In section 3.4, we compare more exact results for two particular wing-fuselage combinations, derived by means of source distributions on the surface of wing and fuselage, with the estimates obtained by means of infinitely long source lines, and in Appendix D a comparison is made with a simple estimate of the interference effect derived 20 years ago[11]. In the present Report, we have

not included any comparisons with experimental results since the latter are modified by viscous effects.

2 A SINGLE KINKED SWEPT SOURCE LINE IN THE PRESENCE OF A CIRCULAR CYLINDRICAL FUSELAGE

2.1 Velocities induced by the source line

Let x, y, z be a cartesian system of coordinates and x, r, θ a system of cylindrical coordinates. We consider an infinitely long cylindrical fuselage of circular cross section $y^2 + z^2 = R^2 = 1$ and an infinite source line in the plane $z = 0$ which is piecewise straight, swept by an angle $\pm\phi$ and which has kinks at $x = 0, y = R$, at $x = R \tan \phi, y = 0$ and at $x = 0, y = -R$ (see Fig.1). The position of the source line is thus given by

$$x = |R - |y|| \tan \phi \quad . \tag{1}$$

The strength of the source line is constant along the span and equal to Q per unit length. In the following equations all lengths are made dimensionless with the radius R of the fuselage.

For the flow field induced by the source line, expressions for the velocity components parallel to the x, y, z axes can be written down in analytic form. Using these one can obtain a formula for the velocity component normal to the surface of the fuselage $v_{nQ}(x,\theta)$; this formula is given in equation (A-3) of Appendix A. Values of $v_{nQ}(x,\theta = 90^o)$ at the top of the fuselage are plotted in Fig.2. We note that at $x = 0$ (the chordwise position where the source line crosses the fuselage) the value of v_{nQ} is independent of the angle of sweep for all values of $\theta \neq 0$ and is given by

$$v_{nQ}(x = 0, \theta \neq 0) = \frac{Q}{2\pi} \quad . \tag{2}$$

Using computed values of $v_{nQ}(x,\theta)$, we have determined the mean value

$$\bar{v}_{nQ}(x) = \frac{1}{2\pi} \int_0^{2\pi} v_{nQ}(x,\theta) d\theta \tag{3}$$

by numerical integration.

The integral of $v_{nQ}(x,\theta)$ over the fuselage is

$$\int_{-\infty}^{\infty}\int_{0}^{2\pi} v_{nQ}(x,\theta)\,d\theta dx = 2Q\sqrt{1+\tan^2\phi} \quad , \tag{4}$$

as is to be expected since the total source strength of that part of the source line which lies inside the fuselage is $2Q\sqrt{1+\tan^2\phi}$. We may note that the normal velocity at the side of the fuselage, $v_{nQ}(x,\theta = 0)$, has non-zero values for $\phi \neq 0$. As x tends to zero,

$$v_{nQ}(x \to 0,\ \theta = 0) = \frac{Q}{4\pi}\sin^2\phi \quad .$$

If we were to extend the source line within the fuselage without forming a kink at the body junction, then the normal velocity in $\theta = 0$ would tend to infinity as $-Q \tan\phi/2\pi x$, when x tends to zero; this type of singular behaviour is of course due to the fact that we are considering an isolated source line.

2.2 Strength of the source distribution on the fuselage which makes the fuselage a stream surface

We have said in the introduction that we intend to cancel the normal velocity $v_{nQ}(x,\theta)$ by a source distribution on the fuselage of strength $q(x,\theta)$. The function $q(x,\theta)$ must satisfy the equation (see section 2.2 of Ref.4):

$$v_{nq}(x,\theta) = -v_{nQ}(x,\theta) \quad ,$$

where

$$v_{nq} = \frac{q(x,\theta)}{2} + \int_{-\infty}^{\infty}\int_{0}^{2\pi} \frac{q(x',\theta')[1-\cos(\theta-\theta')]\,d\theta' dx'}{4\pi\sqrt{(x-x')^2+2[1-\cos(\theta-\theta')]}^3}$$

$$= \frac{q(x,\theta)}{2} + \int_{0}^{2\pi} \frac{q(x,\theta')}{4\pi}\,d\theta'$$

$$+ \int_{-\infty}^{\infty}\int_{0}^{2\pi} \frac{[q(x',\theta')-q(x,\theta')][1-\cos(\theta-\theta')]\,d\theta' dx'}{4\pi\sqrt{(x-x')^2+2[1-\cos(\theta-\theta')]}^3} \quad . \tag{5}$$

An approximate solution of this equation can be derived in the same manner as for the unswept source line (see Ref.1, section 2.2) by an iterative procedure, where the first approximation is given by

$$q^{(0)}(x,\theta) = -2v_{nQ}(x,\theta) + \bar{v}_{nQ}(x) \quad . \tag{6}$$

The mean value

$$\bar{q}^{(0)}(x) = \frac{1}{2\pi}\int_0^{2\pi} q^{(0)}(x,\theta)\,d\theta \tag{7}$$

is equal to $-\bar{v}_{nQ}(x)$.

The second approximation

$$q^{(1)}(x,\theta) = q^{(0)}(x,\theta) + \Delta^{(1)}q(x,\theta) \tag{8}$$

is obtained from

$$\Delta^{(1)}q(x,\theta) + \Delta^{(1)}\bar{q}(x) = K^{(1)}(x,\theta) \quad , \tag{9}$$

where $$K^{(1)}(x,\theta) = -\int_{-\infty}^{\infty}\int_0^{2\pi} \frac{[q^{(0)}(x',\theta') - q^{(0)}(x,\theta')]\,[1 - \cos(\theta - \theta')]\,d\theta'dx'}{2\pi\sqrt{(x - x')^2 + 2[1 - \cos(\theta - \theta')]^3}} \quad . \tag{10}$$

For $\phi = 45^{\circ}$, we have computed values of $K^{(1)}(x,\theta)$ and of

$$\bar{K}^{(1)}(x) = \frac{1}{2\pi}\int_0^{2\pi} K^{(1)}(x,\theta)\,d\theta \quad . \tag{11}$$

It was found that $\left|K^{(1)}(x,\theta) - \bar{K}^{(1)}(x)\right|$ is nowhere larger than $0.05\ \bar{q}^{(0)}(x = 0)$.

For $\phi = 0$, $\left|K^{(1)}(x,\theta) - \bar{K}^{(1)}(x)\right|$ is nowhere larger than $0.032\ \bar{q}^{(0)}(x = 0)$. It has been shown in Ref.1 that the term $K^{(1)}(x,\theta) - \bar{K}^{(1)}(x)$ which occurs in the approximate expression for $q(x,\theta)$, given by equation (19) of Ref.1, has a sufficiently small effect on v_{xq} so that the term may be neglected. To reduce the computational effort, we have therefore neglected it in the approximate source distributions $q(x,\theta)$ for swept source-lines.

Values of $\bar{K}^{(n)}(x)$ can be computed from single integrals. Since

$$\int_0^{2\pi} \frac{[1 - \cos(\theta - \theta')]\,d\theta'}{\sqrt{(x - x')^2 + 2[1 - \cos(\theta - \theta')]^3}} = k[\mathbf{K}(k) - \mathbf{E}(k)]$$

where $\mathbf{K}$ and $\mathbf{E}$ are the complete elliptic integrals (of the first and second kind respectively) with the modulus

$$k^2 = \frac{4}{4 + (x - x')^2} \quad , \tag{12}$$

we can obtain $\bar{K}^{(n)}(x)$ from the relation:

$$\bar{K}^{(n)}(x) = -\int_{-\infty}^{\infty} \frac{\bar{K}^{(n-1)}(x') - \bar{K}^{(n-1)}(x)}{4\pi}\, k[\mathbf{K} - \mathbf{E}]\,dx' \tag{13}$$

with $\bar{K}^{(0)}(x) \equiv 2\bar{q}^{(0)}(x)$. We have calculated values of $\bar{K}^{(n)}(x)$ for $1 \leqslant n \leqslant 6$. It was found that

$$\left|\bar{K}^{(n)}(x)\right|_{max} < \tfrac{1}{2}\left|\bar{K}^{(n-1)}(x)\right|_{max} \quad ,$$

as for $\phi = 0$.

For computing the velocity components induced on the wing and the fuselage, we have therefore used the approximate source distribution

$$q(x,\theta) = -2v_{nQ}(x,\theta) + \bar{v}_{nQ}(x) + \frac{1}{2}\sum_{n=1}^{6} \bar{K}^{(n)}(x) \quad . \tag{14}$$

The mean value

$$\bar{q}(x) = \frac{1}{2\pi}\int_0^{2\pi} q(x,\theta)d\theta \tag{15}$$

is

$$\bar{q}(x) = -\bar{v}_{nQ}(x) + \frac{1}{2}\sum_{n=1}^{6}\bar{K}^{(n)}(x) \quad . \tag{16}$$

To illustrate some of the effects of sweep, we have plotted in Figs.3 and 4 values of the average of the source distributions on the fuselage $\bar{q}^{(0)}(x) = -\bar{v}_{nQ}(x)$ and $\bar{q}(x)$. The function $\bar{q}(x;\phi)$ is of course not symmetric with respect to $x = 0$, when $\phi \neq 0$. The maximum values of $\bar{q}(x;\phi)$ occur at positive values of x . Near the x-value where $\bar{q}(x;\phi)$ has its maximum value, the function $\bar{q}(x;\phi)$ varies less rapidly for non-zero values of ϕ than for $\phi = 0$.

2.3 Streamwise velocity in the plane through the source line and the axis of the fuselage

We consider now the streamwise velocity in the plane $z = 0$, i.e. the plane through the source line and the axis of the fuselage.

The source distribution $q(x,\theta)$ produces the streamwise velocity

$$v_{xq}(x,y,0) = \int_{-\infty}^{\infty}\int_0^{2\pi} \frac{q(x',\theta')(x - x')d\theta'dx'}{4\pi\sqrt{(x - x')^2 + y^2 + 1 - 2y\cos\theta'}^3} \quad . \tag{17}$$

This relation can be written in the form (see equations (26) to (28) of Ref.1):

$$v_{xq}(x,y,0) = \int_{-\infty}^{\infty}\int_0^{\pi} \frac{[q(x',\theta') - q(x,\theta') - q(x',\theta = 0) + q(x,\theta = 0)](x - x')d\theta'dx'}{2\pi\sqrt{(x - x')^2 + y^2 + 1 - 2y\cos\theta'}^3}$$

$$+ \int_{-\infty}^{\infty} \frac{[q(x',\theta = 0) - q(x,\theta = 0)](x - x')E(k)dx'}{\pi[(x - x')^2 + (y - 1)^2]\sqrt{(x - x')^2 + (y + 1)^2}} \tag{18}$$

where E is the complete elliptic integral of the second kind with the modulus

$$k^2 = \frac{4y}{(x - x')^2 + (y + 1)^2} \quad . \tag{19}$$

The numerical evaluation of the integrals in equation (18) does not cause any difficulty, except for $y = 1$ and small values of $|x|$. It is shown in Appendix B that the velocity v_{xq} for $y = 1$ behaves as

$$\frac{v_{xq}(x,y = 1,0)}{Q} = - \frac{\cos^3 \phi - 1 + \frac{3}{2} \sin^2 \phi}{4\pi \sin^3 \phi} \log |x| + \frac{x}{|x|} I(\phi) + f(x;\phi) \tag{20}$$

where $I(\phi)$ can be evaluated numerically from a single integral and $f(x;\phi)$ is a finite continuous function. Values of $v_{xq}(x,y = 1,0)$ for $\phi = 45^\circ$ are plotted in Fig.5.

We have stated above that our aim is to determine the difference between the velocity fields past a swept wing attached to a circular fuselage and past a swept wing attached to an infinite reflection plate. To obtain this interference velocity field for a single source line, $\underline{v}_I$, we have combined the velocity field induced by the source distribution $q(x,\theta)$ on the fuselage with the difference between the velocity fields for the source line with three kinks $\underline{v}_{\wedge\wedge}$, and the velocity field for the ordinary swept source line $\underline{v}_\Lambda$. This means we derive v_{xI} in the plane $z = 0$ from

$$v_{xI}(x,y,0) = v_{xq}(x,y,0) + v_{x\wedge\wedge}(x,y,0) - v_{x\Lambda}(x,y,0) \quad . \tag{21}$$

The relations from which we can derive the values of $v_{x\wedge\wedge} - v_{x\Lambda}$ are given in Appendices A and C, equations (A-4) and (C-2).

For $\phi = 45^\circ$, values of v_{xI} in the wing-body junction are plotted in Fig.5. The figure shows that, for most values of x, the sign of the term $v_{x\wedge\wedge} - v_{x\Lambda}$ is opposite to that of v_{xq}. The largest value of $v_{x\wedge\wedge} - v_{x\Lambda}$ occurs at about $x = \tan \phi$. To judge the magnitude of the interference velocity, we have plotted also the term $-0.2v_{x\Lambda}$

We have computed values of v_{xI} for the angles of sweep $\phi = 30^\circ$, 45°, 60° and for the spanwise stations $y/R = 1.0$, 1.25, 2.0. Values of v_{xI} are

tabulated in Table 1. Fig.6 illustrates how the interference velocity v_{xI} in the wing-body junction varies with the angle of sweep.

For $\phi = 45^{o}$, we have plotted in Fig.7 v_{xI} at $z = 0$ for various spanwise stations. Since chordwise distributions of isolated source lines will be used to represent swept wings and since the pressure distributions on swept wings are usually given as functions of the chordwise coordinate ξ, where ξ is zero at the leading edge of the wing, this coordinate is used in Fig.7. Note that

$$\xi/R = x/R - (|y/R| - 1) \tan \phi \quad . \tag{22}$$

2.4 Streamwise velocity on the fuselage

The isolated infinitely long fuselage does not produce any perturbation to the free stream. Thus the pressure distribution on the fuselage is entirely due to the presence of the wing.

In this section we determine the streamwise velocity due to a single source line in the presence of the fuselage. This velocity is produced by the source line with the triple kink and the source distribution $q(x,\theta)$ on the fuselage.

The source distribution $q(x,\theta)$ produces on the fuselage the velocity

$$v_{xq}(x,\theta) = \int_{-\infty}^{\infty} \int_{0}^{2\pi} \frac{q(x',\theta')(x - x')d\theta'dx'}{4\pi\sqrt{(x - x')^2 + 2[1 - \cos(\theta - \theta')]}^3} \quad . \tag{23}$$

This equation can be written in the form

$$v_{xq}(x,\theta) = \int_{-\infty}^{\infty} \int_{0}^{2\pi} \frac{[q(x',\theta') - q(x,\theta') - q(x',\theta) + q(x,\theta)](x - x')d\theta'dx'}{4\pi\sqrt{(x - x')^2 + 2[1 - \cos(\theta - \theta')]}^3}$$

$$+ \int_{-\infty}^{\infty} \frac{[q(x',\theta) - q(x,\theta)]\mathbf{E}(k)}{\pi(x - x')\sqrt{(x - x')^2 + 4}} dx' \tag{24}$$

with

$$k^2 = \frac{4}{4 + (x - x')^2} \quad .$$

The numerical evaluation of $v_{xq}(x,\theta)$ from equation (24) does not cause any difficulty for $\theta \neq 0$. We have already determined the values for $\theta = 0$ since $v_{xq}(x,\theta = 0)$ from equation (24) is the same as $v_{xq}(x,y = 1,z = 0)$ from equation (18).

The total velocity v_x at the surface of the fuselage is given by

$$v_x(x,\theta) = v_{xq}(x,\theta) + v_{x\wedge}(x,\theta) \tag{25}$$

where $v_{x\wedge}(x,\theta) = v_{x\wedge}(x,y = \cos\theta, z = \sin\theta)$ is given by equation (A-5). Values of $v_x(x,\theta = 90^o)$, i.e. the velocity at the top of the fuselage, are plotted in Fig.8 for various angles of sweep.

Since our aim is the determination of the difference between the velocity fields past a swept wing attached to a circular fuselage and past a swept wing attached to an infinite reflection plate, we have subtracted from $v_x(x,\theta)$ the values of $v_{x\Lambda}$ in the plane $y = 1$, at $z = \sin\theta$, given by equation (C-3) . Values of

$$v_{xI}(x,\theta) = v_{xq}(x,\theta) + v_{x\wedge}(x,\theta) - v_{x\Lambda}(x,y = 1,z = \sin\theta) \tag{26}$$

are quoted in Table 2 and for $\phi = 45^o$, are plotted in Fig.9. Fig.9 shows that, except close to $x = 0$, the magnitude of the values of v_{xI} does not vary much with θ .

For $\phi = 45^o$ and $\theta = 90^o$, we have plotted the various terms v_{xq} , $v_{x\wedge}$, $v_{x\Lambda}$, v_{xI} , v_x in Fig.10. The figure shows that for most values of x , the sign of v_{xI} is opposite to that of $v_{x\Lambda}$ (the same is true for $\theta = 0$, as shown in Fig.5) and the sign of v_{xq} is opposite to that of $v_{x\wedge}$. The velocity at the top of the fuselage $v_x = v_{x\Lambda} + v_{xI}$ is of smaller magnitude than the velocity past the isolated source lines $v_{x\Lambda}$, $v_{x\wedge}$, at the same position. This fact, which is true for all values of ϕ , is to be expected since the fuselage straightens the streamlines past the isolated source lines.

We have stated in the introduction that we prefer to quote the values of v_{xI} instead of the values of the total velocity v_x , because we anticipate

that the magnitude of the interference velocity is appreciably smaller than that of the perturbation velocity of the isolated wing. The assumption holds at the surface of the wing, i.e. in the plane of the wing, and on the fuselage for small values of θ , say $\theta \leqslant 10^{o}$; but it becomes less valid with increasing values of θ . At $\theta = 90^{o}$, the values of v_{xI} , and $v_{x\Lambda}$ are of comparable magnitude; this is because the velocity $|v_{x\Lambda}|$ is appreciably lower for $z = 1$ than for $z = 0$ and not because the magnitude of v_{xI} alters much with increasing z . (The results obtained so far refer only to a single source line. For a wing-fuselage combination, which corresponds to a chordwise distribution of source lines and sink lines, the magnitude of the perturbation velocity near the top of the fuselage varies of course with the distance between the top of the fuselage and the wing plane measured in terms of the wing chord, which means with the ratio R/c between the body radius and the wing chord.) We have nevertheless given in Table 2, also for large values of θ , the values of the term v_{xI} . As stated previously, it seems justified to assume that, for a wing of finite span, we can obtain a reasonably accurate estimate of the body interference on the pressure distribution of the wing by means of the values of v_{xI} , derived from infinitely long source lines of constant strength. This assumption may be less justified for the pressure distribution on the fuselage, particularly for larger values of θ ; but, in practice, a knowledge of the pressure distribution near the wing-body junction is more important than near the top of the fuselage.

2.5 Circumferential velocity on the fuselage

The source line in the plane $z = 0$ and the source distribution $q(x,\theta)$ on the fuselage produce at the fuselage a circumferential velocity

$$v_{\theta}(x,\theta) = v_{\theta\wedge}(x,\theta) + v_{\theta q}(x,\theta) \quad . \tag{27}$$

A relation for $v_{\theta\wedge}(x,\theta)$ is given in Appendix A, equation (A-6). The velocity $v_{\theta q}(x,\theta)$ can be obtained from the equation:

$$v_{\theta q}(x,\theta) = \int_{-\infty}^{\infty}\int_{0}^{2\pi} \frac{q(x',\theta')\sin(\theta-\theta')d\theta'dx'}{4\pi\sqrt{(x-x')^2+2[1-\cos(\theta-\theta')]}^3}$$

$$= \int_{-\infty}^{\infty}\int_{0}^{2\pi} \frac{[q(x'\theta') - q(x,\theta') - q(x',\theta) + q(x,\theta)]\sin(\theta-\theta')d\theta'dx'}{4\pi\sqrt{(x-x')^2+2[1-\cos(\theta-\theta')]}^3}$$

$$+ \int_{0}^{2\pi} \frac{[q(x,\theta') - q(x,\theta)][1+\cos(\theta-\theta')]d\theta'}{4\pi\sin(\theta-\theta')} \quad . \tag{28}$$

The evaluation of $v_{\theta q}$ from equation (28) is straightforward except for the case $x = 0$, $\theta \to 0$. Due to the properties of symmetry of $q(x,\theta)$, the circumferential velocity vanishes for $\theta = 90^{\circ}$ and $\theta = 0$ except for $x = 0$. Calculated values of $v_{\theta q}$ are given in Table 3. When evaluating $v_{\theta q}$ from equation (28), we have used for the source strength $q(x,\theta)$ the approximation given by equation (14). We would of course obtain the same values of $v_{\theta q}$ by using the first approximation $q^{(0)}(x,\theta)$, given by equation (6), since only that part of $q(x,\theta)$ which varies with θ, namely $-2v_{nQ}(x,\theta)$, contributes to $v_{\theta q}$. It is possible that small inaccuracies of the source distribution $q(x,\theta)$ produce some inaccuracy in the values of $v_{\theta q}$ for small values of x, where, for small θ, $v_{\theta q}$ varies fairly rapidly. We do not expect these inaccuracies to be important when we deal with chordwise distributions of source lines.

To determine the pressure distribution on a wing in the presence of a fuselage to second-order accuracy (see section 3.2), we require the velocity component at the surface of the wing to second-order accuracy. We therefore need to know the velocity component v_z at $z \neq 0$ which is induced by the single source line in the presence of the fuselage.

We have not computed values of $v_z(x,y,z \neq 0)$ for points away from the fuselage (which would require the evaluation of more double integrals) but, at the fuselage, v_z can be determined without much further effort since

$$v_z(x,\theta) = \cos\theta\, v_{\theta}(x,\theta) + \sin\theta\, v_n(x,\theta) \quad . \tag{29}$$

The total normal velocity $v_n(x,\theta)$ is zero, so we can obtain $v_z(x,\theta)$ from

$$v_z(x,\theta) = \cos\theta\,[v_{\theta q}(x,\theta) + v_{\theta\wedge}(x,\theta)] \quad . \tag{30}$$

Values of $v_{\theta q}$ are tabulated in Table 3 and values of $v_{\theta\wedge}$ can be determined from equation (A-6).

We have again determined the interference velocity v_{zI}, i.e.

$$v_{zI}(x,\theta) = v_z(x,\theta) - v_{z\Lambda}(x,y = 1, \sin\theta)$$

$$= v_{zq}(x,\theta) + v_{z\wedge}(x,\theta) - v_{z\Lambda}(x,y = 1, \sin\theta) \quad . \tag{31}$$

A relation for $v_{z\Lambda}(x,y = 1,z)$ is given in equation (C-4). Values of $v_{zI}(x,\theta)$ are quoted in Table 4 and for $\phi = 45^o$ are plotted in Fig.11 where we have also plotted values of the downwash induced by the isolated source line $v_{z\Lambda}(x,y = 1,z = \sin\theta)$ for $\theta = 10^o$.

3 PRESSURE DISTRIBUTIONS ON WING-FUSELAGE COMBINATIONS

3.1 Pressure distribution on the wing according to first-order theory

The calculated velocity components due to an isolated source line in the presence of the fuselage can be used to determine the pressure distribution on a wing of given section shape when attached to a fuselage in midwing position.

We consider in this Report only wings of constant chord and constant section shape, $z = z_t(x,y)$, along the span, so that

$$z_t(x,y) = z_t(\xi = x - (|y| - R)\tan\phi) \quad . \tag{32}$$

The wing is in a mainstream of velocity V_0 parallel to the chord plane. In the following, we make all velocity components dimensionless by taking $V_0 = 1$.

Within first-order theory, the source distribution $q_w^{(1)}(x,y)$ in the wing plane $z = 0$ has to produce a velocity $v_z^{(1)}(x,y,z = 0)$ which satisfies the boundary condition

$$v_z^{(1)}(x,y,z = 0) = \frac{\partial z_t(x,y)}{\partial x}$$

$$= \frac{dz_t}{d\xi}\,(\xi = x - (|y| - R)\tan\phi) \tag{33}$$

to first order accuracy. (We use the superscript (1) to denote terms derived by first-order theory.) The source distribution $q(x,\theta)$ on the fuselage does not induce a velocity component $v_z(x,y,z = 0)$ in the plane $z = 0$; therefore, in first-order theory, $q_w^{(1)}(x,y)$ can be chosen to be the same as for the wing alone, i.e.

$$q_w^{(1)}(x,y) = q_w^{(1)}(\xi) = 2\frac{dz_t}{d\xi} \quad . \tag{34}$$

To determine the change in the pressure distribution due to the fuselage - to first-order accuracy - we have to determine only the change in the streamwise velocity, $\Delta v_x^{(1)}(x,y,z = 0)$.

The formulae in section 2 are derived for a single source line for which the strength per unit length along the source line is Q . To derive the velocity components, produced by a source distribution $q(\xi)$, from the results for the single source line, we have to replace Q by $Qdn = \cos\phi\, q(\xi)d\xi$ and perform the integration with respect to ξ . (It is shown in Appendix C, equation (C-6) that, with the factor $\cos\phi$ to $q(\xi)$, we obtain the required value for $v_z(x,y,z = 0)$ at the centre section of the isolated wing.)

We have determined values of $\Delta v_x^{(1)}$ from the relation

$$\Delta v_x^{(1)}(x,y,z = 0) = \cos\phi \int_0^{c/R} q_w^{(1)}(x') \frac{v_{xI}\left(\frac{x - x'}{R}, \frac{y}{R}, 0\right)}{Q/R} d\left(\frac{x'}{R}\right)$$

$$= 2\cos\phi \frac{c}{R} \int_0^1 \frac{d(z_t/c)}{d(x'/c)} \frac{v_{xI}\left(\frac{x - x'}{R}, \frac{y}{R}, 0\right)}{Q/R} d\left(\frac{x'}{c}\right) \tag{35}$$

where c is the wing chord and values of $v_{xI}R/Q$ have been taken from Table 1.

It has been stated above, see equation (20), that v_{xq} and with it $v_{xI}\left(\frac{x - x'}{R}, \frac{y}{R} = 1,0\right)$ tend to infinity when x' tends to x . For $y = R$, we therefore write equation (35) in the form

$$\Delta v_x^{(1)}(x,y = R,\ z = 0) = 2\cos\phi\,\frac{c}{R}\int_0^1 \left[\frac{dz_t(x')}{dx'} - \frac{dz_t(x)}{dx}\right] \frac{v_{xI}\left(\frac{x - x'}{R},\ 1,0\right)}{Q/R}\, d\left(\frac{x'}{c}\right)$$

$$+ 2\cos\phi\,\frac{dz_t(x)}{dx} \int_{-\frac{1-x/c}{R/c}}^{\frac{x/c}{R/c}} \frac{v_{xI}\left(\frac{X}{R},\ 1,0\right)}{Q/R}\, d\left(\frac{X}{R}\right) \quad . \qquad (36)$$

For the second integral in equation (36) we use the relation

$$\int_{-\frac{1-x/c}{R/c}}^{\frac{x/c}{R/c}} \frac{v_{xI}\left(\frac{X}{R},\ 1,0\right)}{Q/R}\, d\left(\frac{X}{R}\right)$$

$$= -\frac{\cos^3\phi - 1 + \frac{3}{2}\sin^2\phi}{4\pi\sin^3\phi}\left[\frac{x/c}{R/c}\left(\log\frac{x/c}{R/c} - 1\right) + \frac{1 - x/c}{R/c}\left(\log\frac{1 - x/c}{R/c} - 1\right)\right]$$

$$+ I(\phi)\left[\frac{x/c}{R/c} - \frac{1 - x/c}{R/c}\right] + \int_{-\frac{1-x/c}{R/c}}^{\frac{x/c}{R/c}} r\left(\frac{X}{R};\ \phi\right)\, d\left(\frac{X}{R}\right) \qquad (37)$$

where $$r(X;\phi) = v_{xI}(X,1,0) + \frac{\cos^3\phi - 1 + \frac{3}{2}\sin^2\phi}{4\pi\sin^3\phi}\log|X| - \frac{X}{|X|}\,I(\phi) \qquad (38)$$

is a finite continuous function, and values of $I(\phi)$ are given in Appendix B.

For sections with finite nose radius, dz_t/dx behaves near the leading edge like $1/\sqrt{x/c}$. To avoid a singular behaviour of the integrand in the first integral of equation (36), or in the integral in equation (35), we have used, for the interval $0 < x'/c < 0.25$, the usual transformation $\tau = \sqrt{x'/c}$.

In order to determine the change in the pressure distribution at spanwise stations away from the wing-body junction, as function of the coordinate ξ , we have to substitute

$$\frac{x}{R} = \frac{\xi}{R} + \left(\left|\frac{y}{R}\right| - 1\right) \tan \phi \quad .$$

For the 10 per cent thick RAE 101 section and for $\frac{c}{R} = 5$, we have computed values of the velocity change in the wing-body junction, $\Delta v_{xJ}^{(1)} = \Delta v_x^{(1)}(x,y = R,0)$, for various angles of sweep; some results are plotted in Fig.12. We have also plotted for comparison values of $-0.1 v_{xw}^{(1)}$, where $v_{xw}^{(1)}$ is the velocity for the wing with an infinite reflection plate at the root. In Fig.13, we have plotted the total streamwise velocity (from first-order theory) in the junction of the wing with a fuselage, v_{xJ} , and in the junction of the wing with an infinite reflection plate, v_{xw} .

Fig.12 shows that, for wings with the same streamwise section shape, the velocity decrement in the wing-body junction, $-\Delta v_x^{(1)}(x,y = R,0)$, decreases with increasing value of ϕ and that the position of the maximum value of $-\Delta v_{xJ}^{(1)}$ moves rearwards with increasing value of ϕ .

We note from Fig.13 that the difference in the type of velocity distribution between a swept and an unswept wing is not much affected by the finite body radius. (Near the leading edge, the values of the velocity from first-order theory are not representative of the actual velocity.)

The rearward movement of the position of the maximum value of $-\Delta v_{xJ}^{(1)}$ can be explained by the asymmetry of the values of $|v_{xI}(x,y = R,0)|$ with respect to $x = 0$, for $\phi \neq 0$. The curves of $v_{xI}(x,y = R,0)$ plotted in Fig.6 show that, for $\phi \neq 0$ and any streamwise length ℓ ,

$$F(\ell,\phi) = \int_{\ell}^{0} v_{xI}(x)dx - \int_{0}^{\ell} - v_{xI}(x)dx > 0$$

and that $F(\ell,\phi)$ increases with ϕ .

In Fig.14, values of $\Delta v_{xJ}^{(1)} / \cos \phi$, for various values of the ratio c/R , have been plotted against the coordinate $x/c - 0.6\phi/\pi$. The figure shows that the values for different angles of sweep collapse approximately on the curve for zero sweep. We note from Fig.14 that the rearward shift, in terms of the wing chord, is nearly independent of the ratio c/R .

To examine how far the results obtained with the RAE 101 section may be generalised, we have also done some calculations for the RAE 103 section. The

results are plotted in Fig.15, which shows a somewhat larger variation of the values of $\Delta v_{xJ}^{(1)} / \cos\phi$ with the angle of sweep. The dependence on ϕ would be larger for elliptic sections, because for $\phi = 0$ the curve $\Delta v_{xJ}^{(1)}$ is symmetrical with respect to $x/c = 0.5$ whilst for increasing values of ϕ we must expect that the curves will become more and more asymmetrical.

For the case $c/R = 5$, we have plotted in Fig.16 the interference velocity at two spanwise stations outboard of the wing-body junction as function of the coordinate $\xi = [x - x_{LE}(y)]/c$. We note that, for both stations, the maximum value of the velocity decrement varies again approximately as $\cos\phi$. The rearward shift of the position of the maximum value of $-\Delta v_x^{(1)}$, as function of ξ, decreases with increasing y. For $y/R = 2$ and $\phi = 60^o$ the maximum value of $-\Delta v_x^{(1)}$ occurs forward of the position of $\left(-\Delta_x^{(1)}\right)_{max}$ for $\phi = 0$. However, the maximum value of $\left(-\Delta v_x^{(1)}\right)_{\phi=60^o}$ as function of x occurs rearward of the position for $\phi = 0$. The results suggest that, near the junction $R \leqslant y \leqslant 2R$, the values of the maximum decrement decrease approximately linearly with the distance from the junction $\left(\frac{|y|}{R} - 1\right)$; for the particular case considered in Fig.16

$$\left[-\Delta v_x^{(1)}(x,y,0;\phi)\right]_{max} = \left[1 - 0.5\left(\frac{|y|}{R} - 1\right)\right]\left[-\Delta v_{xJ}^{(1)}(\phi)\right]_{max} .$$

3.2 Pressure distribution on the wing according to second-order theory

In Ref.1, it has been shown, for unswept wings, that the reduction of the velocity in the wing-body junction derived by second-order theory may be appreciably larger than that derived by first-order theory. The effect of the various second-order terms is therefore of interest also for wing-fuselage combinations with swept wings.

To obtain the pressure distribution to second-order accuracy one has first to determine singularity distributions which satisfy the boundary condition to second order. When the singularity distributions are known, one has to determine the velocity at the wing surface to second-order accuracy; this requires the evaluation of, at least, some terms at $z \neq 0$.

3.2.1 The approximate boundary condition

We consider first the boundary condition. At the surface of the wing, $z = z_t(x,y)$, the velocity field has to satisfy the equation

$$[V_0 + v_x(x,y,z_t)] \frac{\partial z_t}{\partial x} + v_y(x,y,z_t) \frac{\partial z_t}{\partial y} - v_z(x,y,z_t) = 0 \quad . \qquad (39)$$

For a swept wing of constant chord and constant section shape, with the centre section at $y = 0$,

$$\frac{\partial z_t}{\partial y} = - \tan \phi \frac{\partial z_t}{\partial x} \qquad \text{for} \quad y > 0 \quad ,$$

so that the boundary condition on the wing reads for $y \geqslant R$

$$[1 + v_x(x,y,z_t) - \tan \phi \, v_y(x,y,z_t)] \frac{\partial z_t}{\partial x} = v_z(x,y,z_t) \quad . \qquad (40)$$

We intend to retain in this equation all terms of order $(t/c)^2$. The left-hand side can be approximated, correct to second order, by

$$\left[1 + v_{xw}^{(1)}(x,y,0) + \Delta v_x^{(1)}(x,y,0) - \tan \phi \left(v_{yw}^{(1)}(x,y,0) + \Delta v_y^{(1)}(x,y,0)\right)\right] \frac{\partial z_t}{\partial x} \quad .$$

We denote the various terms for the wing attached to an infinite reflection plate by the suffix w and the interference terms by the symbol Δ . The superscript (1) denotes terms computed from the first-order source distribution

$$q_w^{(1)}(\xi) = 2 \frac{dz_t}{d\xi} \quad .$$

We have seen above, see Fig.12, that in the wing-body junction the interference term $\Delta v_x^{(1)}$ is of a magnitude of only about $0.1 v_{xw}^{(1)}$. Further outboard $-\Delta v_{x\ \max}^{(1)}$ is smaller than the value in the junction $\left(-\Delta v_{xJ}^{(1)}\right)_{\max}$; thus within the accuracy required we can neglect the term Δv_x in the boundary condition (even though it is formally a term of order t/c).

We propose to neglect the term $\Delta v_y^{(1)}(x,y,0)$, which is zero in the wing-body junction, for all spanwise stations. (The normal velocity v_{nJ} vanishes in the wing-body junction, so that

$$v_y(x,y_J,z_t) = - \tan \theta_J \, v_z(x,y,z_t) \quad .$$

Therefore $v_y(x,y_J,z_t)$ is approximately equal to $-(z_t/R)dz_t/dx$. The ratio z_t/R is small compared to unity for the configurations we are interested in, so v_{yJ} can be neglected in a second-order theory.)

We therefore approximate the left-hand side of equation (40) by the same term as applies to the isolated nett wing and the approximate boundary condition on the wing at the wing fuselage combination then reads:

$$\left[1 + v_{xw}^{(1)}(x,y,0) - \tan \phi \, v_{yw}^{(1)}(x,y,0)\right] \frac{\partial z_t}{\partial x} = v_z(x,y,z_t) \quad . \qquad (41)$$

The solution of equation (41) for the wing-fuselage combination differs however from the solution for the isolated wing because the velocity $v_z(x,y,z_t)$ contains not only a contribution from the second-order source distribution $q_w^{(2)}$ of the nett wing but also the interference velocity $\Delta v_z(x,y,z_t)$.

3.2.2 The second-order source distribution for the nett wing

We discuss next the determination of source distributions in the wing plane and on the fuselage which satisfy equation (41), approximately. We express the source distribution in the wing plane as the sum of two terms $q_w^{(2)}(x,y) + \Delta q(x,y)$, where $q_w^{(2)}(x,y)$ satisfies the boundary condition, correct to second order, of the wing attached to an infinite reflection plate and $\Delta q(x,y)$ is an interference term.

We consider first the source distribution $q_w^{(2)}(x,y)$, which satisfies the equation

$$\left[1 + v_{xw}^{(1)}(x,y,0) - \tan \phi \, v_{yw}^{(1)}(x,y,0)\right] \frac{\partial z_t}{\partial x}$$

$$= v_{zw}^{(2)}(x,y,z_t) \approx v_{zw}^{(1)}(x,y,z_t) + \tfrac{1}{2}\left[q_w^{(2)}(x,y) - q_w^{(1)}(x,y)\right] \quad . \qquad (42)$$

There exist several possibilities for determining a source distribution $q_w^{(2)}$ (see for example Refs.3 and 5). For the present purpose of deriving only the interference velocity field it seems sufficient to use an approximate expression derived by means of a Taylor series expansion of $v_{zw}^{(1)}(x,y,z_t)$ with respect to

z (even though such an expansion is not strictly permissible at the centre section of the wing, see Ref.5). The resulting relation for $q_w^{(2)}$ reads

$$q_w^{(2)}(x,y) = 2\frac{\partial}{\partial x}\left\{z_t\left[1 + v_{xw}^{(1)}(x,y,0)\right]\right\} + 2\frac{\partial}{\partial y}\left\{z_t v_{yw}^{(1)}(x,y,0)\right\} \quad . \tag{43}$$

We do not evaluate the exact values of $v_{xw}^{(1)}$ and $v_{yw}^{(1)}$ but use the approximate values given by the RAE Standard Method[6]. For a wing with constant chord and constant section shape across the span

$$v_{xw}^{(1)} \approx S^{(1)}(\xi)\cos\phi - K_2(y)f(\phi)\cos\phi\,\frac{dz_t}{d\xi} \tag{44}$$

$$v_{yw}^{(1)} \approx -\left(1 - \left|K_2(y)\right|\right) S^{(1)}(\xi)\sin\phi \quad . \tag{45}$$

(For details concerning the terms $S^{(1)}(\xi)$, $K_2(y)$, $f(\phi)$ see Refs.3 and 6; note that the term $K_3(y)$ in equation (3) of Ref.6 has been replaced by unity.) From equations (43) to (45) we obtain for $q_w^{(2)}$ the relation

$$q_w^{(2)}(x,y) = q_w^{(1)}(\xi) + \frac{1 - \left|K_2\right|\sin^2\phi}{\cos\phi}\,2\frac{d\left(z_t S^{(1)}\right)}{d\xi} - 2K_2 f(\phi)\cos\phi\,\frac{d}{d\xi}\left(z_t\frac{dz_t}{d\xi}\right)$$
$$+ 2\frac{dK_2}{dy}z_t S^{(1)}\sin\phi \quad . \tag{46}$$

For spanwise stations sufficiently far away from the reflection plate (i.e. from the wing-body junction) where $K_2 = 0$, $dK_2/dy = 0$, we obtain

$$q_{ws}^{(2)}(\xi) = q_w^{(2)}(x, y \gg R) = q_w^{(1)}(\xi) + \frac{2}{\cos\phi}\frac{d\left(z_t S^{(1)}\right)}{d\xi} \quad ; \tag{47}$$

for the wing-body junction we obtain with $K_2 = 1$:

$$q_{wJ}^{(2)}(x) = q_w^{(2)}(x, y = R)$$
$$= q_w^{(1)}(\xi) + 2\cos\phi\,\frac{d\left(z_t S^{(1)}\right)}{d\xi}$$
$$- 2f(\phi)\cos\phi\,\frac{d}{d\xi}\left(z_t\frac{dz_t}{d\xi}\right) + 2\left(\frac{dK_2}{dy}\right)_J z_t S^{(1)}\sin\phi \quad . \tag{48}$$

Sells[3] has suggested for the isolated wing, with the centre section at $y = 0$, the function

$$K_2(y) = \frac{0.161 - 0.305y/c}{0.161 + y/c}, \qquad 0 < y/c < 0.53 \quad . \tag{49}$$

This gives for the centre section of the isolated wing

$$(dK_2/dy)_{y=0} \approx -8 \quad ;$$

which means $(dK_2/dy)_J \approx -8$.

3.2.3 The interference source distribution

The interference velocity $\Delta v_z(x,y,z)$, related to $q_w^{(1)}$ or $q_w^{(2)}$, does not vanish at $z = z_t \neq 0$. We shall see that $\Delta v_z^{(1)}(x,y,z_t)$ is numerically small, it is therefore sufficient to determine Δv_z from $q_w^{(1)}$. For the wing-fuselage combination the velocity $v_z(x,y,z_t)$ can be written, to second-order accuracy, as the sum

$$v_z(x,y,z_t) = v_{zw}^{(2)}(x,y,z_t) + \Delta v_z^{(1)}(x,y,z_t) + \Delta v_z^*(x,y,z_t) \tag{50}$$

where Δv_z^* is produced by a source distribution $\Delta q(x,y)$, yet to be determined, in the wing plane. When we combine equations (41), (42) and (50), we learn that the source distribution Δq has to produce a velocity Δv_z^* which satisfies the equation

$$\Delta v_z^*(x,y,z_t;\Delta q) = -\Delta v_z^{(1)}(x,y,z_t) \quad . \tag{51}$$

We have derived in section 2.5, equation (31) values of the interference velocity $v_{zI}(x,\theta)$ on the fuselage, related to a single source line, and have tabulated some values in Table 4. For the case of a wing swept by 45°, with the section RAE 101, $t/c = 0.1$, attached to a fuselage with the radius $R/c = 0.2$, we have computed values of $\Delta v_z^{(1)}(x,\theta)$ for various values of θ . By graphical interpolation, we have determined values of $\Delta v_{zJ}^{(1)}$ in the wing-body junction, i.e. for $\theta_J = \sin^{-1}\left(\frac{c}{R}\frac{z_t}{c}\right)$. These values are plotted in Fig.17, together with the values of $0.1 v_{zw}^{(1)}(x,y,0) = 0.1 dz_t/dx$. The figure

shows that $\Delta v_{zJ}^{(1)}$ is of a magnitude comparable to $0.1 v_{zw}^{(1)}$ (which confirms that we need not consider the source distribution $q_w^{(2)} - q_w^{(1)}$ when we compute Δv_z) .

We have not yet computed values of $v_{zI}(x,y > R,z \neq 0)$ for spanwise stations outboard of the junction. We can therefore make only an estimate of the source distribution $\Delta q(x,y)$ which would cancel the interference velocity $\Delta v_z^{(1)}(x,y,z_t)$ at all spanwise stations. We can expect that $\Delta v_z^{(1)}$ varies rapidly across the span; this would imply that the strength of the source distribution Δq also varies rapidly across the span. Such a source distribution induces at $z \neq 0$ a velocity component $\Delta v_z^*(x,y,z)$ which can be quite different from the velocity induced in $z = 0$, $\Delta v_z^*(x,y,0) = \frac{1}{2}\Delta q(x,y)$.

The aim of deriving an estimate of Δq is of course to estimate its effect on the pressure distribution of the wing, which means on v_x . In view of the uncertainty about the spanwise variation of the interference velocity $\Delta v_z^{(1)}$, we may attempt to obtain an estimate of the effect on v_x by means of a distribution of threedimensional sources along the line $0 < x < c$, $y = R$, $z = 0$. We ignore the fact that such a source distribution produces a normal velocity at the fuselage and determine the strength of the line source distribution such that it induces the velocity

$$\Delta v_z^*(x,y = R,z_t) = - \Delta v_{zJ}^{(1)}(x) \quad . \tag{52}$$

When we approximate the line source distribution by one which varies piecewise linearly, the distribution can be determined by solving a system of linear equations.

We are not able to say whether the streamwise velocity produced by the line source distribution is a fair estimate of the velocity produced by Δq . It is possible that the interference velocity $\Delta v_z^{(1)}$ varies more rapidly across the span than the velocity $\Delta v_z^*(x,y,z_t)$ produced by the line source distribution in $y = R$, $z = 0$. If this were the case then we could derive an overestimate of the effect of Δq on v_x . If $\Delta v_z^{(1)}$ varies very rapidly across the span, then it would be very laborious (and perhaps even impossible) to determine a planar source distribution Δq which cancels $\Delta v_z^{(1)}$. It might prove necessary to use a source distribution on the surface of the wing, and also to modify the source distribution on the fuselage to ensure that the normal

velocity at the body vanishes. We do not intend to apply here such a laborious procedure, but consider the Δv_x induced by the line source distribution to be only a measure of the possible error in v_x if we neglect the interference velocity $\Delta v_z^{(1)}(x,y,z_t)$ in the boundary condition.

3.2.4 The velocity at the wing surface

To evaluate the interference velocity Δv_x at the wing surface to second-order accuracy, we have both to take account of the change in the source distributions and to determine the velocity at the wing surface instead of in the plane $z = 0$.

We consider first the effect of the additional source distribution $q_w^{(2)} - q_w^{(1)}$. We can only make an estimate of the change in Δv_x because this source distribution is no longer of the type considered above, since it varies across the span, see equation (46). To obtain an estimate for the magnitude of the effect of $q_w^{(2)} - q_w^{(1)}$, we have calculated values of Δv_{xJ} for two different source distributions, each of which is of constant strength across the span. We have considered the two extreme cases, firstly the distribution which pertains to the source distributions far away from the fuselage: $q_{ws}^{(2)} - q_w^{(1)} = \frac{2}{\cos\phi} \frac{d\left(z_t S^{(1)}\right)}{d\xi}$ and secondly the distribution which pertains to the wing-body junction: $q_{wJ}^{(2)} - q_w^{(1)}$ given by equation (48). Results are shown in Fig.18.

Next, we examine how the values of Δv_x at the wing surface $z = z_t$ differ from those in the plane $z = 0$. From a Taylor series expansion of Δv_x with respect to z we obtain

$$\Delta v_x(x,y,z) = \Delta v_x(x,y,0) + z\left(\frac{\partial \Delta v_x(x,y,z)}{\partial z}\right)_{z=0} + \ldots$$

$$= \Delta v_x(x,y,0) + z\,\frac{\partial \Delta v_z(x,y,0)}{\partial x} + \ldots \quad . \tag{53}$$

For the interference velocity field, the velocity component $\Delta v_z(x,y,0)$ in the plane $z = 0$ vanishes, because v_{zI} vanishes in $z = 0$, except for $x = 0$, $y = R$ where v_{zI} is finite. The difference $\Delta v_x(x,y,z_t) - \Delta v_x(x,y,0)$ is therefore a term of third order. Nevertheless, we have computed values of $\Delta v_{xJ}^{(2)}(x,z_t)$ in the junction, using the values of the velocity component

$v_{xI}(x,\theta)$ given in Table 2 and the source distribution $q_{ws}^{(2)}$. By graphical interpolation, we have derived values of $\Delta v_{xJ}^{(2)}(x,\theta_J)$ and plotted these in Fig.19 together with the values of $\Delta v_{xJ}^{(2)}(x,\theta = 0)$ and $\Delta v_{xJ}^{(1)}(x,\theta = 0)$. The figure shows that, for the particular case considered, the maximum velocity decrement is increased by about the same amount, when we evaluate Δv_x at $z = z_t$ instead of at $z = 0$ as when we evaluate Δv_x from $q_{ws}^{(2)}$ instead of from $q_w^{(1)}$; the ratio between $\left(-\Delta v_{xJ}^{(2)}(x,\theta_J)\right)_{max}$ and $\left(-\Delta v_{xJ}^{(1)}(x,0)\right)_{max}$ is about 1.5.

Finally, we have determined the strength of the line source distribution, which satisfies equation (52) for the values of $\Delta v_{zJ}^{(1)}$ given in Fig.17, and have computed the streamwise velocity component $\Delta v_x^*(x,y = R,z_t)$ induced by the line source distribution. Values of the sum $\Delta v_{xJ}^{(2)}(x,\theta_J) + \Delta v_x^*(x,R,z_t)$ are also plotted in Fig.19. We note that the ratio between $-\Delta v_{x\,max}^*$ and $-\Delta v_{xJ\,max}^{(1)}$ is about $\frac{1}{3}$. We have, however, to stress again the uncertainty of the estimated Δv_x^* which means of the effect of $\Delta v_z^{(1)}$ in the boundary condition. When we compare the difference between the values of Δv_x computed from $q_{ws}^{(2)} - q_w^{(1)}$ and from $q_{wJ}^{(2)} - q_w^{(1)}$, given in Fig.18, with the magnitude of the somewhat uncertain value of Δv_x^*, then it seems justified to ignore the spanwise variation of $q_w^{(2)}$ and to use only the simpler term $q_{ws}^{(2)}$ when one evaluates the interference velocity Δv_x. (If we were to take account of the term $\frac{\partial z_t}{\partial x}[\Delta v_x - \tan\phi\, \Delta v_y]$ in the boundary condition, see equations (40) (41), we could expect a further, but rather small, increase of the maximum value of $-\Delta v_{xJ}$. For the case considered, $-\Delta v_{x\,max}^{(1)}$ is smaller than 0.02 and $\left|\Delta v_x^{(1)}\right|$ decreases rapidly across the span; we therefore expect that the resulting effect on Δv_x is noticeably smaller than the effect of $\Delta v_z^{(1)}(x,y,z_t)$.)

When we want to compute the pressure coefficient c_p to second-order accuracy, we ought to take account also of the velocity components Δv_y and Δv_z. We have not yet computed values of the spanwise interference velocity Δv_y away from the wing-body junction. It is of course to be expected that the error in c_p, produced by neglecting Δv_y, increases with increasing angle of sweep. The approximate boundary condition of equation (41) states that the velocity component v_z at the surface of the wing attached to the fuselage is the same as for the isolated wing. Within the present approximations, the change in the pressure distribution caused by the fuselage is therefore only produced by the change in the streamwise velocity.

3.3 Pressure distribution on the fuselage

The pressure distribution on the fuselage, to first-order accuracy, can be derived by computing the values of $\Delta v_x^{(1)}(x,\theta)$ (computed with the values of $v_{xI}(x,\theta)$ of Table 2) and adding these to the velocity $v_{xw}^{(1)}$ at the reflection plate at $z = R \sin\theta$ $\left(\text{computed by means of equation (C-3), using } q_w^{(1)}\right)$. For $\theta = 90^\circ$, values of

$$v_x^{(1)}(x,\theta) = v_{xw}^{(1)}(x, y = R, z = R \sin\theta) + \Delta v_x^{(1)}(x,\theta) \quad , \tag{54}$$

are plotted in Fig.20.

More accurate values of v_{xw} can be derived by using $q_w^{(2)}$ instead of $q_w^{(1)}$ with Ledger's program[2] or by means of the iteration technique developed by Sells[3]. However, without further effort, we are not in a position to determine more accurate values of Δv_x, since this would require a knowledge of the additional source distribution $\Delta q(x,y)$, which cancels the velocity $\Delta v_z(x,y,z_t)$.

Fig.20 shows that for the configuration considered, with $c/R = 5$, the maximum perturbation velocity at the top of the fuselage is about half the velocity in the flow past the isolated wing in the plane of symmetry at $z = R$. The maximum velocity at the top of the fuselage decreases with increasing sweep, as for the isolated wing, and the position of the maximum velocity moves rearwards.

3.4 Comparison of the results using the present method with those derived by other methods for particular configurations

The configurations considered so far deal with wings of constant chord and infinite span. We have mentioned already that we assume that the tabulated values of v_{xI} for infinitely long single source lines can also be used to estimate the interference on wings of finite span (when the span is larger than say 5 times the diameter of the fuselage). It has also been suggested that wings of moderate taper can be dealt with. To examine the validity of these assumptions and to provide information about the accuracy of the term Δv_x^*, we now compare results derived by the present method with those from more exact methods.

For symmetrical wing-fuselage configurations at zero lift, it is generally assumed that nominally exact pressure distributions can be derived by means of singularity distributions on the surface of the wing and the fuselage, the

strength of which is chosen such that the exact boundary condition is satisfied at certain points of the surface. A method for solving the problem by means of planar source panels, each of constant source strength, was devised by A.M.O. Smith and J. Hess (see e.g. Ref.7). Recently, A. Roberts[8,9] has produced a computer program for solving the problem by means of curved source panels where the geometry of the panels and the strength of the source distribution vary continuously between adjacent panels.

Using both methods, calculations have been done (unpublished work by A.F. Jones, RAE and A. Roberts, BAC) for two particular wing-fuselage combinations and for the related gross wing without fuselage. Geometric details are given in Fig.21. The velocity components have been computed by Roberts' program for a free stream Mach number $M_0 = 0.4$. In the following analysis, we want to compare only the streamwise perturbation velocity component pertaining to incompressible flow, which we have derived from the values of v_x computed by Roberts' program by multiplying them by the factor $\beta = \sqrt{1 - 0.4^2}$. Somewhat different values would be obtained if Roberts' program were applied for incompressible flow. We may however expect that the difference is small because, for the wing alone, the values of v_x derived in this way from the Roberts' program are very similar to those computed by the A.M.O. Smith program for $M = 0$. Unfortunately, the two programs have produced values for v_x at different spanwise and chordwise positions, so that we have to interpolate or extrapolate the computed values before we can make a comparison. In particular, we have to extrapolate the values of v_x computed by the A.M.O. Smith and the Roberts programs, into the junction. In the neighbourhood of the wing-body junction, the two programs produce different values for v_x , as shown in Fig.22. It seems reasonable to assume that Roberts' program, which uses continuous singularity distributions, produces the more reliable results. (We note also that in Roberts' method special singular source 'modes' are used near the wing-body junction, in accordance with the results of Craggs and Mangler[10]; this feature should also increase the accuracy in this region.)

Some further justification for the assumption can be derived by an examination of the values for the spanwise velocity component obtained by the two methods. The velocity components v_y and v_z at the junction are related by the condition

$$v_{nJ}(x,\theta_J) = \cos\theta_J v_y(x,y_J,z_t) + \sin\theta_J v_z(x,y_J,z_t) = 0 \quad .$$

The values of $v_y(x,y > R,z_t)$ given by Roberts' program can easily be extrapolated to the approximate values

$$- \tan \theta_J \, v_{zw}^{(1)}(x,y,0) \approx - \frac{z_{t/c}}{R/c} \frac{dz_t}{dx} \quad .$$

This is not possible with the values from the A.M.O. Smith program, unless one omits at least the two spanwise stations nearest to the junction. (We may mention that the values of v_y, for lines of constant percentage chord, derived by Roberts' program for the wing-fuselage configuration, vary near the junction more rapidly across the span than the values near the centre section of the isolated wing.)

In the present analysis, we have neglected the difference between the aspect ratio of the gross wing $(A = 6)$ and that of the nett wing $(A = 5.65)$ and have subtracted the values of $v_{xw}(\xi,\eta = 0)$ at the centre section of the gross wing from the $v_{xJ}(\xi,y_J)$ in the wing-body junction at the same percentage-chord point $\xi = \dfrac{x - x_{LE}(y)}{c(y)}$ (where $c(y)$ is the local chord and $x_{LE}(y)$ the coordinate of the leading edge). In both programs, the velocity on the wing-body combination has been computed at values of ξ which differ from those used for the wing alone, i.e. the values of v_{xw} had to be interpolated for the values of ξ for which v_{xJ} was known. With the A.M.O. Smith program the velocity has been computed at a larger number of chordwise and spanwise stations than with the Roberts program. To obtain relatively reliable values of v_{xw}, we have therefore combined the values of v_{xw} derived by the A.M.O. Smith program with those derived by Roberts when we determined the interference velocity Δv_x. Values of Δv_{xJ} are plotted in Fig.23.

To derive an estimate for Δv_x by the method of the present Report, we have approximated the tapered wing by an untapered wing of 30° sweep and the same chord c_J as the tapered wing has in the wing-body junction; the ratio between body radius and wing chord is $R/c_J = 0.24$. For this configuration we have computed values of $\Delta v_x^{(2)}(x,\theta_J)$ using the source distribution $q_{ws}^{(2)}(\xi)$, given by equation (47). (When we use the source distribution $q_{wJ}^{(2)}$, given by equation (48), we obtain for $-\Delta v_{xJ}^{(2)}$ at $x/c_J = 0.35$ the same value as with $q_{ws}^{(2)}$; at $x/c_J = 0.1$ we obtain a value which is smaller by about 0.0015 and at $x/c_J = 0.7$ the value is larger by about 0.001.)

The fuselage is non-cylindrical at distances greater than one diameter forward of the apex of the gross wing. To estimate the effect of the body nose, we have computed, by slender-body theory, values of the streamwise velocity v_{xB} for the isolated fuselage and have added these to $\Delta v_{xJ}^{(2)}$.

In Fig.23 we compare the values of $\Delta v_{xJ}^{(2)} + v_{xB}$ with the values of Δv_{xJ} derived by the two panel methods. We note that for $0.1 < x/c_J < 0.6$ say, the values of $\Delta v_{xJ}^{(2)} + v_{xB}$ agree fairly well with those derived from the Roberts' program.

It is likely that the differences over the rearward part of the chord are taper effects. (We have seen in Fig.12 that the position where Δv_x vanishes moves forward with decreasing angle of sweep.) An improved estimate of Δv_x , at the chordwise position x , would probably be derived if one were to represent the wing by one with the local sweep $\phi(x)$ instead of the sweep of the mid-chord line. Unfortunately, we cannot draw any definite conclusions because we cannot make statements about the accuracy of the interpolated values of v_{xw} . We do not compare the various values of Δv_x near the leading edge because the interpolated values of v_{xw} can be rather inaccurate and because the present method is based on a small-perturbation theory (without leading-edge corrections) which is by nature unreliable near the leading edge.

We have computed values of $\Delta v_{zJ}^{(1)}$ and hence, by means of a line source distribution, values of the corresponding change in the streamwise velocity Δv_x^* . If we consider the values of Δv_x , derived from Roberts' program, as reliable then Fig.23 suggests that the change in Δv_x , which is related to the change Δv_z at the surface of the wing, is smaller than Δv_x^* ; this could imply that the interference term Δv_z decreases more rapidly away from the wing-body junction than the $\Delta v_z^*(x,y,z_t)$ induced by the line source distribution.

A calculation by Roberts' program has also been done for a combination of the same gross wing A with a fuselage, B_0 , for which the diameter of fuselage B_1 has been reduced by the factor $\sqrt{0.5}$. For this configuration, the ratio between the wing chord in the wing-body junction and the body radius $c_J/R = 6$. From the computed results, we have derived values of Δv_{xJ} in the same way as for the larger fuselage. These are plotted in Fig.24 together with the values for the thicker body B_1 . The maximum velocity decrement is larger for the thinner body because the projection of the junction shape into the chordplane,

$y_J(x)$, departs more from a straight line. We have also plotted in Fig.24 the values of $\Delta v_x^{(2)}(x,\theta_J) + v_{xB}$. The values of $\Delta v_x^{(2)}$ are again determined with $q_{ws}^{(2)}$. For the body B_0 , we have taken for v_{xB} half the values of v_{xB} for the body B_1 . Fig.24 shows that the difference between the values of Δv_{xJ} for the two bodies is well predicted by the estimates. The maximum value of $-\Delta v_x^*$, derived from $\Delta v_{zJ}^{(1)}$, is 20 per cent larger for the configuration AB_0 than for AB_1 . If we consider the values of Δv_{xJ} , derived from the Roberts' results, as being correct, then Fig.24 suggests again that the change in Δv_x , related to $\Delta v_z(x,y,z_t)$, is negligible.

We have also derived values of Δv_x for the spanwise stations $y_J + 0.25R$ and $y_J + R$ and have plotted them in Fig.25 together with the estimates of the present method; note that, for $y > R$, $\Delta v_x^{(2)}$ has been computed at $z = 0$, using $q_{ws}^{(2)}$. The differences between the results from the two panel methods decrease away from the junction, see Fig.22. The output of the A.M.O. Smith program enables us to derive values of Δv_x at more chordwise points than the output of Roberts' program. In Fig.25, we have therefore shown mainly the Δv_x from the A.M.O. Smith program; they agree fairly well with the estimate $\Delta v_x^{(2)}(x,y,z = 0) + v_{xB}$.

Summarising, we can say that the comparison of the present method with the results from Roberts' program for two particular configurations suggests that a fair estimate of the interference velocity Δv_{xJ} is given by $\Delta v_x^{(2)}(x,\theta_J)$ and of $\Delta v_x(x,y > R)$ by $\Delta v_x^{(2)}(x,y,0)$, when the terms $\Delta v_x^{(2)}$ are computed from the second-order source distribution and the velocity component v_{xI} related to an infinitely long source line.

4 CONCLUSIONS

The present Report gives tabulated values of the difference between the velocity components induced by a single swept source line in the presence of a circular cylindrical fuselage and those induced by the source line reflected at an infinite plate. It has been shown that, by means of these tables, one can derive fairly accurate estimates of the streamwise interference velocity for wing-fuselage combinations where the wings are of finite span, have some taper and are of uniform section shape. We may expect that estimates of sufficient accuracy can also be obtained for varying section shape if the variation is not too rapid near the wing-body junction.

The recommended procedure for estimating the change of the streamwise velocity Δv_x due to the presence of the fuselage is as follows. For the given section shape $z_t(x)$, one determines the strength of the second-order source distribution $q_{ws}^{(2)}(x)$ of the related infinite sheared wing:

$$q_{ws}^{(2)}(x) = 2 \frac{d}{dx} \left[z_t(x) \left(1 + \frac{S^{(1)}(x)}{\cos \phi} \right) \right]$$

where $S^{(1)}(x) = \frac{1}{\pi} \int_0^c \frac{dz_t(x')}{dx'} \frac{dx'}{x - x'}$.

Using $q_{ws}^{(2)}$ one evaluates $\Delta v_x^{(2)}$ from the single integral

$$\Delta v_x^{(2)}(x,y,z) = \cos \phi \int_0^{c/R} q_{ws}^{(2)}(x') \frac{v_{xI}\left(\frac{x - x'}{R}, \frac{y}{R}, z \right)}{Q/R} d\left(\frac{x'}{R} \right) \quad ;$$

values of v_{xI} are given in Tables 1 and 2. Using the values of Table 1, one can determine the interference velocity in the wing plane. To obtain an improved estimate of Δv_{xJ} in the wing-body junction, it is recommended that $\Delta v_{xJ}^{(2)}(x,z_t)$ be determined by evaluating the integral also with the values of $v_{xI}(x,\theta)$ from Table 2 for various values of θ and to interpolate between the values of $\Delta v_x^{(2)}(x,\theta)$ to derive the value applicable to $\theta_J(x) = \sin^{-1}(z_t(x)/R)$. When the required angle of sweep differs from the values for which v_{xI} is tabulated, it is advisable to compute $\Delta v_x^{(2)}$ with the tabulated values of v_{xI} and to interpolate between the values of $\Delta v_x^{(2)}(x,y,z;\phi)$ to derive $\Delta v_x^{(2)}$ for the required value of ϕ .

Appendix A

VELOCITY FIELD INDUCED BY A SOURCE LINE WITH THREE KINKS

The velocity $\underset{\sim}{v}(x,y,z)$ induced by an infinite source line in $x' = |1 - |y'||\tan\phi$, $z' = 0$ of constant strength Q per unit length can be obtained from the relation

$$\underset{\sim}{v}(x,y,z) = \frac{Q}{4\pi\cos\phi}\left\{\int_1^\infty \frac{[x - (y' - 1)\tan\phi]\,\underline{i} + (y - y')\underline{j} + z\underline{k}}{\sqrt{[x - (y' - 1)\tan\phi]^2 + (y - y')^2 + z^2}^3}\,dy'\right.$$

$$+ \int_0^1 \frac{[x - (1 - y')\tan\phi]\,\underline{i} + (y - y')\underline{j} + z\underline{k}}{\sqrt{[x - (1 - y')\tan\phi]^2 + (y - y')^2 + z^2}^3}\,dy'$$

$$+ \int_0^1 \frac{[x - (1 - y')\tan\phi]\,\underline{i} + (y + y')\underline{j} + z\underline{k}}{\sqrt{[x - (1 - y')\tan\phi]^2 + (y + y')^2 + z^2}^3}\,dy'$$

$$\left.+ \int_1^\infty \frac{[x - (y' - 1)\tan\phi]\,\underline{i} + (y + y')\underline{j} + z\underline{k}}{\sqrt{[x - (y' - 1)\tan\phi]^2 + (y + y')^2 + z^2}^3}\,dy'\right\} \quad (A\text{-}1)$$

where $\underline{i}$, $\underline{j}$, $\underline{k}$ are unit vectors parallel to the x, y, z axes.

Using equation (A-1) we can determine at the fuselage $y^2 + z^2 = R^2 = 1$ the normal velocity $v_{nQ}(x,\theta)$ from

$$v_{nQ}(x,\theta) = v_y\cos\theta + v_z\sin\theta \quad . \qquad (A\text{-}2)$$

We obtain

$$v_{nQ}(x,\theta) = \frac{Q}{4\pi}\left\{ \frac{1 - \cos^2\phi\cos\theta\,(\cos\theta + x\tan\phi + \tan^2\phi) - \dfrac{\cos\phi\,(\sin^2\theta + x^2\cos\theta) - x(1-\cos\theta)\sin\phi}{\sqrt{x^2 + 2(1-\cos\theta)}}}{[(1-\cos\theta)\sin\phi + x\cos\phi]^2 + \sin^2\theta} \right.$$

$$+ \frac{\dfrac{\cos\phi\,(\sin^2\theta + x^2\cos\theta) + x(1-\cos\theta)\sin\phi}{\sqrt{x^2 + 2(1-\cos\theta)}} - \dfrac{\sin\phi\,(x - \tan\phi) + \cos\phi\cos\theta\,(x-\tan\phi)^2}{\sqrt{1 + (x-\tan\phi)^2}}}{[(1-\cos\theta)\sin\phi - x\cos\phi]^2 + \sin^2\theta}$$

$$+ \frac{\dfrac{\cos\phi\,(\sin^2\theta - x^2\cos\theta) + x(1+\cos\theta)\sin\phi}{\sqrt{x^2 + 2(1+\cos\theta)}} - \dfrac{\sin\phi\,(x - \tan\phi) - \cos\phi\cos\theta\,(x-\tan\phi)^2}{\sqrt{1 + (x-\tan\phi)^2}}}{[(1+\cos\theta)\sin\phi - x\cos\phi]^2 + \sin^2\theta}$$

$$\left. + \frac{1 + \cos^2\phi\cos\theta\,(-\cos\theta + x\tan\phi + \tan^2\phi) - \dfrac{\cos\phi\,(\sin^2\theta - x^2\cos\theta) - x(1+\cos\theta)\sin\phi}{\sqrt{x^2 + 2(1+\cos\theta)}}}{[(1+\cos\theta)\sin\phi + x\cos\phi]^2 + \sin^2\theta} \right\} \quad \ldots(A\text{-}3)$$

From equation (A-3) we obtain for $\theta = 0$

$$v_{nQ}(x,\theta = 0) =$$

$$\frac{Q}{4\pi}\left\{\frac{\tan\phi}{x\cos\phi}\,\frac{1-\sqrt{1-2x\sin\phi\cos\phi+x^2\cos^2\phi}}{\sqrt{1+(x-\tan\phi)^2}}-\sqrt{\frac{1+\tan^2\phi}{1+(x-\tan\phi)^2}}\right.$$

$$+\frac{1}{2\sin\phi-x\cos\phi}\left[\frac{x}{\sqrt{x^2+4}}+\frac{\tan\phi-x}{\sqrt{1+(x-\tan\phi)^2}}\right]$$

$$\left.+\frac{1}{2\sin\phi+x\cos\phi}\left[\frac{x}{\sqrt{x^2+4}}+\sin\phi\right]\right\}$$

with

$$\lim_{x\to 0} v_{nQ}(x,\theta = 0) = \frac{Q}{4\pi}\sin^2\phi \quad .$$

From equation (A-3) we obtain for $x = 0$

$$v_{nQ}(x = 0,\theta) = \frac{Q}{2\pi}$$

which means

$$\bar{v}_{nQ}(x = 0) = \frac{Q}{2\pi}$$

for all values of ϕ .

For the streamwise velocity component in the plane $z = 0$ we obtain from equation (A-1) the relation:

$$v_{x_{\wedge\wedge}}(x,y,0) =$$

$$\frac{Q}{4\pi\cos\phi}\left\{\frac{1}{x+(y-1)\tan\phi}\left[\frac{y}{\sqrt{(x-\tan\phi)^2+y^2}}-\frac{y-1}{\sqrt{x^2+(y-1)^2}}\right]\right.$$

$$+\frac{1}{x-(y+1)\tan\phi}\left[\frac{-y}{\sqrt{(x-\tan\phi)^2+y^2}}+\frac{y+1}{\sqrt{x^2+(y+1)^2}}\right]$$

$$+\frac{1}{x-(y-1)\tan\phi}\left[\cos\phi+\frac{y-1}{\sqrt{x^2+(y-1)^2}}\right]$$

$$\left.+\frac{1}{x+(y+1)\tan\phi}\left[\cos\phi-\frac{y+1}{\sqrt{x^2+(y+1)^2}}\right]\right\} \quad . \qquad \text{(A-4)}$$

For the velocity on the fuselage we obtain

$$v_{x/\!\!/}(x,\theta) =$$

$$\frac{Q}{4\pi \cos\phi}\left\{\frac{1}{[x - \tan\phi\ (1 - \cos\theta)]^2 + \sin^2\theta\ (1 + \tan^2\phi)}\left[\frac{(x - 2\tan\phi)(1 - \cos\theta)}{\sqrt{x^2 + 2(1 - \cos\theta)}} + \frac{x\cos\theta + \tan\phi\ (1 - \cos\theta)}{\sqrt{(x - \tan\phi)^2 + 1}}\right]\right.$$

$$+ \frac{1}{[x - \tan\phi\ (1 + \cos\theta)]^2 + \sin^2\theta\ (1 + \tan^2\phi)}\left[\frac{(x - 2\tan\phi)(1 + \cos\theta)}{\sqrt{x^2 + 2(1 + \cos\theta)}} + \frac{-x\cos\theta + \tan\phi\ (1 + \cos\theta)}{\sqrt{(x - \tan\phi)^2 + 1}}\right]$$

$$+ \frac{1}{[x + \tan\phi\ (1 - \cos\theta)]^2 + \sin^2\theta\ (1 + \tan^2\phi)}\left[x\cos\phi + \sin\phi\ (1 - \cos\theta) - \frac{(x + 2\tan\phi)(1 - \cos\theta)}{\sqrt{x^2 + 2(1 - \cos\theta)}}\right]$$

$$\left.+ \frac{1}{[x + \tan\phi\ (1 + \cos\theta)]^2 + \sin^2\theta\ (1 + \tan^2\phi)}\left[x\cos\phi + \sin\phi\ (1 + \cos\theta) - \frac{(x + 2\tan\phi)(1 + \cos\theta)}{\sqrt{x^2 + 2(1 + \cos\theta)}}\right]\right\}$$

...(A-5)

$$v_{\theta/\!\!\wedge}(x,\theta) =$$

$$\frac{Q}{4\pi}\left\{\frac{\sin\theta\cos\phi}{[(1-\cos\theta)\sin\phi + x\cos\phi]^2 + \sin^2\theta}\left[\sin\phi\,(x+\tan\phi) + \cos\phi\cos\theta + \frac{x(x+\tan\phi)+1-\cos\theta}{\sqrt{x^2+2(1-\cos\theta)}}\right]\right.$$

$$+\frac{\sin\theta\cos\phi}{[(1-\cos\theta)\sin\phi - x\cos\phi]^2 + \sin^2\theta}\left[\sqrt{1+(x-\tan\phi)^2} - \frac{x(x-\tan\phi)+1-\cos\theta}{\sqrt{x^2+2(1-\cos\theta)}}\right]$$

$$-\frac{\sin\theta\cos\phi}{[(1+\cos\theta)\sin\phi - x\cos\phi]^2 + \sin^2\theta}\left[\sqrt{1+(x-\tan\phi)^2} - \frac{x(x-\tan\phi)+1+\cos\theta}{\sqrt{x^2+2(1+\cos\theta)}}\right]$$

$$\left.-\frac{\sin\theta\cos\phi}{[(1+\cos\theta)\sin\phi + x\cos\phi]^2 + \sin^2\theta}\left[\sin\phi\,(x+\tan\phi) - \cos\phi\cos\theta + \frac{x(x+\tan\phi)+1+\cos\theta}{\sqrt{x^2+2(1+\cos\theta)}}\right]\right\}$$

...(A-6)

Appendix B

THE BEHAVIOUR OF $v_{xq}(x,y = 1,0)$ FOR SMALL VALUES OF $|x|$

By using the relations

$$\int_{-\infty}^{\infty} \frac{(x - x')dx'}{\sqrt{(x - x')^2 + 2(1 - \cos\theta)}^3} = 0$$

$$\int_{0}^{\pi} \frac{d\theta'}{\sqrt{(x - x')^2 + 2(1 - \cos\theta)}^3} = \frac{2\mathbf{E}(k)}{(x - x')^2\sqrt{(x - x')^2 + 4}}$$

and $q(x,\theta)$ given by equation (14), we can derive $v_{xq}(x,y = 1,0)$ from the equation

$$v_{xq}(x,y = 1,0) = -\int_{-\infty}^{\infty}\int_{0}^{\pi} \frac{v_{nQ}(x',\theta)(x - x')d\theta dx'}{\pi\sqrt{(x - x')^2 + 2(1 - \cos\theta)}^3}$$

$$+ \int_{-\infty}^{\infty} \frac{\left[\bar{v}_{nQ}(x') - \bar{v}_{nQ}(x) + \tfrac{1}{2}\bar{\sum K}^{(n)}(x') - \tfrac{1}{2}\bar{\sum K}^{(n)}(x)\right]\mathbf{E}(k)dx'}{\pi(x - x')\sqrt{(x - x')^2 + 4}} \quad . \qquad \ldots(B\text{-}1)$$

The single integral is a finite continuous function for all values of x. The singular behaviour of the double integral for small values of $|x|$ arises from

$$I_1 = -\int_{-a}^{b} dx' \int_{0}^{\delta} \frac{v_{nQ}(x',\theta)(x - x')d\theta}{\pi\sqrt{(x - x')^2 + 2(1 - \cos\theta)}^3} \qquad (B\text{-}2)$$

where a, b, δ are large compared to $|x|$. By using equation (A-1) for $v_{nQ}(x,\theta)$ it can be shown that, for $\theta \ll 1$ and $x \ll 1/\sin 2\phi$, the leading terms in $v_{nQ}(x,\theta)$ are

$$v_{nQ}(x,\theta) = \frac{Q}{4\pi}\left\{2 - \frac{x^2\cos^2\phi\,(2\cos^2\phi - \sin^2\phi)}{x^2\cos^2\phi + \theta^2} - \frac{2x^4\sin^2\phi\cos^4\phi}{[x^2\cos^2\phi + \theta^2]^2}\right.$$

$$\left. + \frac{x\sin\phi\,[3x^2\theta^2\cos^2\phi + \theta^4(1 + 2\cos^2\phi)]}{\sqrt{x^2 + \theta^2}\,[x^2\cos^2\phi + \theta^2]^2} + O(x,\theta^2)\right\}. \quad \text{(B-3)}$$

We consider first the contribution I_2 to $v_{xq}(x,1,0)$ where

$$I_2(x) = -\frac{1}{4\pi^2}\int_{-d}^{d}\int_{0}^{\delta}\frac{x'\sin\phi\,[3x'^2\theta^2\cos^2\phi + \theta^4(1 + 2\cos^2\phi)](x - x')d\theta dx'}{\sqrt{x'^2 + \theta^2}\,[x'^2\cos^2\phi + \theta^2]^2\sqrt{(x - x')^2 + \theta^2}^3}$$

$$= -\frac{\sin\phi}{4\pi^2}\int_{0}^{d}\int_{0}^{\delta}\frac{3x'^2\theta^2\cos^2\phi + \theta^4(1 + 2\cos^2\phi)}{[x'^2\cos^2\phi + \theta^2]^2}\frac{x'}{\sqrt{x'^2 + \theta^2}}\times$$

$$\times\left[\frac{x - x'}{\sqrt{(x - x')^2 + \theta^2}^3} - \frac{x + x'}{\sqrt{(x + x')^2 + \theta^2}^3}\right]d\theta dx' \quad . \quad \text{(B-4)}$$

We choose $\delta = d$ and introduce the variable σ, defined by

$$\theta = \sigma x'$$

$$I_2 = -\frac{\sin\phi}{4\pi^2}\left\{\int_{0}^{1} d\sigma\,\frac{3\sigma^2\cos^2\phi + \sigma^4(1 + 2\cos^2\phi)}{[\cos^2\phi + \sigma^2]^2\sqrt{1 + \sigma^2}}\times\right.$$

$$\times\int_{0}^{d}\left[\frac{x'(x - x')}{\sqrt{(x - x')^2 + \sigma^2x'^2}^3} - \frac{x'(x + x')}{\sqrt{(x + x')^2 + \sigma^2x'^2}^3}\right]dx'$$

$$+\int_{1}^{\infty} d\sigma\,\frac{3\sigma^2\cos^2\phi + \sigma^4(1 + 2\cos^2\phi)}{[\cos^2\phi + \sigma^2]^2\sqrt{1 + \sigma^2}}\times$$

$$\left.\times\int_{0}^{d/\sigma}\left[\frac{x'(x - x')}{\sqrt{(x - x')^2 + \sigma^2x'^2}^3} - \frac{x'(x + x')}{\sqrt{(x + x')^2 + \sigma^2x'^2}^3}\right]dx'\right\}.$$

The integrals

$$\int_0^d \left[\frac{x'(x - x')}{\sqrt{(x - x')^2 + \sigma^2 x'^2}^3} - \frac{x'(x + x')}{\sqrt{(x + x')^2 + \sigma^2 x'^2}^3} \right] dx'$$

and

$$\int_0^{d/\sigma} \left[\frac{x'(x - x')}{\sqrt{(x - x')^2 + \sigma^2 x'^2}^3} - \frac{x'(x + x')}{\sqrt{(x + x')^2 + \sigma^2 x'^2}^3} \right] dx'$$

contain the term $\frac{2}{\sqrt{1 + \sigma^2}^3} \log |x|$. This means that I_2 contains the term $\kappa \log |x|$, where

$$\kappa = - \frac{\sin \phi}{4\pi^2} \int_0^\infty 2 \frac{3\sigma^2 \cos^2 \phi + \sigma^4 (1 + 2 \cos^2 \phi)}{[\cos^2 \phi + \sigma^2]^2 [1 + \sigma^2]^2} d\sigma$$

$$= - \frac{\cos^3 \phi - 1 + \frac{3}{2} \sin^2 \phi}{4\pi \sin^3 \phi} \quad . \tag{B-5}$$

We now consider the contribution I_3 to $v_{xq}(x,1,0)$ where

$$I_3(x) = - \frac{1}{4\pi^2} \int_{x-\varepsilon}^{x+\varepsilon} \int_0^\delta \left\{ \frac{- x'^2 \cos^2 \phi (2 \cos^2 \phi - \sin^2 \phi)}{x'^2 \cos^2 \phi + \theta^2} - \frac{2x'^4 \sin^2 \phi \cos^4 \phi}{[x'^2 \cos^2 \phi + \theta^2]^2} \right\}$$

$$\times \frac{(x - x') d\theta dx'}{\sqrt{(x - x')^2 + \theta^2}^3} \quad . \tag{B-6}$$

$I_3(x)$ is discontinuous at $x = 0$. The value

$$I(\phi) = \lim_{x \to +0} I_3(x > 0, \phi) \tag{B-7}$$

can be determined by a technique similar to that of Appendix A of Ref.1. This leads to the expression

$$I(\phi) = -\frac{\cos^2\phi}{4\pi^2}\int_{-\infty}^{\infty}\left\{\frac{(1+\tau)^2[2(\sin^2\phi-\cos^2\phi)\tau^2+(2-\sin^2\phi)\cos^2\phi\,(1+\tau)^2]}{\tau[\tau^2-(1+\tau)^2\cos^2\phi]^2}\right.$$

$$\left.+\frac{\tau|1+\tau|[2\tau^2-(2+\sin^2\phi)(1+\tau)^2]}{\sqrt{|\tau^2-(1+\tau)^2\cos^2\phi|^5}}f(\tau)\right\}d\tau \qquad \text{(B-8)}$$

where $f(\tau) = \tan^{-1}\frac{\sqrt{\tau^2-(1+\tau)^2\cos^2\phi}}{|1+\tau|\cos\phi}$ for

$$-\infty < \tau < -\frac{\cos\phi}{1+\cos\phi} \quad \text{and} \quad \frac{\cos\phi}{1-\cos\phi} < \tau < \infty$$

and $f(\tau) = \frac{1}{2}\log\frac{(1+\tau)\cos\phi+\sqrt{(1+\tau)^2\cos^2\phi-\tau^2}}{(1+\tau)\cos\phi-\sqrt{(1+\tau)^2\cos^2\phi-\tau^2}}$ for

$$-\frac{\cos\phi}{1+\cos\phi} < \tau < \frac{\cos\phi}{1-\cos\phi} \quad .$$

We have evaluated the integral in equation (B-8) numerically and have obtained the values

ϕ	$I(\phi)$
0	-0.05305
30^o	-0.04853
45^o	-0.04240
60^o	-0.03288

The remaining contributions to $v_{xq}(x,1,0)$ are finite continuous functions. Thus $v_{xq}(x,y=1,0)$ behaves as

$$\frac{v_{xq}(x,y=1,0)}{Q} = -\frac{\cos^3\phi-1+\frac{3}{2}\sin^2\phi}{4\pi\sin^3\phi}\log|x| + \frac{x}{|x|}I(\phi) + f(x;\phi) \qquad \text{(B-9)}$$

where $f(x;\phi)$ is a finite continuous function.

Appendix C

VELOCITY FIELD INDUCED BY A SWEPT SOURCE LINE

The velocity field $\underline{v}_\Lambda(x,y,z)$ induced by an infinite swept source line with the kink at $x' = 0$, $y' = 1$ can be obtained from the relation

$$\underline{v}_\Lambda(x,y,z) = \frac{Q}{4\pi \cos\phi}\left\{\int_1^\infty \frac{[x - (y' - 1)\tan\phi]\,\underline{i} + (y - y')\underline{j} + z\underline{k}}{\sqrt{[x - (y' - 1)\tan\phi]^2 + (y - y')^2 + z^2}^3}\,dy' + \int_{-\infty}^1 \frac{[x - (1 - y')\tan\phi]\,\underline{i} + (y - y')\underline{j} + z\underline{k}}{\sqrt{[x - (1 - y')\tan\phi]^2 + (y - y')^2 + z^2}^3}\,dy'\right\} \quad (C\text{-}1)$$

This equation gives for the x-component of the velocity in the plane $z = 0$ the relation:

$$v_{x\Lambda}(x,y,0) = \frac{Q}{4\pi \cos\phi}\left\{\frac{1}{x + (y - 1)\tan\phi}\left[\cos\phi - \frac{y - 1}{\sqrt{x^2 + (y - 1)^2}}\right] + \frac{1}{x - (y - 1)\tan\phi}\left[\cos\phi + \frac{y - 1}{\sqrt{x^2 + (y - 1)^2}}\right]\right\} . \quad (C\text{-}2)$$

For the velocity components in the plane $y = 1$, we obtain the relations:

$$v_{x\Lambda}(x,y = 1,z) = \frac{Q}{2\pi}\frac{1}{x^2\cos^2\phi + z^2}\left\{x\cos^2\phi - \frac{z^2\sin\phi}{\sqrt{x^2 + z^2}}\right\} \quad (C\text{-}3)$$

$$v_{z\Lambda}(x,y = 1,z) = \frac{Q}{2\pi}\frac{z}{x^2\cos^2\phi + z^2}\left\{1 + \frac{x\sin\phi}{\sqrt{x^2 + z^2}}\right\} . \quad (C\text{-}4)$$

When we substitute for Q in equation (C-4) the term $f(\xi)d\xi$ and perform the integration with respect to ξ, we obtain

$$v_z(x,y=1,z) = \frac{1}{2\pi}\int_0^1 f(\xi)\,\frac{z}{(x-\xi)^2\cos^2\phi + z^2}\left\{1 + \frac{(x-\xi)\sin\phi}{\sqrt{(x-\xi)^2+z^2}}\right\}d\xi$$

$$= \frac{f(x)}{2\pi}\int_0^1 \frac{z}{(x-\xi)^2\cos^2\phi + z^2}\,d\xi$$

$$+ \frac{z}{2\pi}\int_0^1 \left\{\frac{f(\xi)-f(x)}{(x-\xi)^2\cos^2\phi + z^2} + \right.$$

$$\left. + \frac{(x-\xi)f(\xi)\sin\phi}{[(x-\xi)^2\cos^2\phi + z^2]\sqrt{(x-\xi)^2+z^2}}\right\}d\xi \quad . \quad (C\text{-}5)$$

The first term on the right-hand side is equal to

$$\frac{f(x)}{2\pi}\,\frac{z}{z\cos\phi}\left[\tan^{-1}\frac{(1-x)\cos\phi}{z} + \tan^{-1}\frac{x\cos\phi}{z}\right] \quad ;$$

when z tends to zero the term tends to $f(x)/2\cos\phi$. The integrand of the second term changes its sign at $\xi = x$; the second term therefore vanishes when z tends to zero. With $f(\xi) = \cos\phi\, q(\xi)$, we obtain therefore from equation (C-5) the limit

$$\lim_{z\to 0} v_z(x,y=1,z) = \frac{q(\xi)}{2} \quad .$$

Appendix D

COMPARISON BETWEEN RESULTS FROM THE PRESENT METHOD AND FROM THE APPROXIMATE 'SOURCE METHOD' GIVEN IN REF.11

At the time when Ref.11 was written, the evaluation of a series of double integrals seemed too laborious a procedure. Therefore an estimate of the interference effect produced by a fuselage was derived by means of only a source distribution on the axis of the fuselage. For an unswept isolated source line in $x = 0$, the effect of the source distribution $q(x,\theta)$ on the fuselage, used in the present method, was approximated by the velocity field of a single sink in $x = y = z = 0$. The strength of the source was chosen such that there is no overall flow through the fuselage, which means the condition of zero normal velocity at the surface of the fuselage is satisfied in the average but not locally, as by means of $q(x,\theta)$.

With a swept wing attached to a circular fuselage, the source distribution in the wing plane was the same as in the present method, however the difference between the velocity fields for a source line with three kinks and for a source line with one kink, $\underline{v}_{\wedge} - \underline{v}_{\Lambda}$, was neglected. For a single source line through $x = |1 - |y|| \tan \phi$, the source distribution $q(x,\theta)$ on the fuselage was approximated by a sink distribution in $0 < x < \tan \phi$ of strength $E(x) = -2Q/\sin \phi$. This sink distribution induces the streamwise velocity component

$$v_{xs}(x,y,z = 0) = \frac{-2Q}{4\pi \sin \phi} \int_0^{\tan \phi} \frac{x - x'}{\sqrt{(x - x')^2 + y^2}^3} \, dx'$$

$$= -\frac{Q}{2\pi \sin \phi} \left[\frac{1}{\sqrt{(\tan \phi - x)^2 + y^2}} - \frac{1}{\sqrt{x^2 + y^2}} \right] . \quad \text{(D-1)}$$

To judge how good an approximation can be derived by means of the axial source distribution, we compare first some results for an isolated source line. For $\phi = 45^{\circ}$ and $y = 1$, we have plotted in Fig.26 v_{xs} from equation (D-1) together with v_{xq} and v_{xI} from Fig.5. We note, for larger values of $|x|$, that v_{xs} gives an overestimate of v_{xq} (the same is true for $\phi = 0$ as shown in Fig.5 of Ref.1). The axial source distribution was suggested as an approximation of the interference effect; we are therefore more interested in a

comparison of v_{xs} with v_{xI}. Fig.26 shows that v_{xs} produces, for most values of x, a large overestimate of the magnitude of the interference velocity $|v_{xI}|$. We have seen in Fig.5 that the terms v_{xq} and $v_{x\mathcal{M}} - v_{x\Lambda}$ are for most values of x of opposite sign, therefore the neglect of the term $v_{x\mathcal{M}} - v_{x\Lambda}$ in the 'source method' of Ref.11 produces a less satisfactory approximation to v_{xI} for larger values of ϕ.

We are of course more interested in a comparison of the results for a complete wing-fuselage combination than in a comparison of the results for a single source line. For an unswept wing, a comparison is made in Fig.27 between the values of Δv^{**}_{xJ} from the 'source method' with the values of $\Delta v^{(1)}_{xJ}$ computed from equation (35); we learn that the maximum value of $-\Delta v^{**}_{xJ}$ is about twice the maximum value of $-\Delta v^{(1)}_{xJ}$. We have plotted in Fig.27 also the values of $\Delta v^{(2)}_{xJ}(x,\theta_J)$ and of $\Delta v^{(2)}_{xJ} + \Delta v^{*}_{x}$. For the particular values of wing thickness, $t/c = 0.1$, and ratio between wing chord and body radius, $c/R = 5$, the agreement between the values of Δv^{**}_{xJ} from the 'source method' (related to the wing source distribution of first-order theory $q^{(1)}_{w}$) and the values Δv_{xJ} from second-order theory seems to be sufficient for preliminary estimates.

When we apply the 'source method' to configurations with wings of the same chordwise section but with varying angle of sweep, then we find that the maximum velocity decrement in the junction is almost independent of sweep in contrast to the results shown for example in Fig.12. We follow therefore a suggestion made by D.A. Treadgold[12] who found that an improved estimate of Δv_x can be obtained from the 'source method' of Ref.11, when the strength of the axial source distribution is reduced by the factor $\cos\phi$. For a wing-fuselage combination with a wing swept by 45°, we have plotted in Fig.28 the estimate of the interference velocity, Δv^{**}_{xJ}, determined from the 'source method' multiplied by the factor $\cos\phi$ (i.e. from equation (35) when v_{xI} is replaced by $\cos\phi\, v_{xs}$, with v_{xs} from equation (D-1)), together with the values of $\Delta v^{(1)}_{xJ}$ and $\Delta v^{(2)}_{xJ}$ from Fig.19. When we compare Figs.27 and 28, we note that the relations between Δv^{**}_{xJ} and $\Delta v^{(1)}_{xJ}$ and also between Δv^{**}_{xJ} and Δv_{xJ} from second-order theory are for the swept wing similar to those for the unswept wing; this fact demonstrates the beneficial effect of the factor $\cos\phi$ applied to the 'source method' of Ref.11.

In Ref.11, a further estimate for the interference effect was suggested by means of the 'vortex method'. This estimate was based on the assumption that

the curved shape of the intersection line between a thick wing and a fuselage (in particular the projection into the plane of the wing) were mainly responsible for the velocity decrement in the junction. If this were true, then the velocity decrement would be nearly independent of the angle of sweep; however the results in Figs.12 and 14 show that the assumption is invalid.

Table I

STREAMWISE COMPONENT OF THE INTERFERENCE VELOCITY ON THE WING, $\frac{v_{xI}(x,y,z=0)}{Q/R}$, FOR A SINGLE SOURCE LINE

x \ y	$\phi = 0$			$\phi = 30^\circ$			$\phi = 45^\circ$			$\phi = 60^\circ$		
	1	1.25	2	1	1.25	2	1	1.25	2	1	1.25	2
-10	0.0014	0.0015	0.0015	0.0011	0.0011	0.0011	0.0009	0.0009	0.0009	0.0008	0.0007	0.0008
-5	0.0051	0.0052	0.0045	0.0041	0.0041	0.0038	0.0037	0.0037	0.0035	0.0034	0.0033	0.0032
-4.5	0.0060	0.0061	0.0051	0.0049	0.0049	0.0044	0.0045	0.0045	0.0041	0.0041	0.0040	0.0038
-4	0.0072	0.0072	0.0059	0.0060	0.0060	0.0053	0.0055	0.0055	0.0050	0.0050	0.0049	0.0046
-3.5	0.0086	0.0084	0.0068	0.0074	0.0073	0.0063	0.0069	0.0068	0.0060	0.0063	0.0062	0.0057
-3	0.0104	0.0102	0.0078	0.0093	0.0091	0.0077	0.0087	0.0085	0.0074	0.0081	0.0080	0.0067
-2.5	0.0128	0.0123	0.0089	0.0118	0.0114	0.0091	0.0112	0.0109	0.0090	0.0107	0.0104	0.0088
-2	0.0160	0.0152	0.0100	0.0152	0.0146	0.0108	0.0147	0.0143	0.0110	0.0143	0.0138	0.0111
-1.75	0.0180	0.0168	0.0104	0.0174	0.0166	0.0117	0.0170	0.0164	0.0121	0.0167	0.0161	0.0124
-1.5	0.0202	0.0187	0.0106	0.0201	0.0191	0.0127	0.0199	0.0191	0.0133	0.0196	0.0190	0.0138
-1.25	0.0228	0.0208	0.0105	0.0233	0.0219	0.0134	0.0235	0.0223	0.0145	0.0235	0.0225	0.0154
-1	0.0259	0.0228	0.0101	0.0275	0.0254	0.0139	0.0282	0.0263	0.0155	0.0286	0.0270	0.0169
-0.9	0.0274	0.0235	0.0097	0.0295	0.0270	0.0141	0.0305	0.0282	0.0159	0.0312	0.0292	0.0174
-0.8	0.0288	0.0243	0.0092	0.0319	0.0286	0.0141	0.0332	0.0303	0.0161	0.0342	0.0316	0.0179
-0.7	0.0303	0.0248	0.0085	0.0346	0.0304	0.0139	0.0364	0.0326	0.0163	0.0377	0.0343	0.0184
-0.6	0.0321	0.0252	0.0077	0.0378	0.0322	0.0137	0.0401	0.0350	0.0163	0.0419	0.0373	0.0188
-0.5	0.0341	0.0252	0.0068	0.0413	0.0340	0.0133	0.0446	0.0377	0.0162	0.0470	0.0407	0.0190
-0.4	0.0364	0.0243	0.0056	0.0464	0.0356	0.0127	0.0503	0.0402	0.0159	0.0536	0.0443	0.0191
-0.3	0.0389	0.0222	0.0044	0.0526	0.0365	0.0119	0.0578	0.0425	0.0154	0.0623	0.0479	0.0190
-0.2	0.0423	0.0181	0.0030	0.0612	0.0358	0.0109	0.0685	0.0437	0.0148	0.0749	0.0510	0.0187
-0.1	0.0467	0.0106	0.0015	0 0742	0.0320	0.0097	0.0850	0.0422	0.0139	0.0967	0.0519	0.0182
-0.05	0.0495	0.0056	0.0008	0.0869	0.0284	0.0091	0.1033	0.0397	0.0134	0.1185	0.0510	0.0179
-0.02	0.0516	0.0022		0.1033	0.0256		0.1259	0.0377		0.1470	0.0498	
0	±0.0530	0	0	-	0.0237	0.0084	-	0.0362	0.0128	-	0.0488	0.0175
0.02	-0.0516	-0.0022		0.0063	0.0216		0.0431	0.0344		0.0856	0.0476	
0.05	-0.0495	-0.0056	-0.0008	-0.0066	0.0185	0.0077	0.0213	0.0316	0.0122	0.0547	0.0454	0.0170
0.1	-0.0467	-0.0106	-0.0015	-0.0152	0.0128	0.0070	0.0066	0.0264	0.0116	0.0341	0.0412	0.0165
0.2	-0.0423	-0.0181	-0.0030	-0.0220	0.0029	0.0055	-0.0058	0.0161	0.0102	0.0161	0.0317	0.0155
0.3	-0.0389	-0.0222	-0.0044	-0.0241	-0.0044	0.0040	-0.0119	0.0076	0.0088	0.0058	0.0227	0.0142
0.4	-0.0364	-0.0243	-0.0056	-0.0246	-0.0093	0.0025	-0.0150	0.0013	0.0073	-0.0004	0.0154	0.0129
0.5	-0.0341	-0.0252	-0.0068	-0.0243	-0.0125	0.0011	-0.0167	-0.0033	0.0059	-0.0045	0.0095	0.0115
0.6	-0.0321	-0.0252	-0.0077	-0.0237	-0.0145	-0.0002	-0.0176	-0.0066	0.0045	-0.0073	0.0049	0.0101
0.7	-0.0303	-0.0248	-0.0085	-0.0231	-0.0157	-0.0016	-0.0179	-0.0089	0.0031	-0.0093	0.0014	0.0087
0.8	-0.0288	-0.0243	-0.0092	-0.0222	-0.0164	-0.0027	-0.0179	-0.0105	0.0018	-0.0107	-0.0014	0.0074
0.9	-0.0274	-0.0235	-0.0097	-0.0215	-0.0168	-0.0036	-0.0178	-0.0116	0.0007	-0.0116	-0.0036	0.0061
1.0	-0.0259	-0.0228	-0.0101	-0.0208	-0.0169	-0.0044	-0.0175	-0.0124	-0.0004	-0.0123	-0.0053	0.0049
1.25	-0.0228	-0.0208	-0.0105	-0.0192	-0.0167	-0.0060	-0.0167	-0.0134	-0.0025	-0.0130	-0.0080	0.0023
1.5	-0.0202	-0.0187	-0.0106	-0.0179	-0.0161	-0.0070	-0.0160	-0.0137	-0.0041	-0.0130	-0.0095	0.0002
1.75	-0.0180	-0.0168	-0.0104	-0.0167	-0.0153	-0.0076	-0.0153	-0.0136	-0.0052	-0.0128	-0.0103	-0.0015
2	-0.0160	-0.0152	-0.0100	-0.0156	-0.0145	-0.0079	-0.0147	-0.0133	-0.0060	-0.0125	-0.0107	-0.0028
2.5	-0.0128	-0.0123	-0.0089	-0.0136	-0.0128	-0.0080	-0.0134	-0.0124	-0.0068	-0.0121	-0.0109	-0.0044
3	-0.0104	-0.0102	-0.0078	-0.0116	-0.0113	-0.0076	-0.0120	-0.0114	-0.0069	-0.0113	-0.0107	-0.0053
3.5	-0.0086	-0.0084	-0.0068	-0.0100	-0.0099	-0.0069	-0.0106	-0.0105	-0.0067	-0.0105	-0.0105	-0.0056
4	-0.0072	-0.0072	-0.0059	-0.0086	-0.0087	-0.0063	-0.0093	-0.0095	-0 0063	-0.0096	-0.0102	-0.0057
4.5	-0.0060	-0.0061	-0.0051	-0.0073	-0.0076	-0.0057	-0.0081	-0.0085	-0.0058	-0.0086	-0.0096	-0.0056
5	-0.0051	-0.0052	-0.0045	-0.0064	-0.0067	-0.0052	-0.0070	-0.0077	-0.0054	-0.0076	-0.0089	-0.0054
10	-0.0014	-0.0015	-0.0015	-0.0018	-0.0022	-0.0020	-0.0019	-0.0028	-0.0024	-0.0019	-0.0038	-0.0030

Table 2

STREAMWISE COMPONENT OF THE INTERFERENCE VELOCITY ON THE FUSELAGE, $\frac{v_{xI}(x,\theta)}{Q/R}$, FOR A SINGLE SOURCE LINE

x \ θ	φ = 0					φ = 30°					φ = 45°					φ = 60°				
	5°	10°	30°	60°	90°	5°	10°	30°	60°	90°	5°	10°	30°	60°	90°	5°	10°	30°	60°	90°
-10	0.0014	0.0014	0.0015	0.0018	0.0019	0.0010	0.0011	0.0011	0.0011	0.0012	0.0009	0.0009	0.0009	0.0009	0.0009	0.0008	0.0008	0.0008	0.0008	0.0008
-5	0.0051	0.0052	0.0055	0.0062	0.0066	0.0041	0.0041	0.0042	0.0045	0.0046	0.0037	0.0037	0.0037	0.0038	0.0038	0.0034	0.0034	0.0034	0.0033	0.0033
-4.5	0.0060	0.0061	0.0065	0.0074	0.0080	0.0050	0.0050	0.0051	0.0054	0.0056	0.0045	0.0045	0.0045	0.0046	0.0047	0.0041	0.0041	0.0041	0.0040	0.0040
-4	0.0072	0.0073	0.0079	0.0091	0.0098	0.0060	0.0060	0.0062	0.0067	0.0070	0.0055	0.0055	0.0056	0.0058	0.0059	0.0051	0.0051	0.0051	0.0051	0.0050
-3.5	0.0086	0.0087	0.0096	0.0114	0.0123	0.0074	0.0074	0.0077	0.0085	0.0089	0.0069	0.0069	0.0070	0.0074	0.0076	0.0064	0.0064	0.0064	0.0065	0.0065
-3	0.0104	0.0106	0.0119	0.0147	0.0159	0.0093	0.0094	0.0099	0.0111	0.0117	0.0087	0.0087	0.0090	0.0097	0.0101	0.0082	0.0082	0.0083	0.0086	0.0087
-2.5	0.0129	0.0132	0.0152	0.0194	0.0212	0.0118	0.0120	0.0129	0.0150	0.0162	0.0112	0.0113	0.0119	0.0133	0.0140	0.0107	0.0107	0.0110	0.0118	0.0122
-2	0.0161	0.0165	0.0199	0.0263	0.0289	0.0152	0.0154	0.0174	0.0212	0.0230	0.0148	0.0149	0.0162	0.0190	0.0203	0.0143	0.0144	0.0151	0.0170	0.0180
-1.75	0.0182	0.0187	0.0231	0.0309	0.0340	0.0175	0.0178	0.0204	0.0257	0.0280	0.0171	0.0173	0.0192	0.0231	0.0250	0.0167	0.0169	0.0181	0.0209	0.0222
-1.5	0.0205	0.0212	0.0272	0.0365	0.0396	0.0202	0.0206	0.0243	0.0313	0.0343	0.0200	0.0203	0.0231	0.0286	0.0309	0.0196	0.0199	0.0218	0.0259	0.0277
-1.25	0.0233	0.0243	0.0325	0.0428	0.0456	0.0235	0.0241	0.0295	0.0387	0.0415	0.0237	0.0241	0.0283	0.0357	0.0382	0.0236	0.0239	0.0270	0.0327	0.0347
-1.0	0.0265	0.0282	0.0395	0.0492	0.0506	0.0279	0.0288	0.0370	0.0477	0.0508	0.0285	0.0292	0.0356	0.0449	0.0478	0.0288	0.0293	0.0341	0.0416	0.0442
-0.9	0.0280	0.0302	0.0430	0.0510	0.0516	0.0300	0.0312	0.0404	0.0517	0.0542	0.0309	0.0318	0.0394	0.0491	0.0516	0.0315	0.0321	0.0379	0.0456	0.0483
-0.8	0.0297	0.0323	0.0466	0.0530	0.0524	0.0325	0.0340	0.0452	0.0557	0.0576	0.0337	0.0349	0.0438	0.0536	0.0557	0.0345	0.0354	0.0423	0.0504	0.0525
-0.7	0.0316	0.0348	0.0504	0.0536	0.0514	0.0354	0.0374	0.0504	0.0596	0.0607	0.0369	0.0385	0.0491	0.0582	0.0597	0.0381	0.0393	0.0475	0.0553	0.0569
-0.6	0.0338	0.0380	0.0545	0.0528	0.0498	0.0388	0.0415	0.0562	0.0631	0.0630	0.0408	0.0429	0.0552	0.0628	0.0634	0.0425	0.0441	0.0537	0.0603	0.0612
-0.5	0.0364	0.0420	0.0582	0.0502	0.0462	0.0430	0.0467	0.0630	0.0658	0.0643	0.0458	0.0487	0.0623	0.0669	0.0662	0.0478	0.0501	0.0609	0.0653	0.0654
-0.4	0.0399	0.0477	0.0584	0.0451	0.0404	0.0486	0.0539	0.0692	0.0668	0.0642	0.0520	0.0562	0.0700	0.0702	0.0685	0.0549	0.0581	0.0691	0.0697	0.0687
-0.3	0.0450	0.0553	0.0551	0.0372	0.0327	0.0563	0.0640	0.0746	0.0660	0.0623	0.0607	0.0668	0.0776	0.0721	0.0699	0.0646	0.0693	0.0778	0.0734	0.0711
-0.2	0.0535	0.0642	0.0446	0.0269	0.0229	0.0686	0.0787	0.0764	0.0627	0.0586	0.0743	0.0827	0.0832	0.0720	0.0693	0.0794	0.0860	0.0855	0.0755	0.0721
-0.1	0.0683	0.0603	0.0254	0.0141	0.0118	0.0916	0.0943	0.0713	0.0565	0.0529	0.1000	0.1032	0.0840	0.0697	0.0664	0.1074	0.1090	0.0903	0.0759	0.0722
-0.05	0.0629	0.0384	0.0131	0.0072	0.0059	0.1064	0.0932	0.0653	0.0526	0.0496	0.1198	0.1090	0.0817	0.0676	0.0646	0.1300	0.1188	0.0907	0.0755	0.0718
-0.02	0.0382	0.0154	0.0052	0.0029	0.0024	0.1020	0.0840	0.0610	0.0500	0.0477	0.1245	0.1062	0.0791	0.0661	0.0635	0.1400	0.1203	0.0903	0.0754	0.0715
0	0	0	0	0	0	0.0845	0.0735	0.0574	0.0478	0.0464	0.1165	0.1012	0.0773	0.0651	0.0624	0.1388	0.1184	0.0896	0.0749	0.0711
0.02	-0.0382	-0.0154	-0.0052	-0.0029	-0.0024	0.0571	0.0613	0.0530	0.0460	0.0446	0.0990	0.0935	0.0761	0.0640	0.0613	0.1305	0.1155	0.0887	0.0743	0.0707
0.05	-0.0629	-0.0384	-0.0131	-0.0072	-0.0059	0.0121	0.0391	0.0471	0.0433	0.0419	0.0606	0.0775	0.0710	0.0619	0.0594	0.1054	0.1067	0.0864	0.0732	0.0698
0.1	-0.0683	-0.0603	-0.0254	-0.0141	-0.0118	-0.0280	0.0026	0.0345	0.0377	0.0377	0.0090	0.0449	0.0628	0.0583	0.0566	0.0586	0.0844	0.0818	0.0713	0.0684
0.2	-0.0535	-0.0642	-0.0446	-0.0269	-0.0229	-0.0366	-0.0351	0.0111	0.0256	0.0273	-0.0198	-0.0044	0.0428	0.0494	0.0489	0.0097	0.0386	0.0687	0.0661	0.0647
0.3	-0.0450	-0.0553	-0.0551	-0.0372	-0.0327	-0.0329	-0.0411	-0.0101	0.0127	0.0167	-0.0222	-0.0237	0.0218	0.0388	0.0399	-0.0040	0.0089	0.0529	0.0592	0.0594
0.4	-0.0399	-0.0477	-0.0584	-0.0451	-0.0404	-0.0301	-0.0389	-0.0254	0.0003	0.0060	-0.0219	-0.0286	0.0036	0.0276	0.0318	-0.0086	-0.0063	0.0368	0.0510	0.0525
0.5	-0.0364	-0.0420	-0.0582	-0.0502	-0.0462	-0.0283	-0.0359	-0.0346	-0.0103	-0.0039	-0.0216	-0.0288	-0.0104	0.0165	0.0229	-0.0108	-0.0136	0.0224	0.0422	0.0454
0.6	-0.0338	-0.0380	-0.0545	-0.0528	-0.0498	-0.0264	-0.0325	-0.0392	-0.0201	-0.0133	-0.0211	-0.0277	-0.0201	0.0061	0.0128	-0.0121	-0.0168	0.0102	0.0334	0.0379
0.7	-0.0316	-0.0348	-0.0504	-0.0536	-0.0514	-0.0251	-0.0300	-0.0414	-0.0283	-0.0216	-0.0206	-0.0262	-0.0263	-0.0031	0.0045	-0.0131	-0.0182	0.0006	0.0249	0.0301
0.8	-0.0297	-0.0323	-0.0466	-0.0530	-0.0524	-0.0238	-0.0278	-0.0407	-0.0326	-0.0284	-0.0201	-0.0249	-0.0299	-0.0109	-0.0031	-0.0137	-0.0187	-0.0069	0.0170	0.0226
0.9	-0.0280	-0.0302	-0.0430	-0.0510	-0.0516	-0.0227	-0.0260	-0.0399	-0.0362	-0.0341	-0.0195	-0.0236	-0.0316	-0.0172	-0.0106	-0.0141	-0.0187	-0.0125	0.0098	0.0156
1.0	-0.0265	-0.0282	-0.0395	-0.0492	-0.0506	-0.0218	-0.0246	-0.0379	-0.0385	-0.0357	-0.0189	-0.0224	-0.0322	-0.0222	-0.0166	-0.0143	-0.0185	-0.0165	0.0035	0.0098
1.25	-0.0233	-0.0243	-0.0325	-0.0428	-0.0456	-0.0199	-0.0217	-0.0332	-0.0399	-0.0392	-0.0176	-0.0201	-0.0310	-0.0298	-0.0265	-0.0143	-0.0175	-0.0220	-0.0089	-0.0035
1 5	-0.0205	-0.0212	-0.0272	-0.0365	-0.0396	-0.0184	-0.0199	-0.0290	-0.0375	-0.0390	-0.0167	-0.0183	-0.0285	-0.0324	-0.0317	-0.0139	-0.0164	-0.0235	-0.0168	-0.0128
1.75	-0.0182	-0.0187	-0.0231	-0.0309	-0.0340	-0.0171	-0.0184	-0.0255	-0.0345	-0.0367	-0.0158	-0.0172	-0.0259	-0.0323	-0.0327	-0.0135	-0.0154	-0.0234	-0.0214	-0.0187
2	-0.0161	-0.0165	-0.0199	-0.0263	-0.0289	-0.0158	-0.0167	-0.0226	-0.0309	-0.0336	-0.0151	-0.0162	-0.0236	-0.0308	-0.0318	-0.0131	-0.0146	-0.0224	-0.0237	-0.0219
2.5	-0.0129	-0.0132	-0.0152	-0.0194	-0.0212	-0.0137	-0.0142	-0.0180	-0.0245	-0.0268	-0.0136	-0.0143	-0.0195	-0.0263	-0.0282	-0.0124	-0.0135	-0.0200	-0.0243	-0.0245
3	-0.0104	-0.0106	-0.0119	-0.0147	-0.0159	-0.0116	-0.0121	-0.0147	-0.0198	-0.0214	-0.0122	-0.0125	-0.0163	-0.0219	-0.0236	-0.0116	-0.0125	-0.0176	-0.0225	-0.0237
3.5	-0.0086	-0.0087	-0.0096	-0.0114	-0.0123	-0.0110	-0.0103	-0.0120	-0.0160	-0.0172	-0.0107	-0.0110	-0.0138	-0.0182	-0.0197	-0.0108	-0.0114	-0.0155	-0.0202	-0.0214
4	-0.0072	-0.0073	-0.0079	-0.0091	-0.0098	-0.0086	-0.0088	-0.0100	-0.0130	-0.0139	-0.0094	-0.0096	-0.0118	-0.0152	-0.0166	-0.0099	-0.0104	-0.0136	-0.0178	-0.0190
4.5	-0.0060	-0.0061	-0.0065	-0.0074	-0.0080	-0.0073	-0.0074	-0.0085	-0.0107	-0.0115	-0.0082	-0.0083	-0.0101	-0.0129	-0.0140	-0.0089	-0.0091	-0.0119	-0.0156	-0.0168
5	-0.0051	-0.0052	-0.0055	-0.0062	-0.0066	-0.0064	-0.0065	-0.0073	-0.0090	-0.0097	-0.0071	-0.0072	-0.0086	-0.0111	-0.0120	-0.0078	-0.0080	-0.0104	-0.0138	-0.0149
10	-0.0014	-0.0014	-0.0015	-0.0018	-0.0019	-0.0018	-0.0018	-0.0021	-0.0028	-0.0032	-0.0019	-0.0020	-0.0026	-0.0037	-0.0038	-0.0019	-0.0021	-0.0033	-0.0055	-0.0063

Table 3

CIRCUMFERENTIAL VELOCITY COMPONENT, $\frac{v_{\theta q}(x,\theta)}{Q/R}$, FOR A SINGLE SOURCE LINE

x \ θ	φ = 30°							φ = 45°							φ = 60°						
	5°	10°	20°	30°	45°	60°	75°	5°	10°	20°	30°	45°	60°	75°	5°	10°	20°	30°	45°	60°	75°
-10	0 0001	0 0001	0.0002	0.0003	0.0003	0.0003	0 0001	0.0000	0.0001	0.0001	0.0001	0.0002	0.0001	0.0001	0.0000	0.0000	0.0001	0.0001	0.0001	0 0001	0 0000
-5	0.0002	0.0005	0 0009	0.0012	0.0014	0.0012	0.0007	0.0002	0 0003	0.0006	0.0007	0.0009	0.0007	0.0004	0.0001	0.0002	0.0003	0.0004	0.0005	0.0004	0 0003
-4 5	0 0003	0.0006	0.0011	0.0015	0.0017	0 0015	0.0009	0.0002	0 0004	0.0007	0.0010	0.0011	0.0010	0.0005	0.0001	0.0002	0.0004	0.0006	0.0007	0.0006	0.0003
-4	0.0004	0.0008	0 0015	0.0020	0.0023	0.0020	0.0011	0.0003	0.0005	0.0010	0.0013	0.0015	0.0013	0.0007	0.0002	0.0003	0.0006	0.0008	0.0009	0.0008	0.0005
-3 5	0.0005	0.0011	0.0020	0.0027	0.0031	0.0026	0.0015	0.0004	0.0007	0.0013	0.0018	0.0021	0.0018	0.0010	0.0002	0.0005	0.0009	0.0012	0.0013	0.0012	0.0007
-3	0 0008	0 0015	0.0028	0.0038	0.0043	0.0037	0.0021	0.0005	0.0010	0.0019	0.0026	0.0030	0.0025	0.0015	0.0004	0.0007	0.0013	0.0018	0.0020	0.0017	0 0010
-2 5	0 0011	0.0022	0.0042	0.0055	0.0063	0.0053	0.0030	0.0008	0.0016	0.0030	0.0040	0.0045	0.0038	0.0022	0.0006	0.0011	0.0021	0.0028	0.0032	0.0027	0.0016
-2	0.0018	0.0035	0.0065	0.0086	0.0096	0.0080	0.0045	0.0013	0.0026	0.0048	0.0064	0.0071	0.0060	0.0034	0.0010	0.0019	0.0035	0.0047	0.0053	0.0045	0.0025
-1 75	0.0023	0 0045	0.0083	0.0109	0.0120	0.0099	0.0055	0.0017	0.0033	0.0062	0.0082	0.0091	0.0076	0.0042	0.0013	0.0026	0.0047	0.0062	0.0069	0.0058	0 0032
-1 5	0.0030	0.0059	0.0109	0.0141	0.0151	0.0122	0.0067	0.0023	0.0045	0.0083	0.0108	0.0117	0.0096	0.0052	0.0018	0.0034	0.0063	0.0083	0.0090	0.0074	0.0042
-1 25	0.0041	0.0080	0.0144	0.0183	0.0190	0.0149	0.0081	0.0031	0.0061	0.0111	0.0142	0.0149	0.0118	0.0064	0.0024	0.0048	0.0086	0.0110	0.0116	0.0093	0 0051
-1 0	0 0058	0 0111	0 0195	0.0238	0.0234	0.0177	0.0093	0.0045	0.0086	0.0152	0.0188	0.0187	0.0142	0.0076	0.0035	0.0068	0.0119	0.0148	0.0148	0 0113	0.0060
-0 9	0.0067	0.0128	0.0221	0.0265	0.0252	0.0186	0 0097	0.0052	0.0100	0.0174	0.0210	0.0203	0.0151	0.0079	0.0041	0.0078	0.0136	0.0165	0.0161	0.0120	0.0063
-0 8	0.0078	0.0149	0.0252	0.0293	0.0269	0.0194	0.0100	0.0061	0.0117	0.0198	0.0233	0.0218	0.0159	0.0082	0.0048	0.0092	0.0156	0.0184	0.0173	0.0126	0.0066
-0 7	0 0093	0.0176	0.0287	0.0322	0.0284	0.0199	0 0101	0.0072	0.0138	0.0227	0.0258	0.0231	0.0164	0.0084	0.0057	0.0108	0.0179	0.0204	0.0183	0 0131	0.0067
-0.6	0 0112	0 0209	0.0327	0.0351	0.0294	0.0201	0.0100	0.0088	0.0164	0.0259	0.0282	0.0241	0.0166	0.0084	0.0069	0.0129	0.0205	0.0223	0.0191	0.0132	0 0067
-0 5	0.0139	0.0253	0.0370	0.0374	0.0297	0.0198	0.0098	0.0109	0.0199	0.0295	0.0303	0.0245	0.0165	0.0082	0 0085	0.0156	0.0232	0.0239	0.0193	0.0130	0.0065
-0 4	0 0177	0.0310	0.0412	0.0388	0.0292	0 0190	0.0094	0.0139	0.0245	0.0331	0.0317	0.0242	0.0159	0.0079	0.0109	0.0192	0.0259	0.0248	0.0189	0.0124	0.0061
-0 3	0.0237	0.0385	0.0443	0.0386	0.0278	0 0179	0.0088	0.0186	0.0305	0.0358	0.0317	0.0231	0 0150	0.0074	0.0145	0.0238	0.0278	0 0244	0.0177	0.0114	0.0056
-0 2	0.0339	0.0471	0.0444	0.0362	0.0255	0 0164	0.0081	0.0266	0.0375	0.0361	0.0298	0.0211	0.0136	0.0067	0.0206	0.0290	0.0274	0.0223	0.0156	0.0100	0.0049
-0 1	0.0499	0.0499	0.0395	0.0320	0.0230	0.0150	0.0074	0.0395	0.0402	0.0320	0.0259	0.0186	0.0122	0.0060	0.0302	0.0300	0.0230	0.0182	0.0129	0.0084	0.0041
-0.05	0 0525	0 0447	0.0359	0.0298	0.0218	0.0144	0.0071	0 0420	0.0358	0.0285	0.0236	0.0173	0.0114	0.0057	0.0310	0.0252	0.0192	0.0157	0.0114	0.0075	0.0037
-0 02	0.0460	0.0407	0.0338	0.0287	0.0212	0.0141	0.0070	0.0363	0.0315	0 0264	0.0223	0.0166	0.0110	0.0055	0 0249	0.0205	0.0167	0.0141	0.0105	0.0070	0.0035
0	0 0405	0.0380	0 0331	0.0281	0.0209	0.0139	0.0069	0.0302	0.0285	0.0250	0.0215	0.0161	0.0108	0.0054	0.0178	0.0169	0.0150	0 0130	0.0099	0.0067	0.0033
0 02	0.0419	0.0371	0 0325	0 0277	0.0207	0.0137	0.0069	0.0282	0.0265	0.0240	0.0208	0.0157	0.0105	0.0053	0.0125	0.0137	0.0134	0.0120	0.0093	0.0063	0.0032
0 05	0.0534	0.0391	0.0322	0.0274	0.0204	0.0136	0.0068	0.0351	0.0258	0.0227	0.0200	0.0152	0.0102	0.0051	0.0118	0.0103	0.0112	0.0106	0.0085	0.0058	0.0030
0 1	0 0790	0 0511	0.0343	0 0278	0.0204	0.0135	0.0067	0.0663	0.0336	0.0226	0.0191	0.0145	0.0098	0.0049	0.0346	0.0111	0.0087	0.0086	0.0072	0.0051	0.0026
0 2	0.0792	0.0765	0.0463	0.0327	0.0220	0.0141	0.0069	0.0901	0.0649	0.0307	0.0211	0.0146	0.0095	0.0047	0 0837	0.0342	0.0100	0.0069	0.0055	0.0039	0.0020
0 3	0.0630	0 0816	0.0607	0 0414	0.0257	0.0157	0.0076	0.0803	0.0844	0.0462	0.0278	0.0166	0.0102	0.0050	0.0948	0.0636	0.0194	0.0090	0.0052	0 0034	0.0017
0 4	0 0502	0.0758	0 0706	0.0509	0.0308	0.0183	0.0086	0.0673	0.0882	0.0620	0.0379	0.0207	0.0120	0.0056	0.0892	0.0834	0.0338	0.0149	0.0065	0.0036	0.0017
0.5	0.0409	0.0674	0.0745	0.0587	0.0365	0 0214	0.0100	0.0567	0.0843	0.0737	0.0488	0.0265	0.0147	0.0067	0.0800	0.0925	0.0495	0.0236	0.0096	0.0047	0 0021
0 6	0.0341	0.0591	0 0741	0.0636	0.0418	0.0243	0 0116	0.0483	0.0778	0.0803	0.0585	0.0330	0.0182	0.0082	0.0711	0.0944	0.0636	0.0338	0.0141	0.0066	0.0028
0 7	0.0290	0.0519	0.0710	0 0657	0.0459	0 0278	0.0131	0.0418	0.0707	0.0827	0.0660	0.0396	0.0221	0.0100	0.0634	0.0923	0.0748	0.0444	0.0198	0.0093	0.0039
0 8	0.0250	0.0457	0.0667	0.0656	0.0487	0.0304	0.0144	0.0366	0.0641	0.0822	0.0710	0.0455	0.0260	0.0118	0.0568	0.0884	0.0829	0.0544	0.0262	0.0127	0.0053
0 9	0.0217	0 0404	0.0618	0.0640	0.0502	0 0323	0 0155	0.0323	0.0580	0.0798	0.0736	0.0504	0.0297	0.0137	0.0513	0.0836	0.0880	0.0632	0.0330	0.0165	0.0069
1 0	0.0191	0 0359	0.0570	0.0614	0.0505	0.0334	0.0163	0.0288	0.0526	0.0762	0.0742	0.0539	0.0329	0.0154	0.0466	0.0787	0 0907	0.0705	0.0396	0.0206	0 0088
1 25	0.0143	0 0273	0 0459	0.0531	0.0479	0.0337	0.0170	0.0221	0.0415	0.0655	0.0703	0.0575	0.0378	0.0184	0.0375	0.0669	0.0903	0 0815	0.0539	0.0307	0.0138
1 5	0.0111	0.0213	0 0370	0.0446	0.0427	0.0316	0.0164	0.0174	0.0332	0.0550	0.0628	0.0556	0.0387	0.0194	0.0308	0.0568	0.0842	0.0840	0.0628	0.0388	0.0182
1 75	0 0088	0.0170	0.0301	0.0373	0.0342	0.0284	0.0150	0.0140	0.0269	0.0460	0.0545	0.0510	0.0370	0.0189	0.0257	0.0480	0.0756	0.0808	0.0656	0.0434	0.0210
2	0.0071	0.0138	0.0248	0.0313	0.0322	0.0251	0 0135	0.0115	0.0222	0.0387	0.0470	0.0458	0.0341	0.0179	0.0215	0.0408	0.0667	0.0747	0.0648	0.0445	0.0222
2 5	0.0049	0.0096	0.0175	0.0225	0.0240	0.0193	0.0106	0.0080	0.0156	0.0280	0.0351	0.0359	0.0279	0.0150	0 0156	0.0299	0.0511	0.0604	0.0567	0.0412	0.0213
3	0 0036	0.0070	0.0129	0.0168	0.0182	0.0150	0.0083	0.0059	0.0116	0.0210	0.0268	0.0282	0.0225	0.0122	0.0117	0.0225	0.0395	0.0483	0.0474	0.0357	0 0187
3 5	0.0027	0 0053	0.0098	0.0129	0.0143	0.0118	0.0066	0.0046	0.0089	0.0163	0.0211	0.0226	0.0184	0.0101	0.0091	0.0176	0.0313	0.0391	0.0395	0.0305	0.0163
4	0.0021	0.0042	0.0077	0.0102	0.0114	0.0095	0 0054	0 0036	0.0071	0.0130	0.0170	0.0185	0.0152	0 0084	0.0073	0.0141	0.0254	0.0322	0.0333	0.0262	0.0141
4 5	0.0017	0.0034	0.0062	0.0083	0.0093	0.0078	0.0044	0.0029	0.0058	0.0106	0.0139	0.0153	0.0127	0 0071	0.0059	0.0116	0 0210	0.0269	0.0284	0.0226	0 0123
5	0.0014	0.0028	0.0051	0.0068	0.0077	0.0065	0 0037	0 0024	0.0048	0.0088	0.0116	0.0129	0.0108	0.0060	0.0050	0.0097	0.0177	0.0228	0.0244	0.0197	0 0108
10	0 0004	0.0007	0.0014	0.0019	0.0021	0.0018	0.0011	0.0007	0.0013	0.0025	0.0033	0.0038	0.0033	0 0019	0.0015	0.0029	0 0054	0.0071	0.0080	0.0068	0.0038

Table 4

z-COMPONENT OF THE INTERFERENCE VELOCITY ON THE FUSELAGE, $\frac{v_{zI}(x,\theta)}{Q/R}$, FOR A SINGLE SOURCE LINE

x \ θ	φ = 0				φ = 30°				φ = 45°				φ = 60°			
	5°	10°	20°	30°	5°	10°	20°	30°	5°	10°	20°	30°	5°	10°	20°	30°
-10	0.0001	0.0003	0.0004	0.0004	0.0000	0.0000	0.0000	-0.0001	0.0000	0.0000	-0.0001	-0.0002	0.0000	-0.0001	-0.0002	-0.0003
-5	0.0006	0.0011	0.0017	0.0016	0.0001	0.0002	0.0002	-0.0001	0.0000	-0.0001	-0.0003	-0.0006	-0.0001	-0.0003	-0.0006	-0.0010
-4.5	0.0007	0.0013	0.0021	0.0020	0.0001	0.0003	0.0003	-0.0002	0.0000	-0.0001	-0.0004	-0.0006	-0.0002	-0.0003	-0.0007	-0.0011
-4	0.0009	0.0017	0.0027	0.0026	0.0002	0.0004	0.0005	-0.0001	0.0000	0.0000	-0.0004	-0.0007	-0.0002	-0.0003	-0.0007	-0.0013
-3.5	0.0012	0.0022	0.0035	0.0033	0.0003	0.0006	0.0007	0.0000	0.0001	0.0000	-0.0004	-0.0007	-0.0002	-0.0003	-0.0008	-0.0015
-3	0.0016	0.0030	0.0048	0.0045	0.0005	0.0008	0.0011	0.0003	0.0001	0.0001	-0.0003	-0.0007	-0.0001	-0.0003	-0.0009	-0.0017
-2.5	0.0022	0.0042	0.0067	0.0063	0.0007	0.0014	0.0020	0.0012	0.0003	0.0005	0.0004	-0.0005	-0.0001	-0.0002	-0.0007	-0.0019
-2	0.0034	0.0063	0.0099	0.0090	0.0013	0.0024	0.0035	0.0024	0.0006	0.0011	0.0013	0.0000	0.0001	0.0001	-0.0003	-0.0022
-1.75	0.0042	0.0079	0.0123	0.0110	0.0017	0.0032	0.0047	0.0033	0.0009	0.0016	0.0021	0.0005	0.0003	0.0005	0.0001	-0.0018
-1.5	0.0054	0.0102	0.0154	0.0131	0.0023	0.0044	0.0065	0.0046	0.0014	0.0025	0.0033	0.0013	0.0006	0.0010	0.0007	-0.0015
-1.25	0.0071	0.0133	0.0195	0.0155	0.0033	0.0062	0.0089	0.0061	0.0021	0.0038	0.0050	0.0021	0.0011	0.0019	0.0018	-0.0012
-1.0	0.0098	0.0179	0.0248	0.0173	0.0049	0.0090	0.0123	0.0075	0.0032	0.0058	0.0074	0.0029	0.0019	0.0033	0.0035	-0.0011
-0.9	0.0113	0.0205	0.0271	0.0174	0.0058	0.0105	0.0140	0.0079	0.0039	0.0070	0.0087	0.0031	0.0024	0.0042	0.0043	-0.0013
-0.8	0.0131	0.0235	0.0298	0.0167	0.0068	0.0124	0.0159	0.0079	0.0047	0.0084	0.0101	0.0029	0.0030	0.0052	0.0052	-0.0017
-0.7	0.0154	0.0272	0.0324	0.0149	0.0083	0.0147	0.0178	0.0074	0.0057	0.0102	0.0115	0.0023	0.0038	0.0065	0.0061	-0.0026
-0.6	0.0184	0.0317	0.0343	0.0115	0.0101	0.0177	0.0198	0.0057	0.0072	0.0124	0.0130	0.0008	0.0048	0.0082	0.0070	-0.0044
-0.5	0.0226	0.0373	0.0349	0.0053	0.0127	0.0215	0.0213	0.0024	0.0091	0.0154	0.0141	-0.0022	0.0063	0.0103	0.0075	-0.0075
-0.4	0.0285	0.0442	0.0327	-0.0040	0.0164	0.0264	0.0214	-0.0035	0.0120	0.0192	0.0140	-0.0075	0.0085	0.0131	0.0069	-0.0127
-0.3	0.0375	0.0515	0.0252	-0.0168	0.0221	0.0322	0.0183	-0.0129	0.0164	0.0238	0.0113	-0.0161	0.0118	0.0164	0.0038	-0.0211
-0.2	0.0508	0.0543	0.0110	-0.0321	0.0316	0.0375	0.0095	-0.0262	0.0239	0.0280	0.0035	-0.0288	0.0174	0.0191	-0.0040	-0.0336
-0.1	0.0646	0.0401	-0.0075	-0.0451	0.0452	0.0327	-0.0066	-0.0418	0.0348	0.0239	-0.0118	-0.0448	0.0252	0.0141	-0.0193	-0.0505
-0.05	0.0545	0.0256	-0.0144	-0.0490	0.0440	0.0218	-0.0158	-0.0491	0.0340	0.0139	-0.0215	-0.0531	0.0231	0.0039	-0.0296	-0.0592
-0.02	0.0425	0.0191	-0.0164	-0.0501	0.0340	0.0144	-0.0209	-0.0530	0.0248	0.0058	-0.0273	-0.0580	0.0136	-0.0048	-0.0361	-0.0646
0.0	0.0355	0.0181	-0.0169	-0.0504	0.0264	0.0098	-0.0234	-0.0552	0.0162	0.0005	-0.0309	-0.0610	0.0038	-0.0110	-0.0403	-0.0683
0.02	0.0425	0.0191	-0.0164	-0.0501	0.0268	0.0075	-0.0254	-0.0571	0.0124	-0.0036	-0.0340	-0.0638	-0.0037	-0.0167	-0.0444	-0.0718
0.05	0.0545	0.0256	-0.0144	-0.0490	0.0389	0.0087	-0.0273	-0.0593	0.0187	-0.0064	-0.0381	-0.0676	-0.0062	-0.0230	-0.0501	-0.0769
0.1	0.0646	0.0401	-0.0075	-0.0451	0.0680	0.0219	-0.0265	-0.0610	0.0520	0.0007	-0.0414	-0.0723	0.0172	-0.0250	-0.0575	-0.0843
0.2	0.0508	0.0543	0.0110	-0.0321	0.0735	0.0541	-0.0121	-0.0566	0.0810	0.0361	-0.0348	-0.0750	0.0700	-0.0009	-0.0616	-0.0943
0.3	0.0375	0.0515	0.0252	-0.0168	0.0596	0.0656	0.0086	-0.0445	0.0742	0.0610	-0.0165	-0.0687	0.0843	0.0319	-0.0529	-0.0966
0.4	0.0285	0.0442	0.0327	-0.0040	0.0479	0.0643	0.0257	-0.0291	0.0629	0.0696	0.0041	-0.0563	0.0809	0.0553	-0.0366	-0.0920
0.5	0.0226	0.0373	0.0349	0.0053	0.0393	0.0588	0.0366	-0.0143	0.0531	0.0693	0.0212	-0.0414	0.0732	0.0677	-0.0181	-0.0826
0.6	0.0184	0.0317	0.0343	0.0115	0.0329	0.0526	0.0422	-0.0079	0.0454	0.0655	0.0334	-0.0266	0.0652	0.0726	-0.0008	-0.0705
0.7	0.0154	0.0272	0.0324	0.0149	0.0281	0.0468	0.0444	0.0075	0.0394	0.0606	0.0411	-0.0135	0.0581	0.0730	0.0139	-0.0573
0.8	0.0131	0.0235	0.0298	0.0167	0.0243	0.0418	0.0444	0.0142	0.0345	0.0556	0.0454	-0.0026	0.0521	0.0712	0.0254	-0.0443
0.9	0.0113	0.0205	0.0271	0.0174	0.0213	0.0374	0.0431	0.0187	0.0306	0.0509	0.0474	0.0060	0.0469	0.0682	0.0341	-0.0322
1.0	0.0098	0.0179	0.0248	0.0173	0.0189	0.0336	0.0412	0.0215	0.0273	0.0466	0.0478	0.0125	0.0425	0.0647	0.0404	-0.0214
1.25	0.0071	0.0133	0.0195	0.0155	0.0144	0.0262	0.0355	0.0241	0.0213	0.0376	0.0452	0.0220	0.0341	0.0558	0.0483	-0.0005
1.5	0.0054	0.0102	0.0154	0.0131	0.0114	0.0209	0.0300	0.0233	0.0171	0.0309	0.0406	0.0255	0.0281	0.0481	0.0499	0.0128
1.75	0.0042	0.0079	0.0123	0.0110	0.0092	0.0170	0.0254	0.0213	0.0140	0.0257	0.0358	0.0258	0.0236	0.0414	0.0480	0.0204
2	0.0034	0.0063	0.0099	0.0090	0.0075	0.0141	0.0216	0.0191	0.0117	0.0217	0.0315	0.0248	0.0201	0.0360	0.0450	0.0243
2.5	0.0022	0.0042	0.0067	0.0063	0.0053	0.0101	0.0159	0.0150	0.0086	0.0161	0.0244	0.0214	0.0152	0.0278	0.0381	0.0264
3	0.0016	0.0030	0.0048	0.0045	0.0040	0.0076	0.0122	0.0119	0.0065	0.0124	0.0193	0.0179	0.0119	0.0220	0.0319	0.0252
3.5	0.0012	0.0022	0.0035	0.0033	0.0031	0.0058	0.0095	0.0095	0.0052	0.0098	0.0156	0.0151	0.0096	0.0179	0.0269	0.0230
4	0.0009	0.0017	0.0027	0.0026	0.0024	0.0047	0.0076	0.0078	0.0042	0.0080	0.0128	0.0128	0.0080	0.0149	0.0229	0.0207
4.5	0.0007	0.0013	0.0021	0.0020	0.0020	0.0039	0.0062	0.0065	0.0034	0.0066	0.0107	0.0108	0.0066	0.0126	0.0197	0.0185
5	0.0006	0.0011	0.0017	0.0016	0.0017	0.0032	0.0052	0.0055	0.0029	0.0056	0.0091	0.0094	0.0057	0.0108	0.0172	0.0165
10	0.0001	0.0003	0.0004	0.0004	0.0005	0.0009	0.0015	0.0016	0.0009	0.0017	0.0028	0.0031	0.0019	0.0036	0.0060	0.0065

SYMBOLS

c	wing chord
$c(y)$	local wing chord
$K^{(1)}(x,\theta)$	see equation (10)
$\bar{K}^{(1)}(x)$	see equation (11)
$\bar{K}^{(n)}(x)$	see equation (13)
Q	strength of single infinite source line
$q(x,\theta)$	strength of source distribution on the fuselage related to a single source line with triple kink in the plane $z = 0$
$q^{(0)}(x,\theta)$	first approximation to $q(x,\theta)$, see equation (6)
$q^{(1)}(x,\theta)$	second approximation to $q(x,\theta)$, see equations (8) to (10)
$\bar{q}(x)$	mean value of source strength $q(x,\theta)$ at a station x , see equation (15)
$q_f(x,\theta)$	strength of source distribution on the fuselage related to the source distribution in the plane $z = 0$
$q_w(x,y)$	strength of source distribution in the wing plane representing the wing attached to an infinite reflection plate
$q_w^{(1)}(x,y)$	source distribution in first-order theory
$q_w^{(2)}(x,y)$	source distribution in second-order theory
$q_{ws}^{(2)}$, $q_{wJ}^{(2)}$	see equations (47) and (48)
$\Delta q(x,y)$	interference term of source distribution in the plane $z = 0$, which cancels the velocity $\Delta v_z^{(1)}(x,y,z_t)$, see equation (51)
R	radius of fuselage
t/c	thickness-to-chord ratio
x,y,z	rectangular coordinate system, x along the axis of the fuselage
x,r,θ	system of cylindrical coordinates
$z_t(\xi)$	section shape
$\theta_J(x)$	$= \sin^{-1}\left(\frac{c}{R}\frac{z_t(x)}{c}\right)$
ξ	$= x - (\lvert y\rvert - R)\tan\phi$
ϕ	angle of sweep
ϕ_{LE}	sweep of leading edge
V_0	free stream velocity, taken as unity
$\underline{v}$	perturbation velocity
$\underline{v}_{\wedge\wedge}$	velocity induced by single source line with three kinks, see equation (A-1)

SYMBOLS (concluded)

$\underline{v}_{\Lambda}$	velocity induced by single source line with one kink
$\underline{v}_{q}$	velocity induced by source distribution on fuselage, $q(x,\theta)$
$\underline{v}_{I}$	$= \underline{v}_{q} + \underline{v}_{\wedge\wedge} - \underline{v}_{\Lambda}$, interference velocity, related to single source line
$\underline{v}_{w}$	velocity field past the wing attached to an infinite reflection plate
v_x, v_y, v_z	components of perturbation velocity
v_n	velocity component normal to the surface of the fuselage
v_{nQ}	normal velocity induced by single source line with three kinks, $= v_{n\wedge\wedge}$
$\bar{v}_n(x)$	mean value of $v_n(x,\theta)$
v_θ	circumferential velocity component at the surface of the fuselage
v_{xB}	streamwise velocity on isolated fuselage
$v_{xw}^{(1)}$	streamwise velocity component in the flow past the wing attached to an infinite reflection plate according to first-order theory
$v_{xw}^{(2)}$	v_{xw} according to second-order theory
$\Delta\underline{v}$	difference between the velocity field past the wing-fuselage combination and the velocity field past the wing attached to an infinite reflection plate
$\Delta v_x^{(1)}$, $\Delta v_z^{(1)}$	interference velocity components derived from the source distribution $q_w^{(1)}$
$\Delta v_x^{(2)}$	interference velocity derived from the source distribution $q_{ws}^{(2)}$
Δv_{xJ}, Δv_{zJ}	interference velocity components in the wing-body junction
Δv_x^*	streamwise velocity induced by line source distribution in $y = R$, $z = 0$ for which $\Delta v_z^*(x,y = R,z_t) = -\Delta v_{zJ}^{(1)}(x)$
Δv_x^{**}	interference velocity according to the 'source method' of Ref.11, multiplied by factor $\cos\phi$

REFERENCES

No.	Author	Title, etc.
1	J. Weber M.G. Joyce	Interference problems on wing-fuselage combinations. Part II: Symmetrical unswept wing at zero incidence attached to a cylindrical fuselage at zero incidence in midwing position. RAE Technical Report 71179 (ARC 33437) (1971)
2	J.A. Ledger	Computation of the velocity field induced by a planar source distribution, approximating a symmetrical non-lifting wing in subsonic flow. ARC R & M 3751 (1972)
3	C.C.L. Sells	Iterative solution for thick symmetrical wings at incidence in incompressible flow. RAE Technical Report 73047 (ARC 34959) (1973)
4	J. Weber	Interference problems on wing-fuselage combinations. Part I: Lifting unswept wing attached to a cylindrical fuselage at zero incidence in midwing position. RAE Technical Report 69130 (ARC 31532) (1969)
5	J. Weber	Second-order small-perturbation theory for finite wings in incompressible flow. ARC R & M 3759 (1972)
6	-	Method for predicting the pressure distribution on swept wings with subsonic attached flow. Roy. Aero. Soc. Trans. Data Memo. 6312 (1963). (Revised version to be issued as TDM 73012)
7	J.L. Hess A.M.O. Smith	Calculation of potential flow about arbitrary bodies. Progress in Aeron. Sci., Vol.8 (1967)
8	A. Roberts K. Rundle	Computation of incompressible flow about bodies and thick wings using the spline mode system. BAC, Weybridge, Ma Report 19 (1972) ARC 33775
9	A. Roberts K. Rundle	The computation of first order compressible flow about wing-body combinations. BAC Ma Report 20 (1973)

REFERENCES (concluded)

No.	Author	Title, etc.
10	J.W. Craggs K.W. Mangler	Some remarks on the behaviour of surface source distributions near the edge of a body. Aeron. Quarterly, 24, 25 (1973) RAE Technical Report 71085 (ARC 33185) (1971)
11	D. Küchemann J. Weber	The subsonic flow past swept wings at zero lift without and with body. ARC R & M 2908 (1953)
12	D.A. Treadgold	RAE paper, unpublished

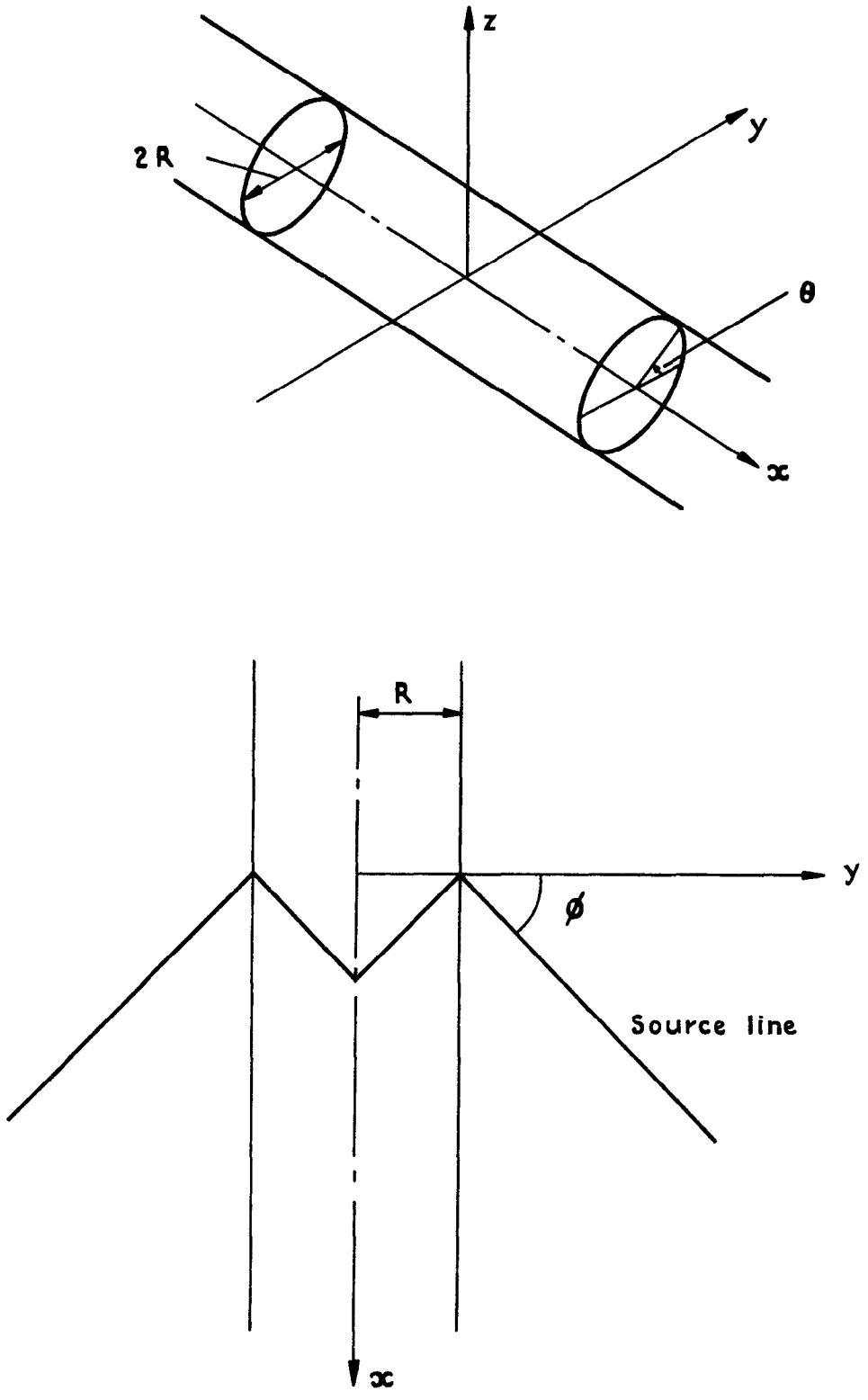

Fig. 1 Notation

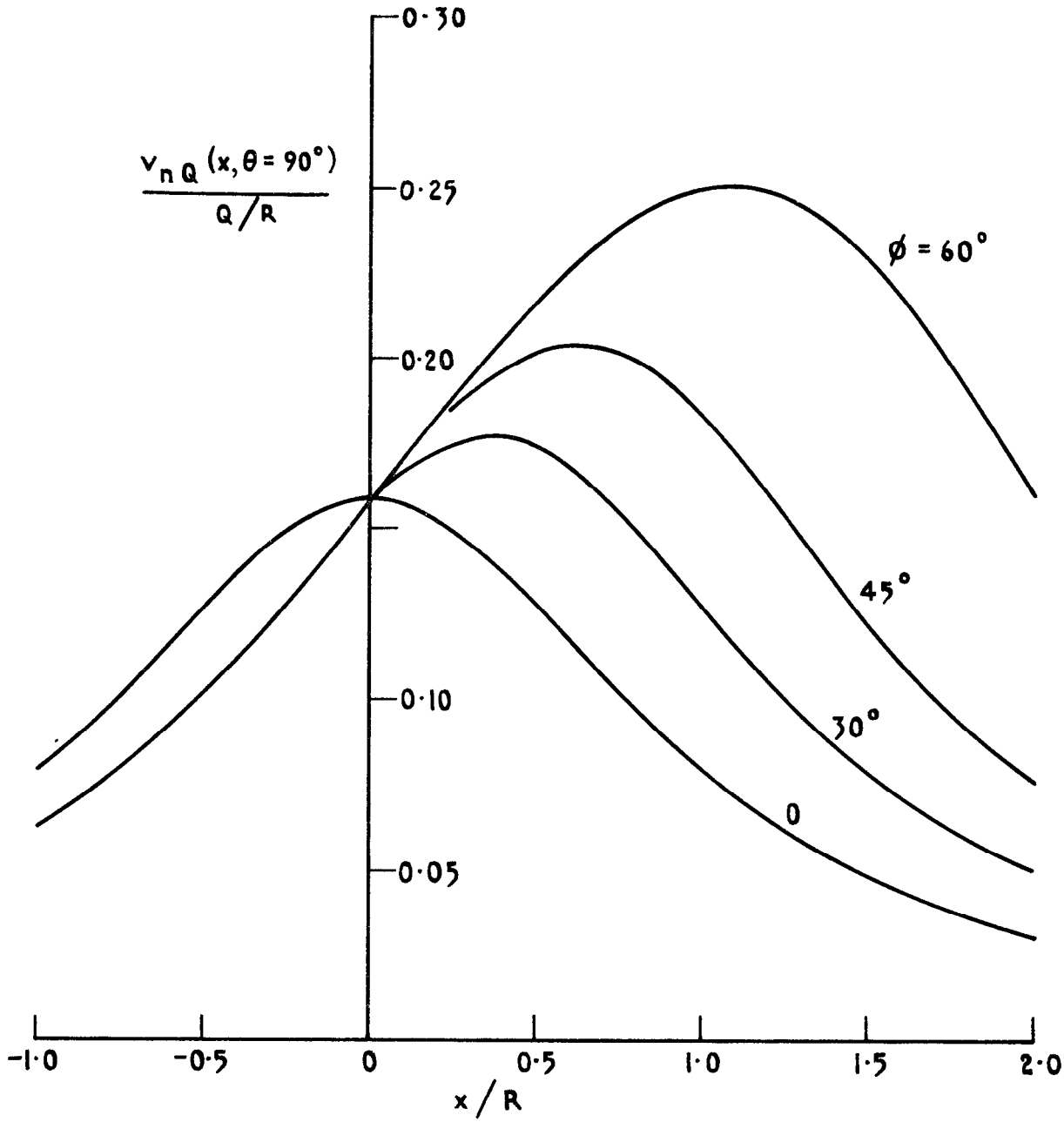

Fig. 2 Normal velocity at the top of the fuselage induced by a swept source line

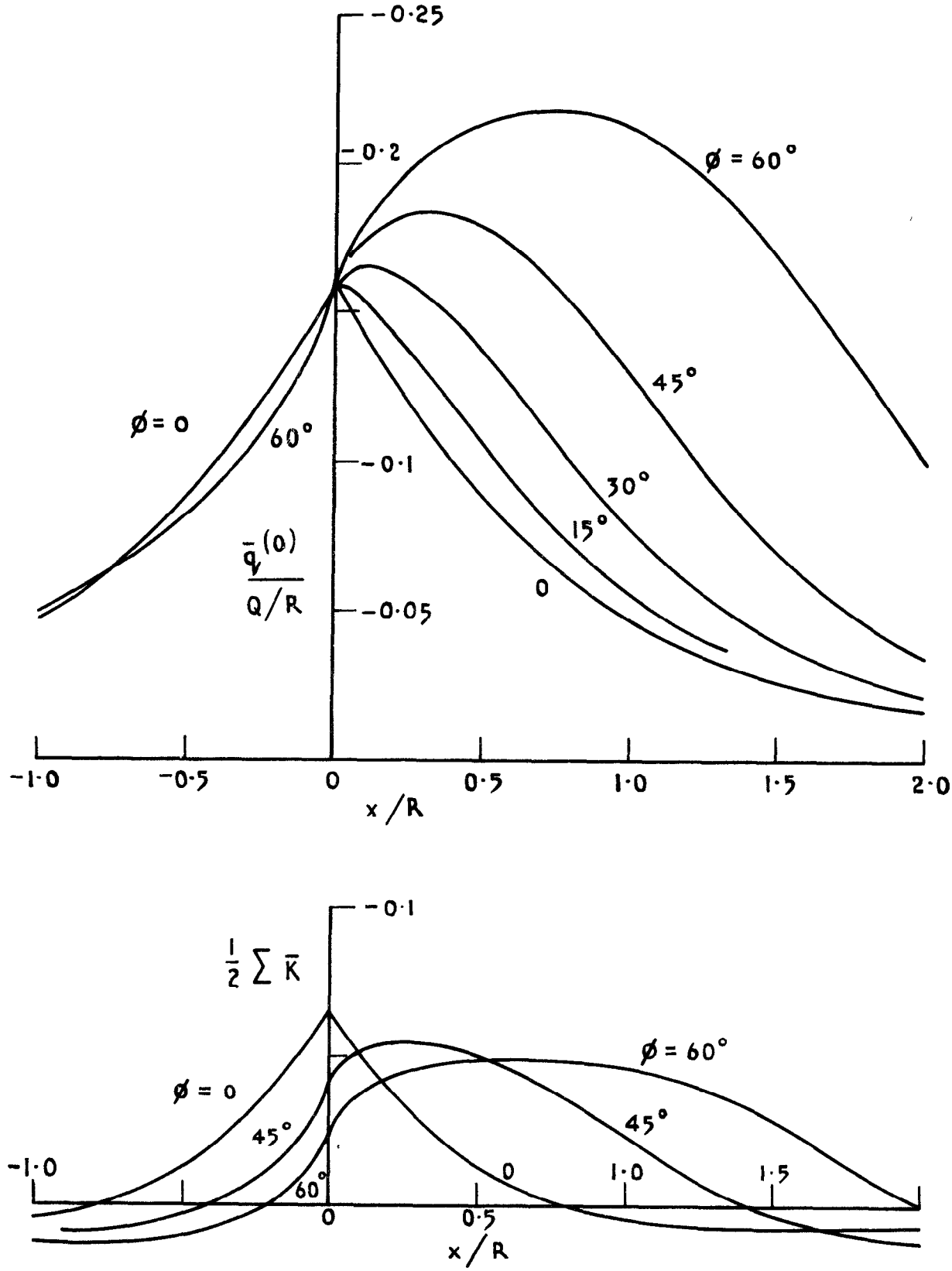

Fig. 3 Average strength of source distribution on fuselage

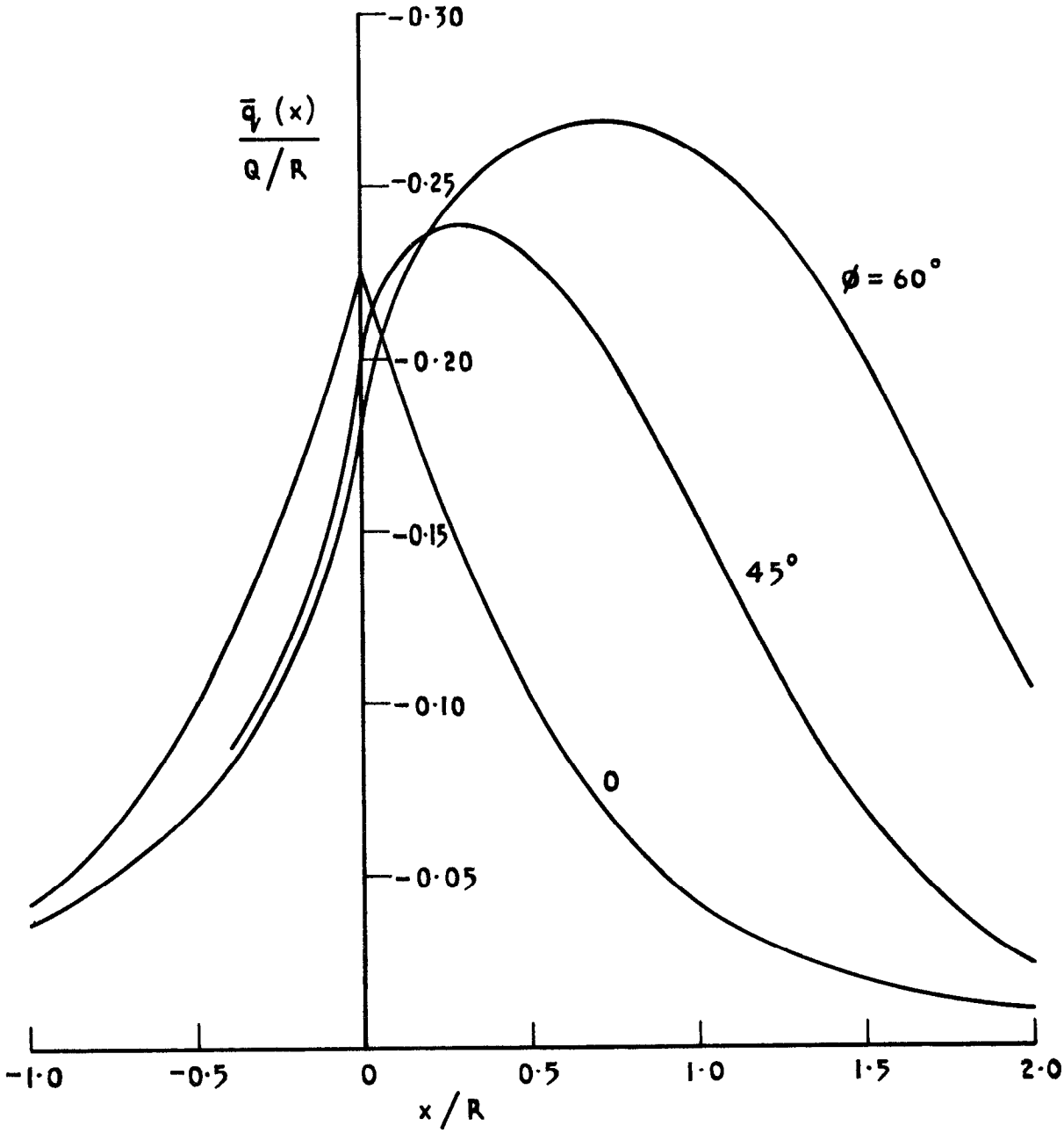

Fig. 4 Average strength of source distribution on fuselage

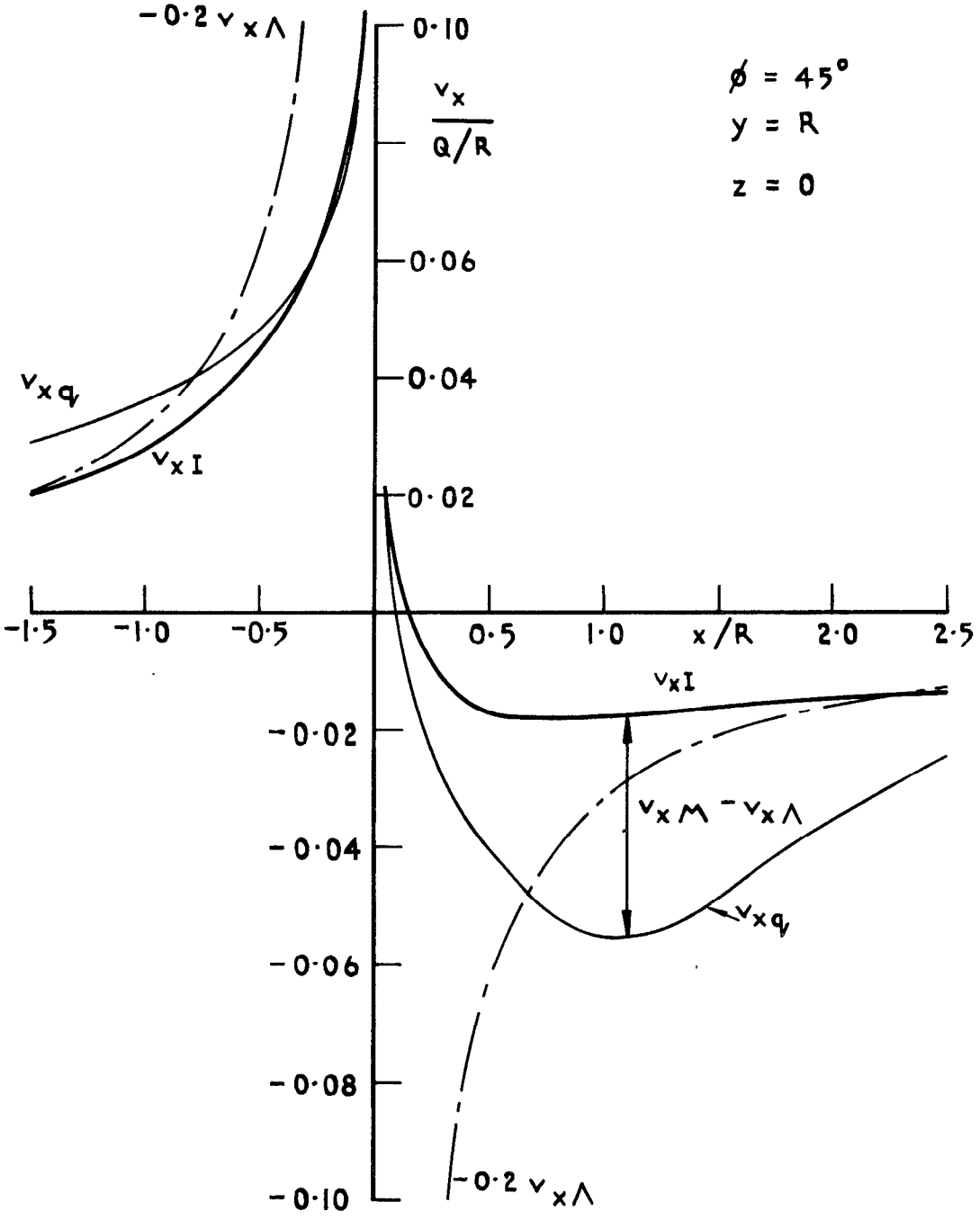

Fig. 5 Additional streamwise velocity in the wing-body junction

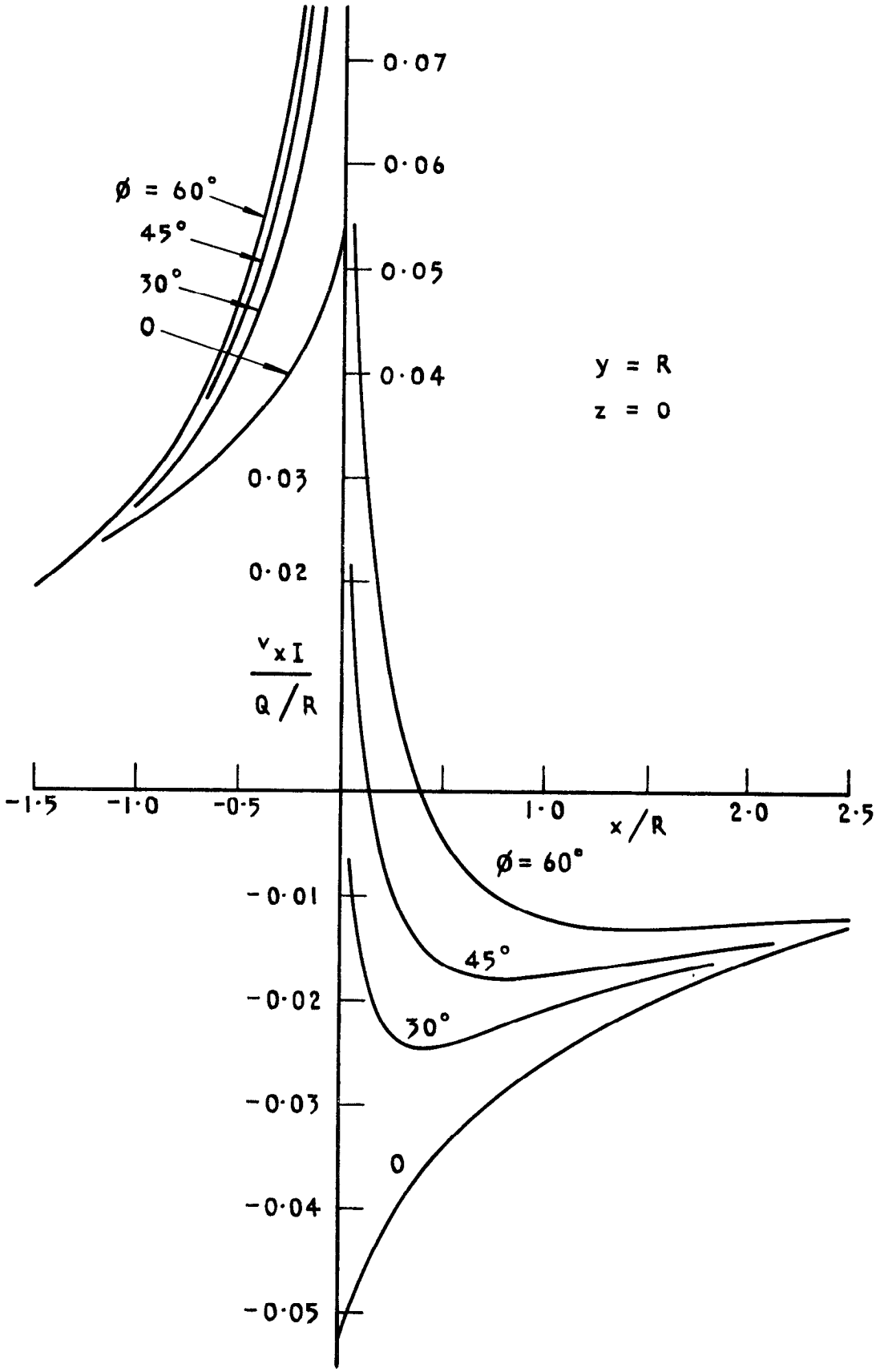

Fig. 6 Additional streamwise velocity in the wing-body junction

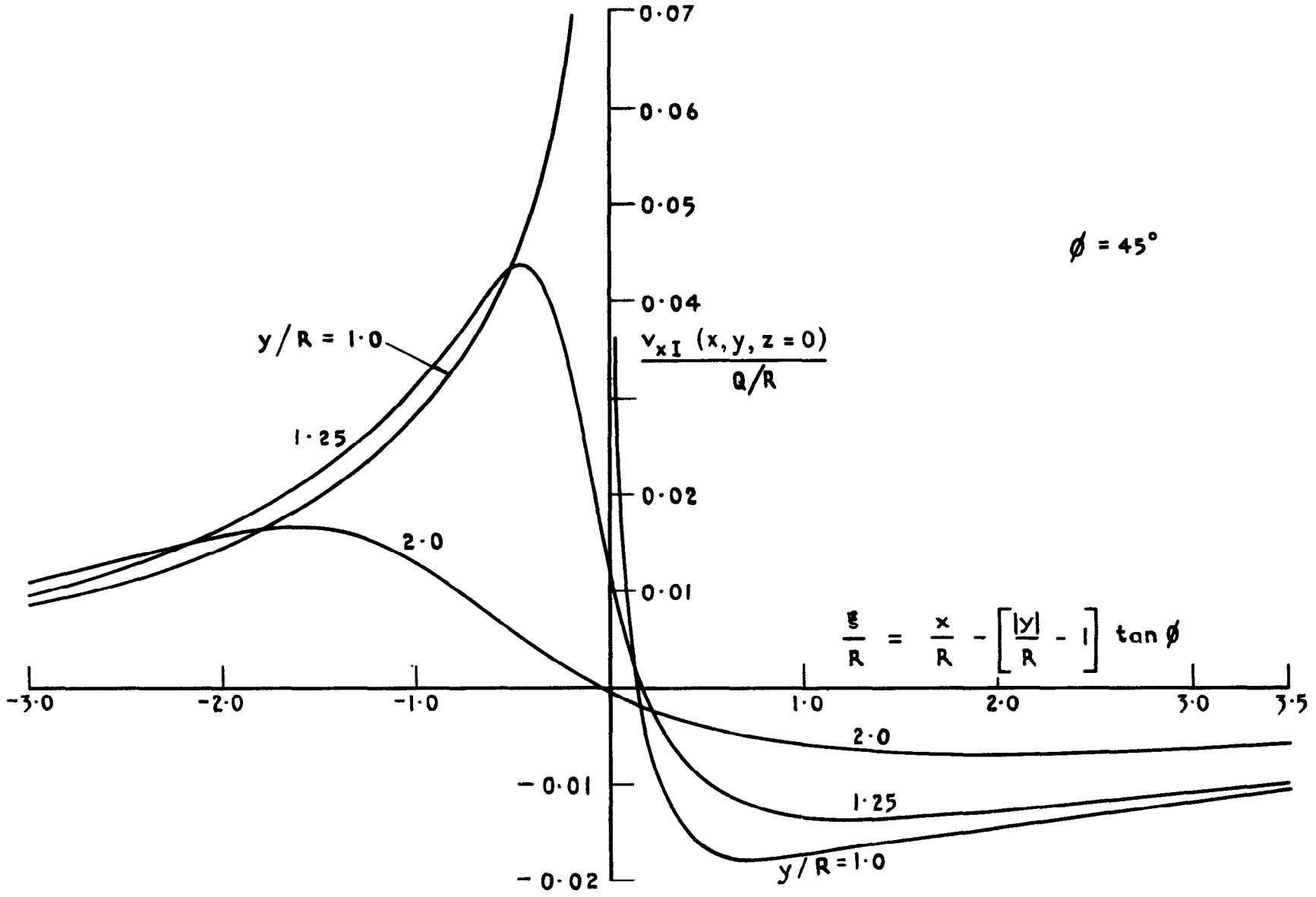

Fig. 7 Additional streamwise velocity in the plane z = O

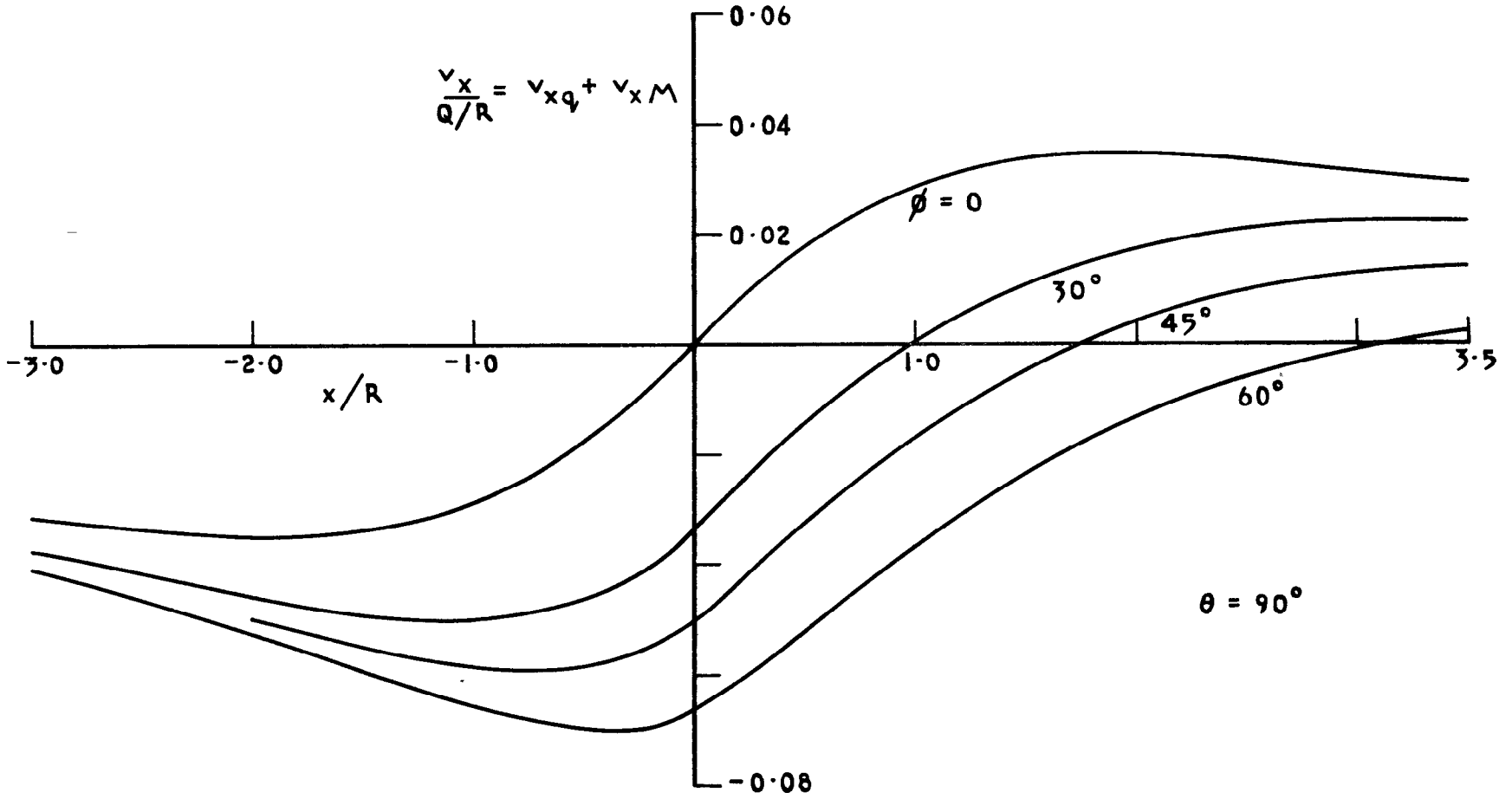

Fig. 8 Velocity on top of fuselage

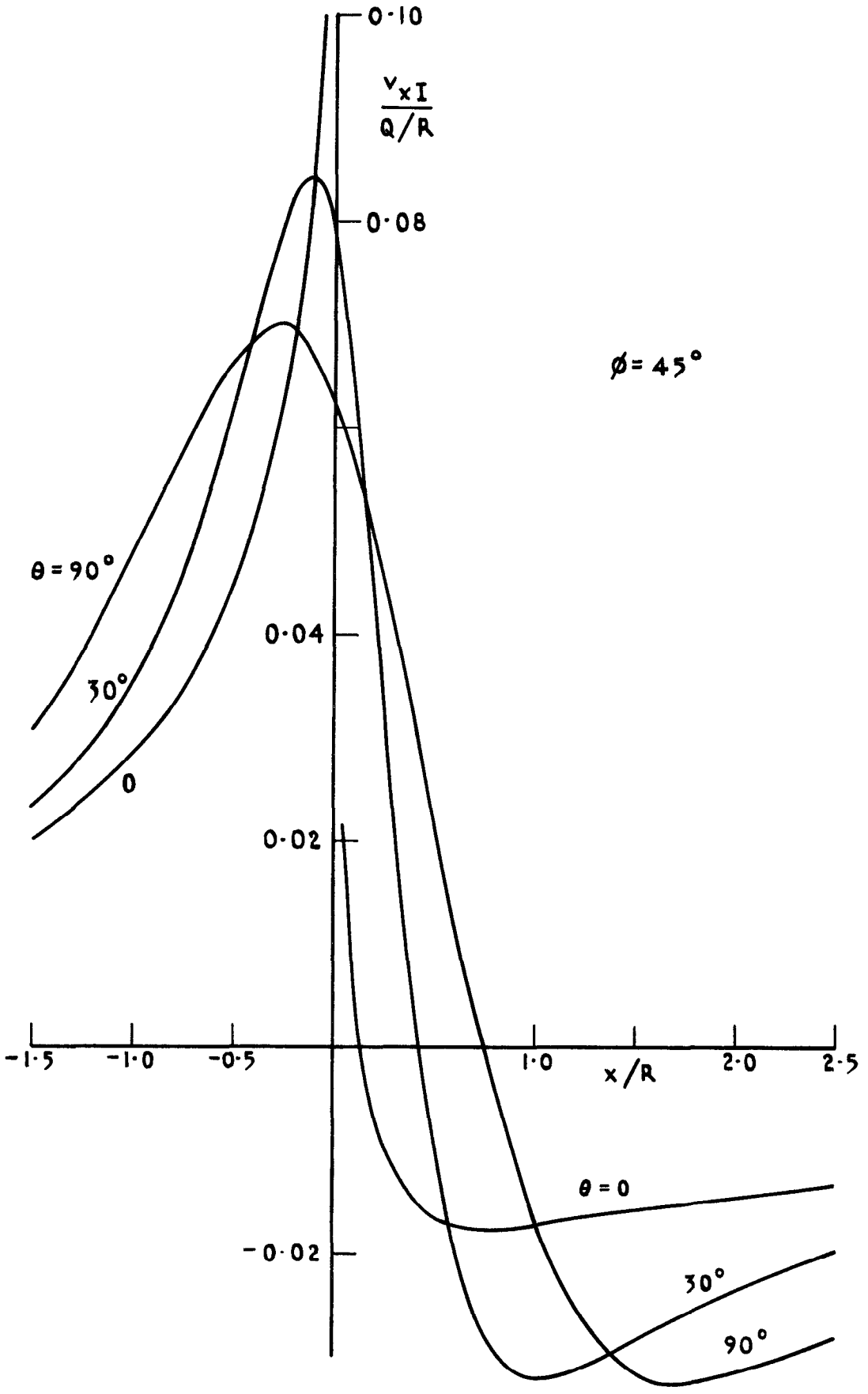

Fig. 9 Interference velocity on fuselage

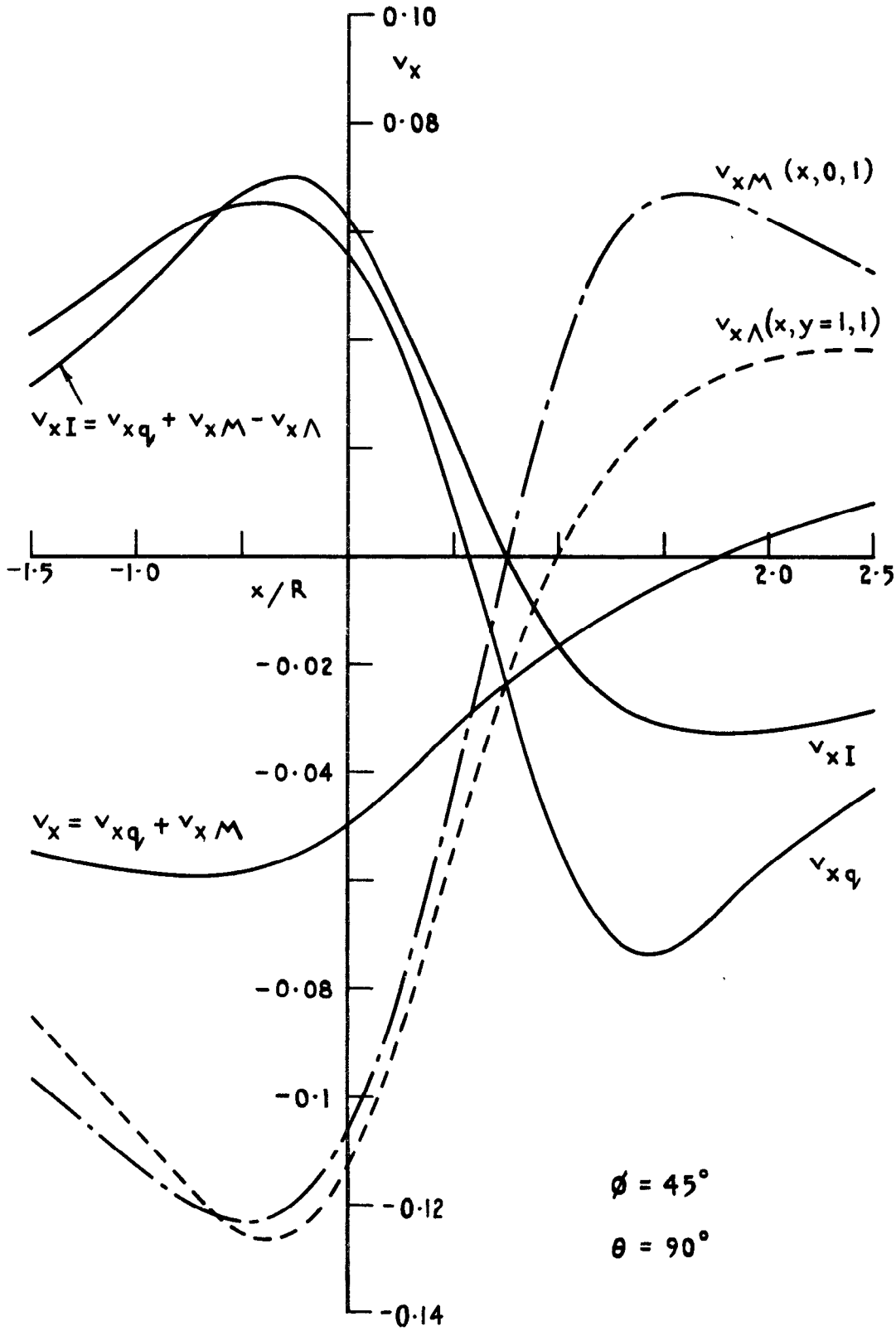

Fig. 10 Streamwise velocity on top of the fuselage

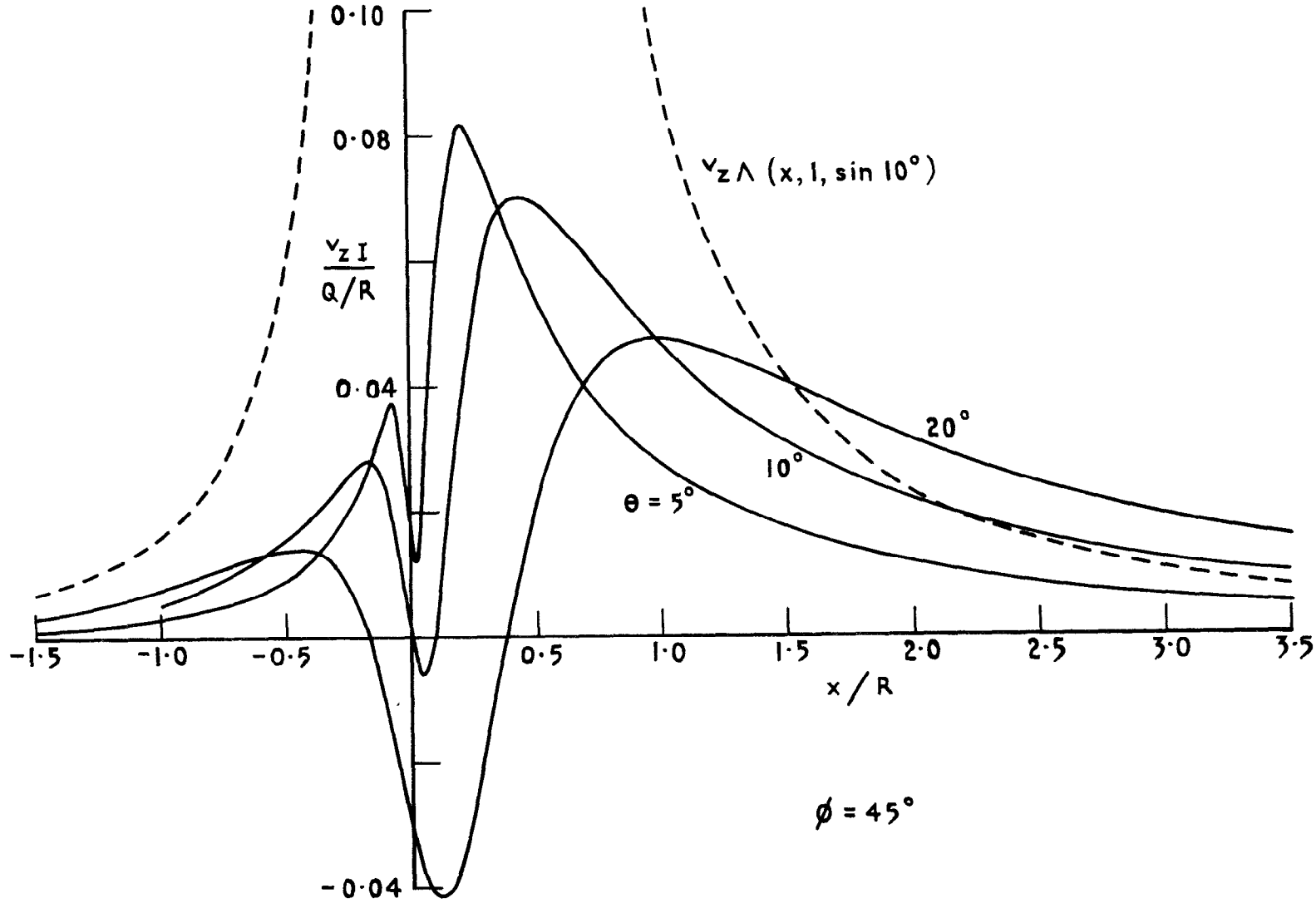

Fig. 11 z - component of the interference velocity at the fuselage

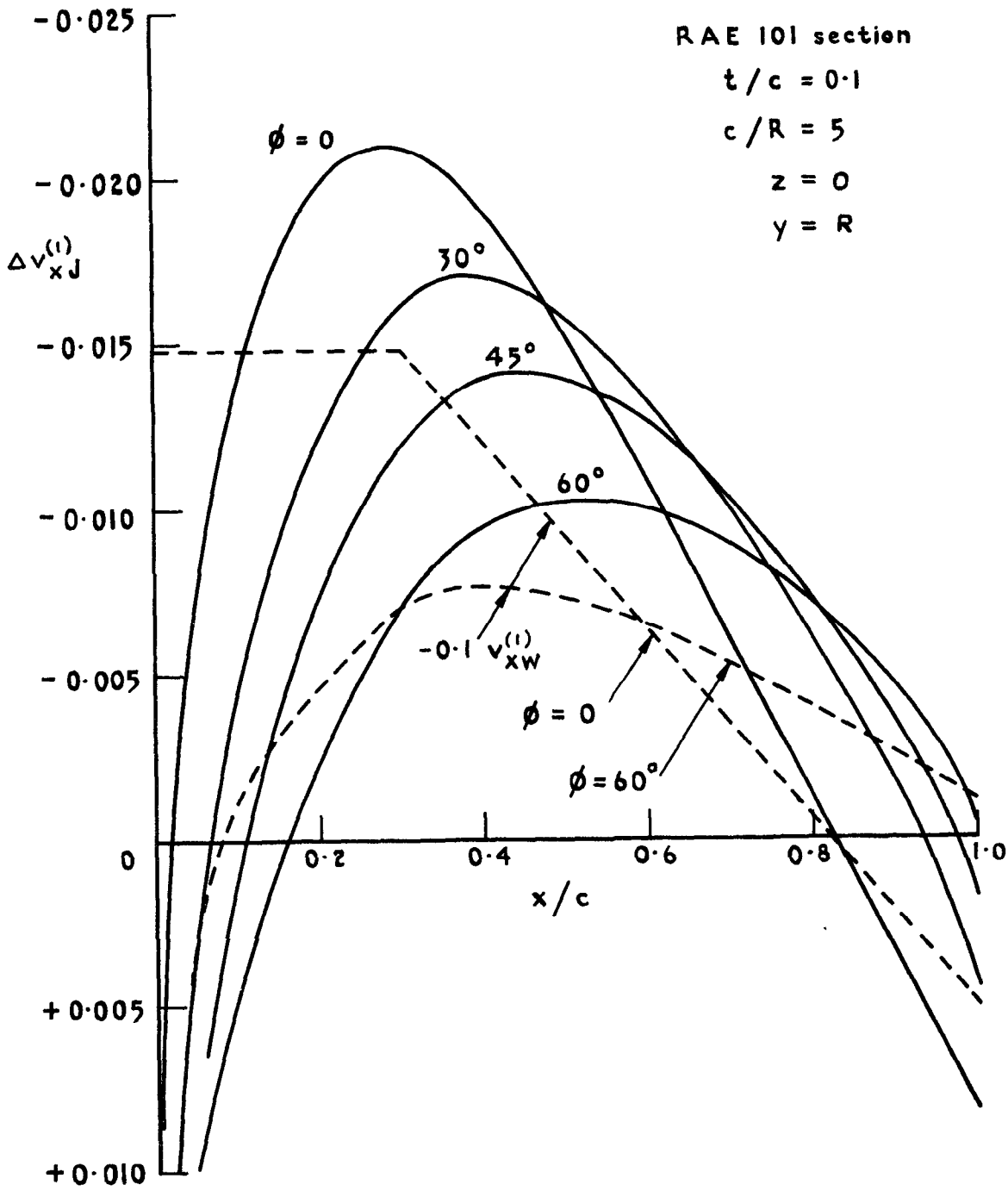

Fig. 12 Interference velocity in the wing-body junction according to first-order theory

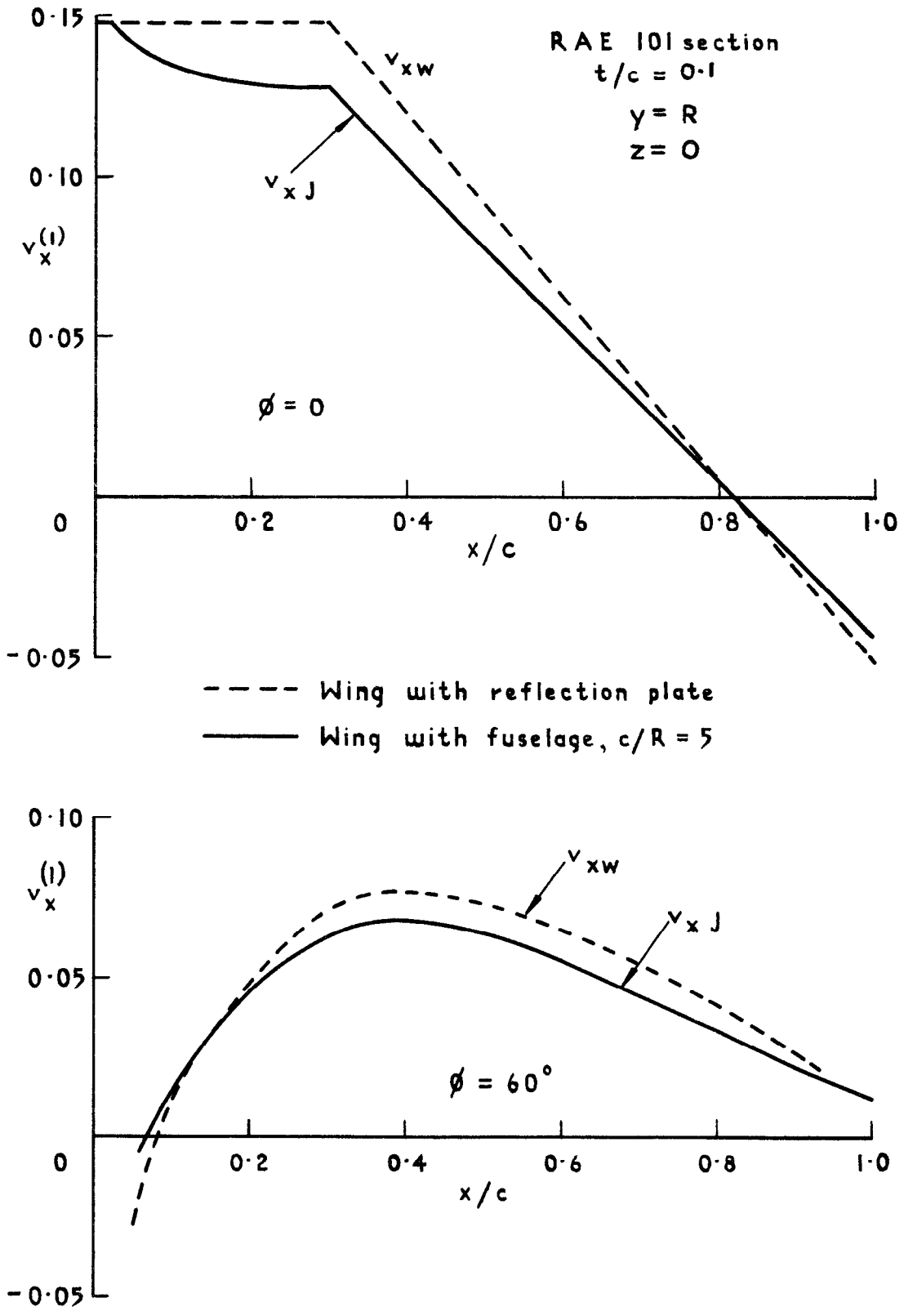

Fig.13 Velocity in wing-body junction

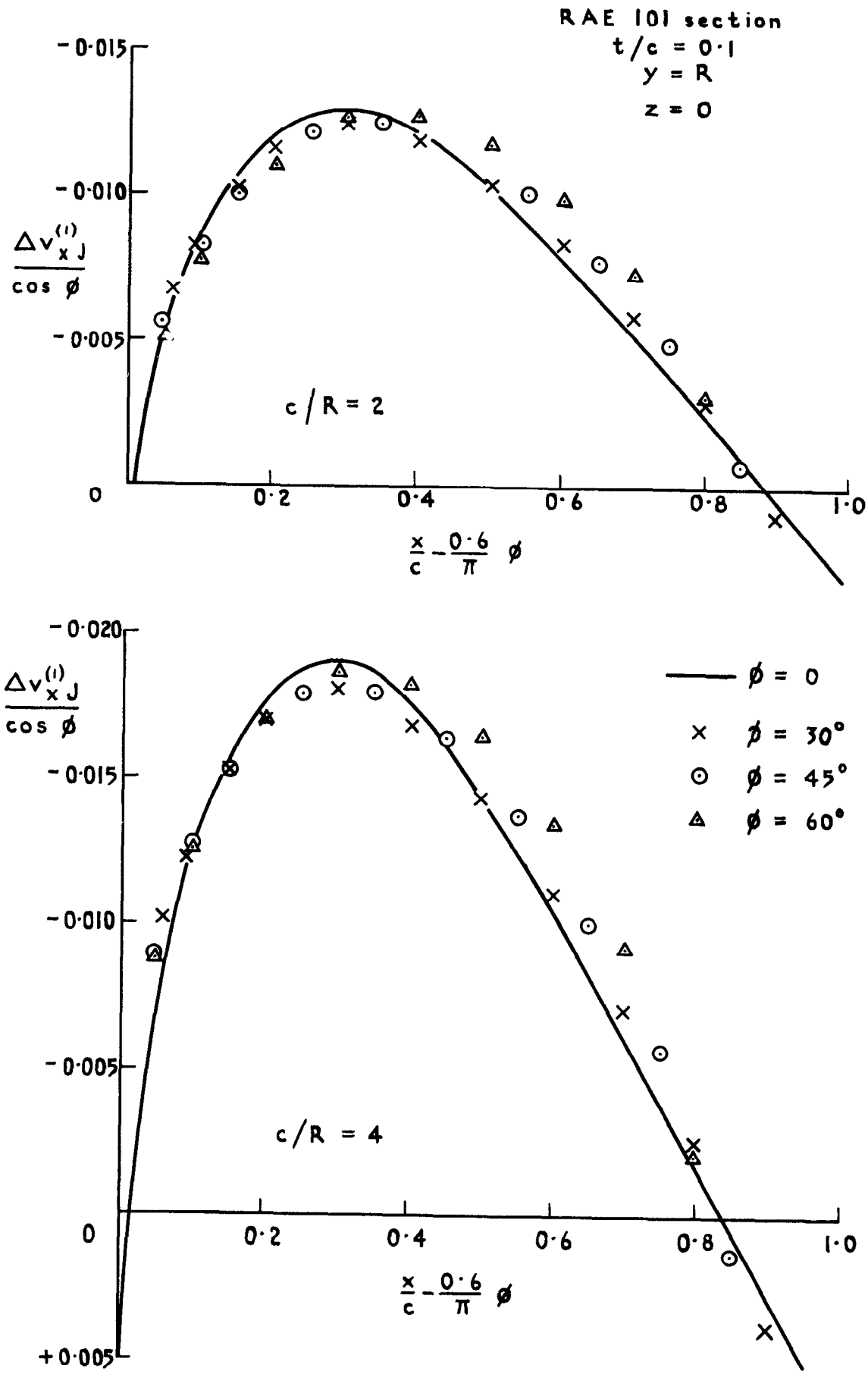

Fig. 14a Interference velocity in the wing-body junction

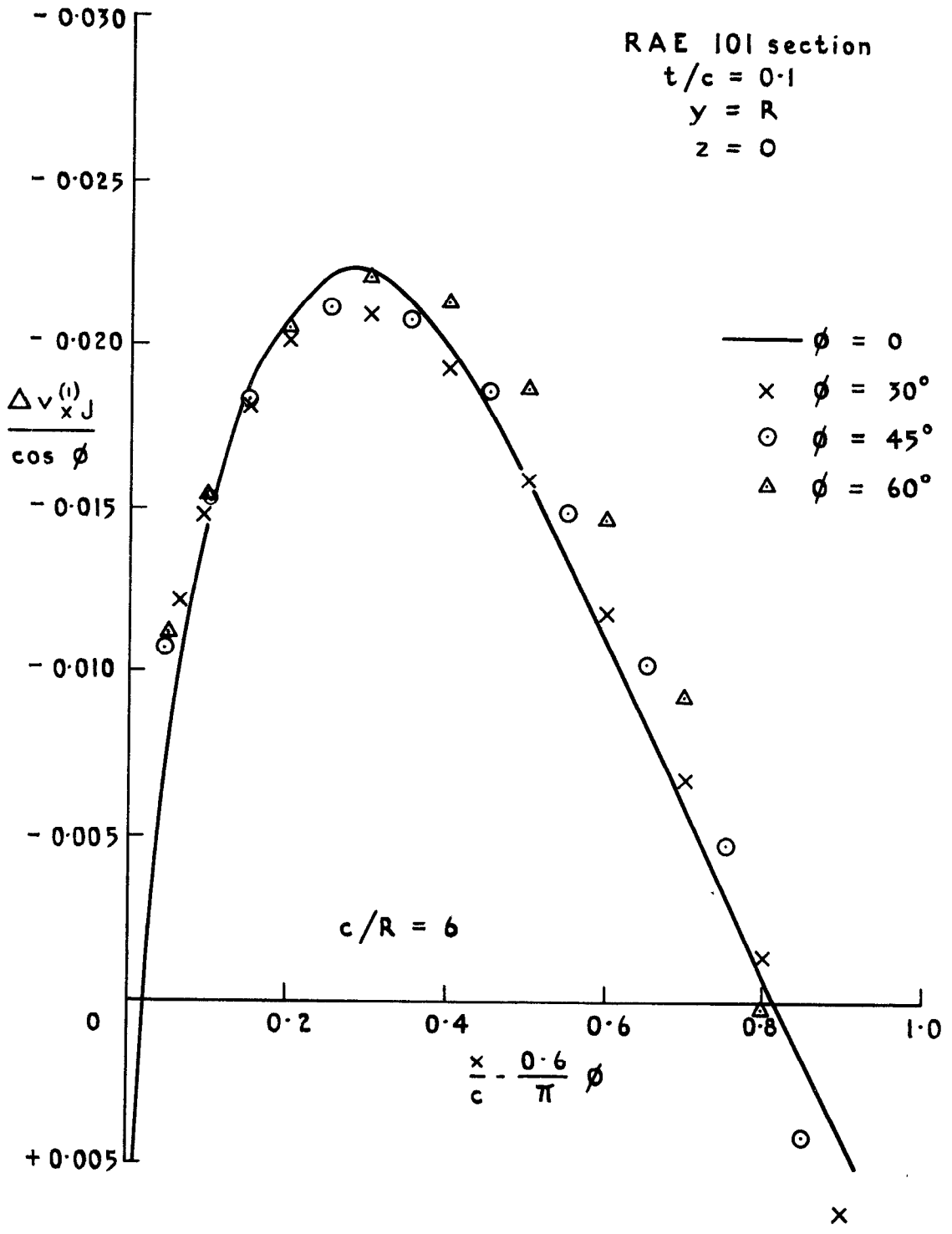

Fig. 14b Interference velocity in the wing - body junction

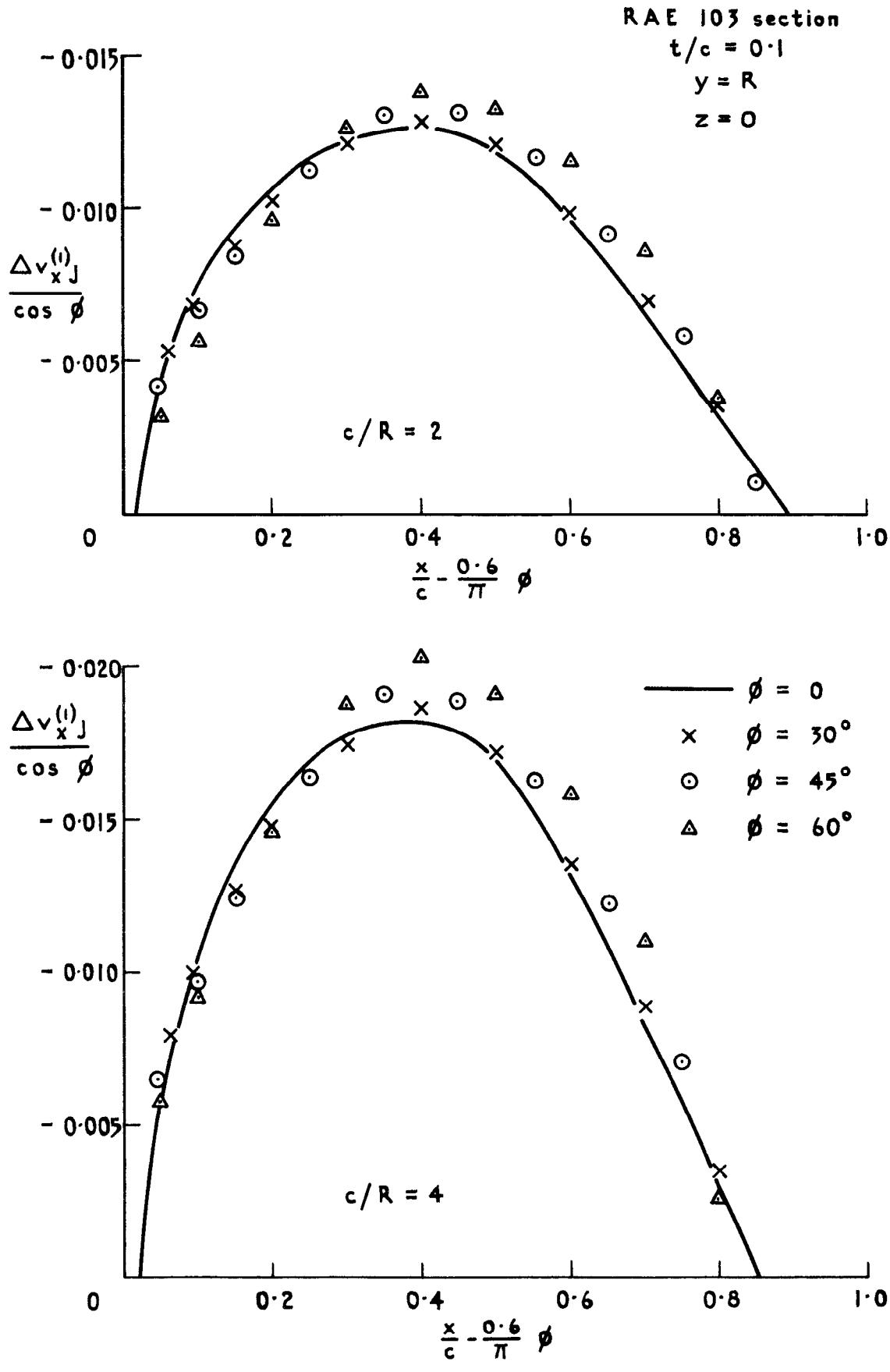

Fig. 15a Interference velocity in the wing-body junction

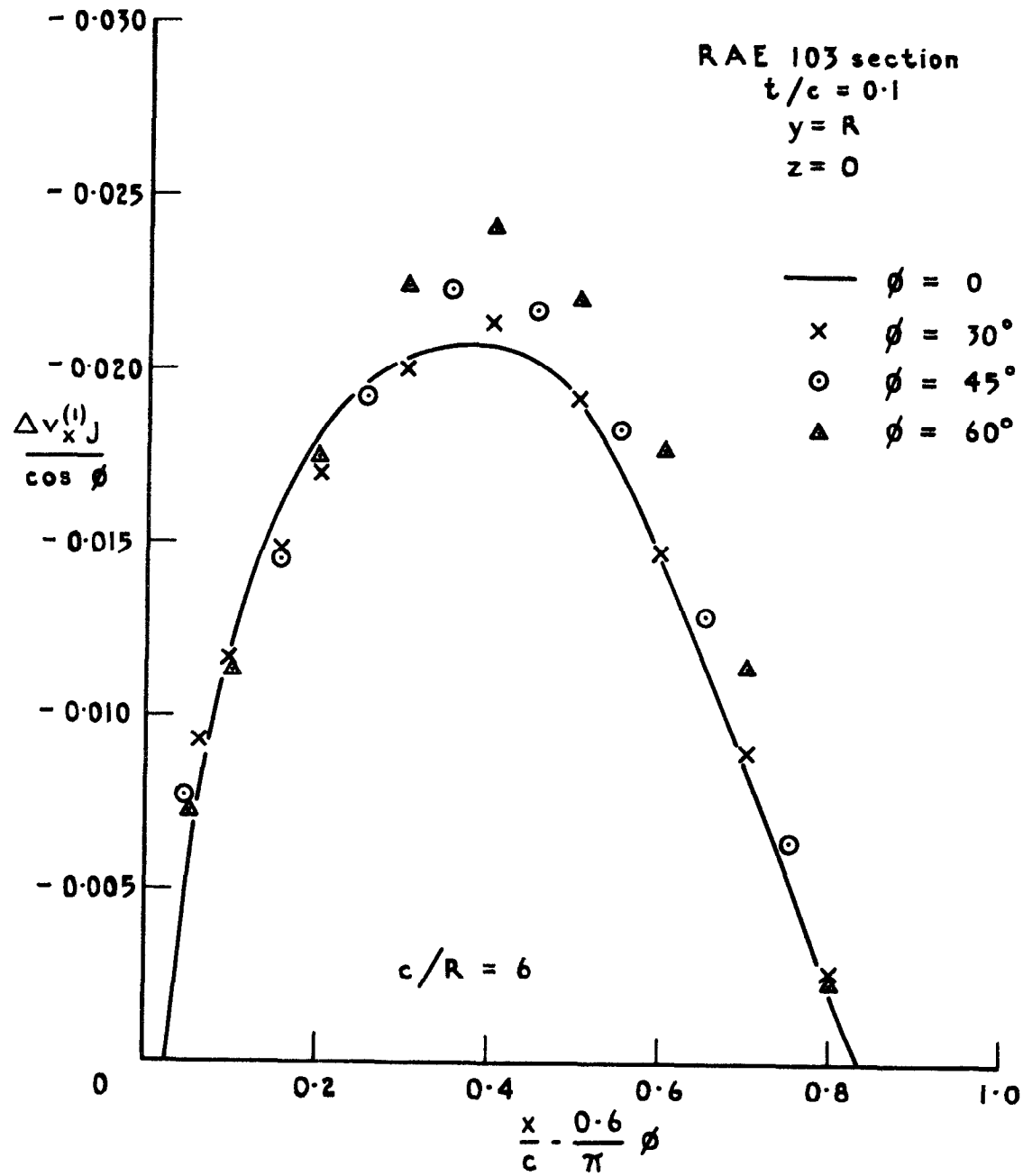

Fig. 15b Interference velocity in the wing-body junction

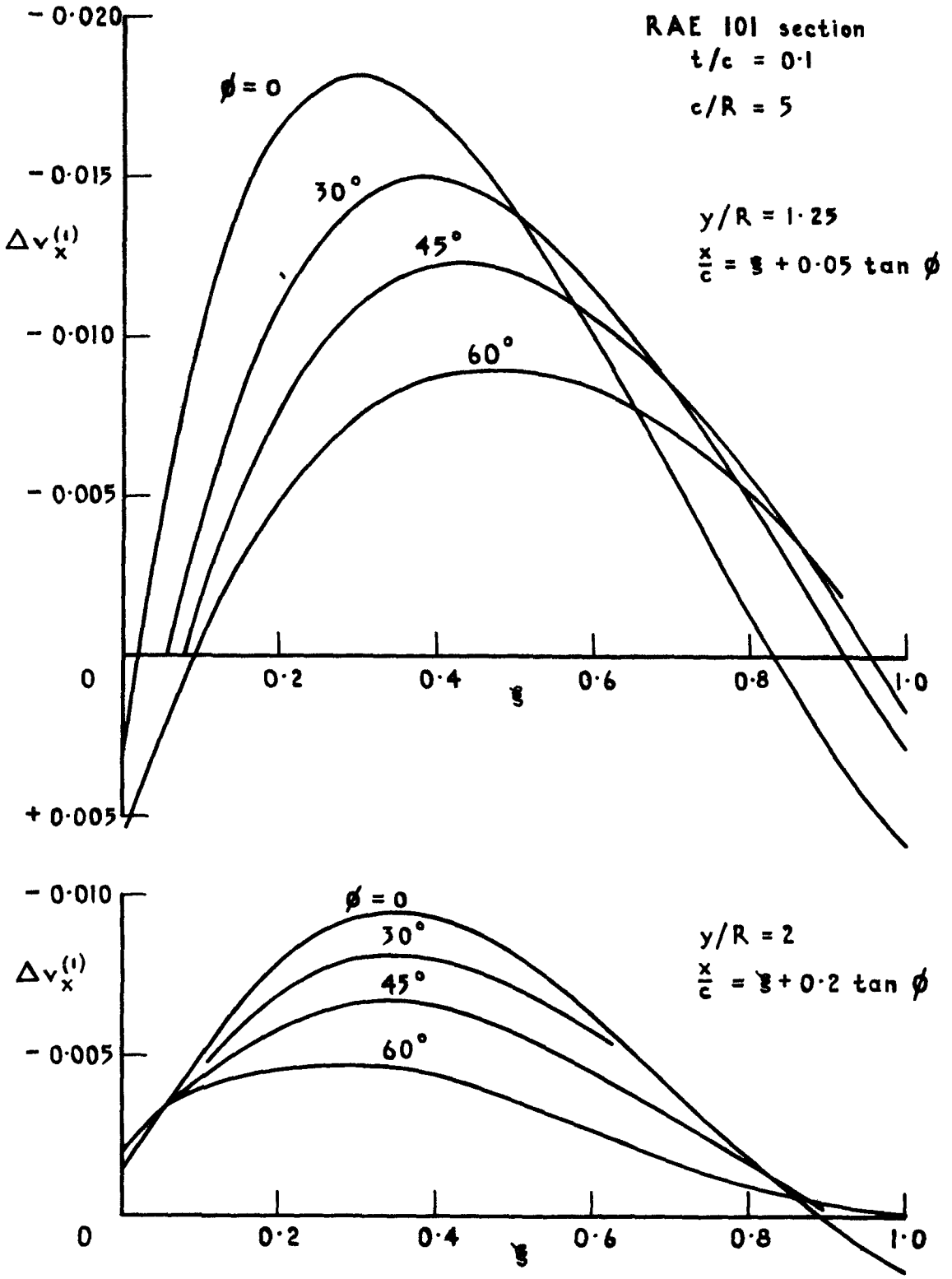

Fig. 16 Interference velocity in the plane of the wing

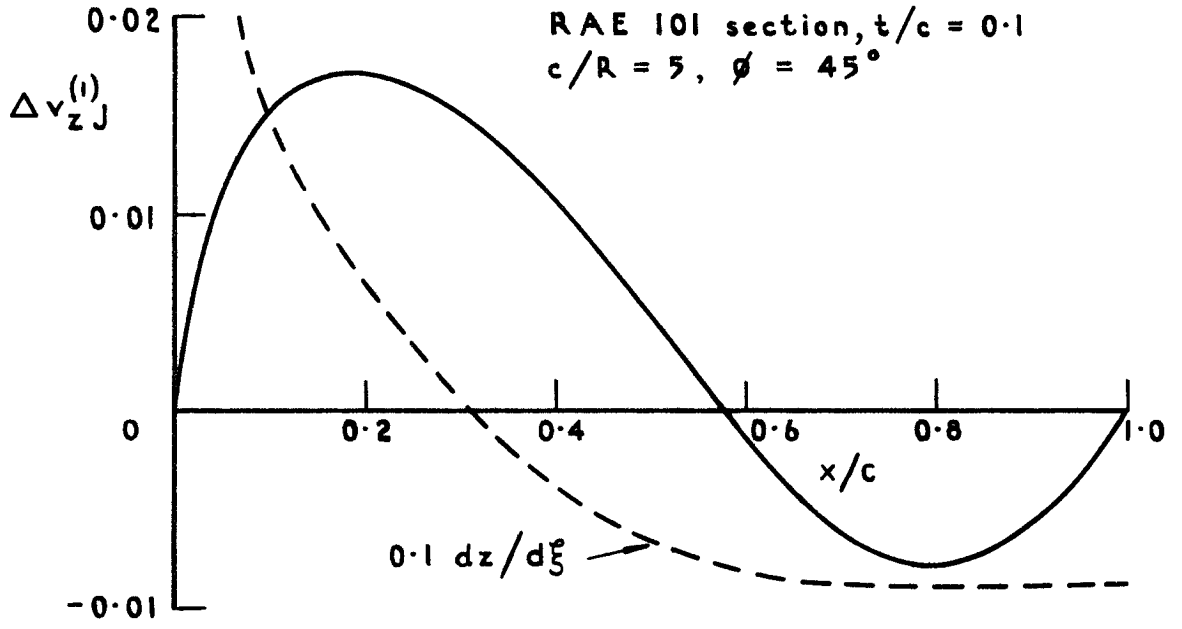

Fig. 17 Interference velocity $\Delta v_z (x, y_J, z_t)$ in the wing–body junction

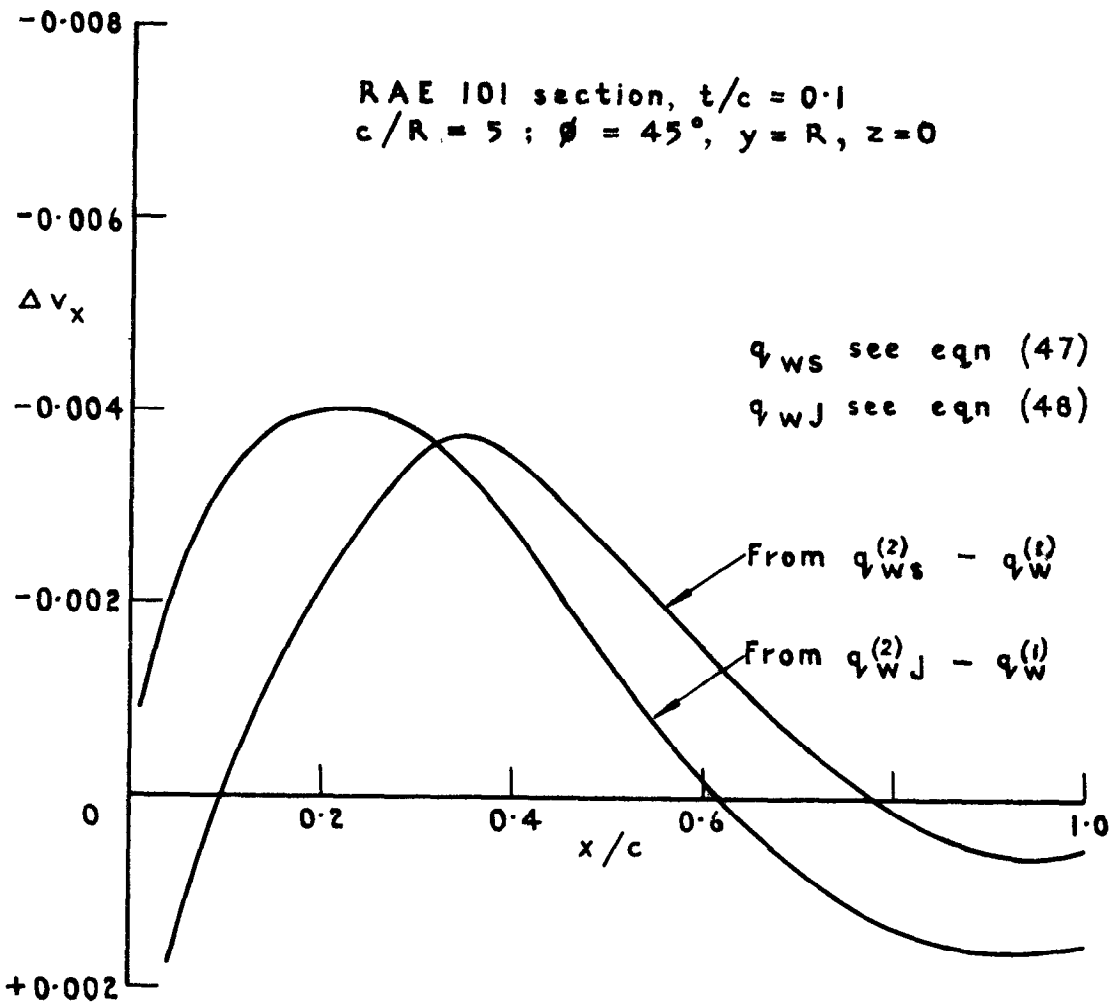

Fig. 18 Change of interference velocity in the wing-body junction due to $q_w^{(2)} - q_w^{(1)}$

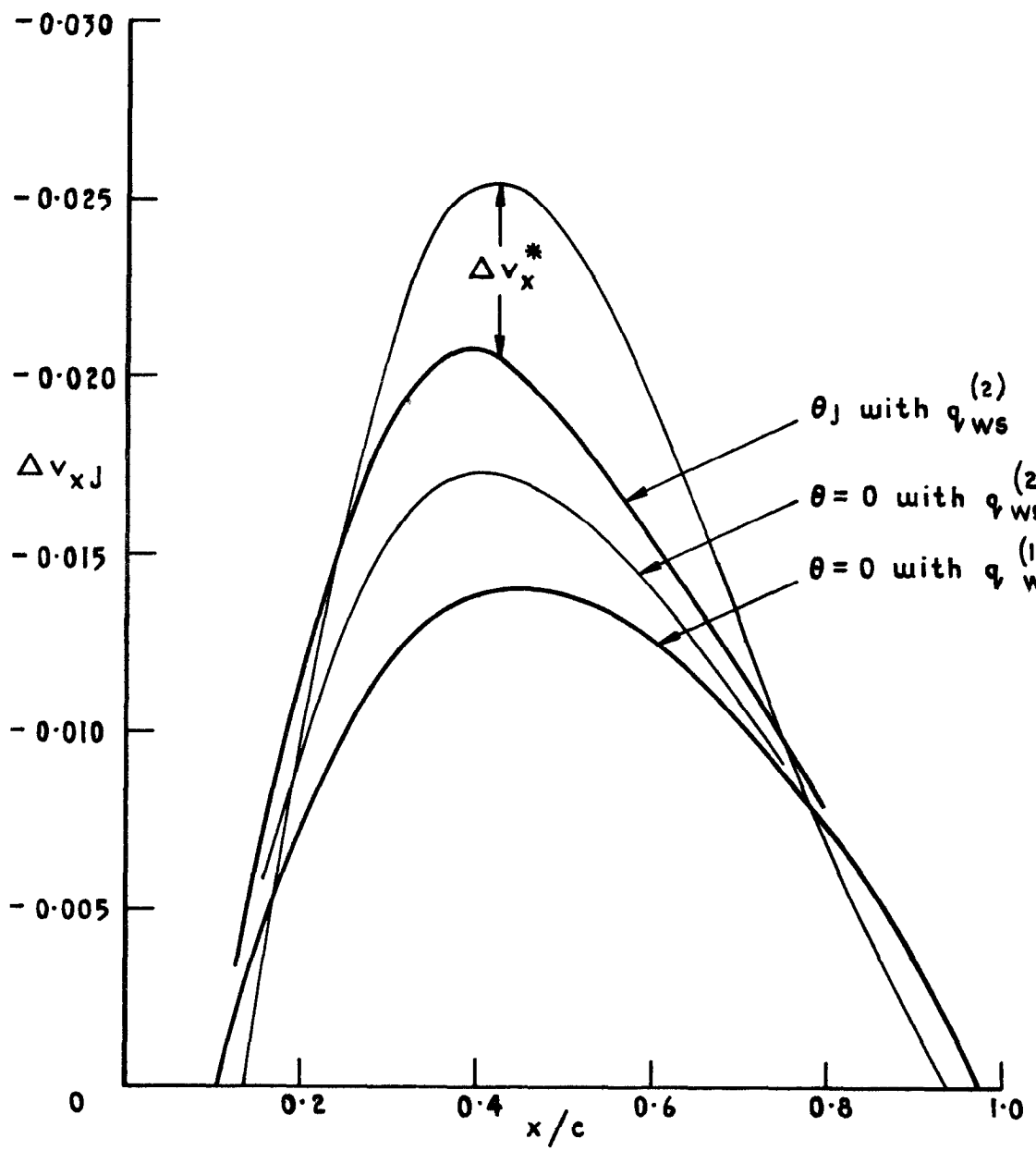

RAE 101 section, t/c = 0·1
$\phi = 45°$, c/R = 5

Fig. 19 Interference velocity in the wing - body junction

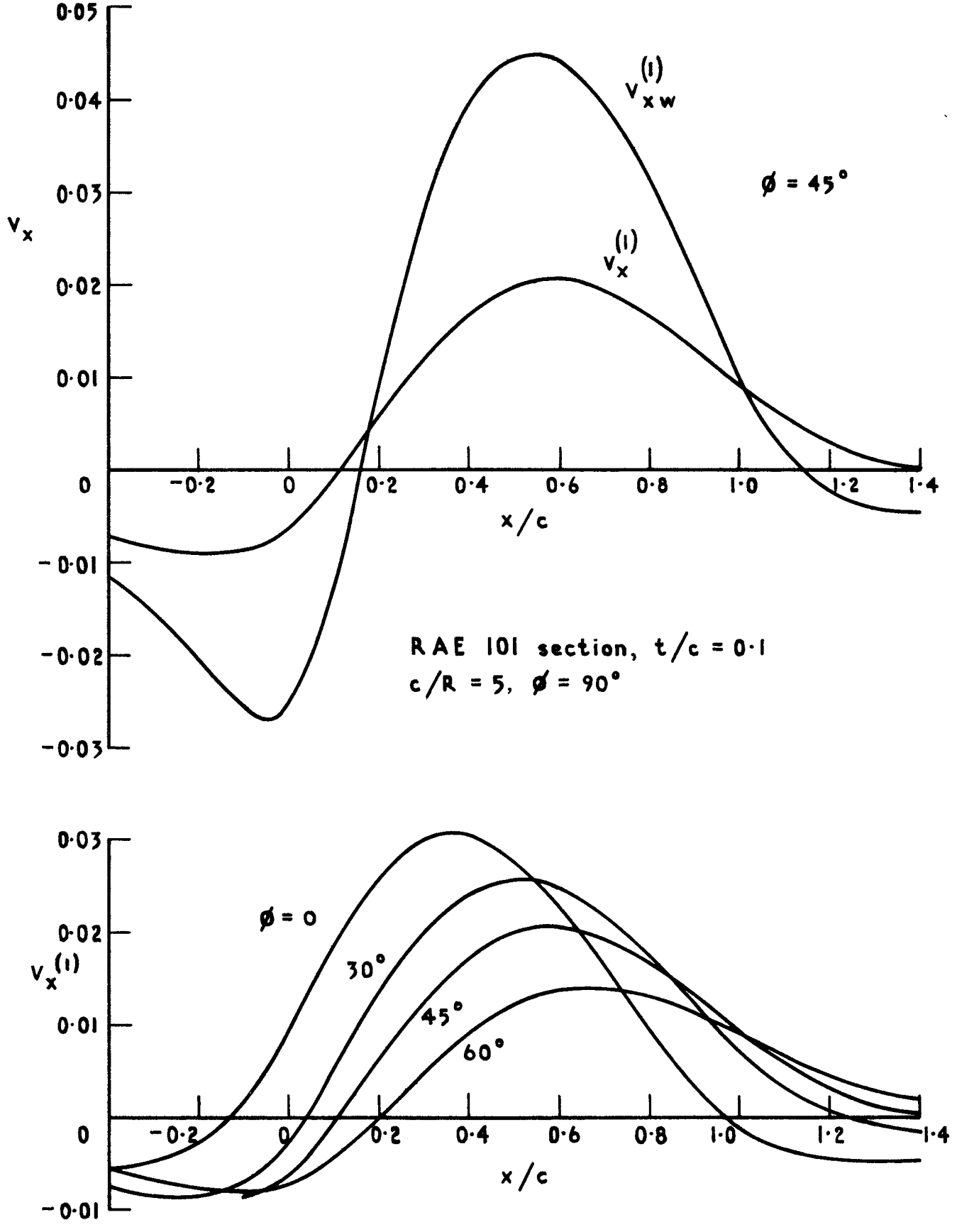

Fig. 20 Velocity at the top of the fuselage

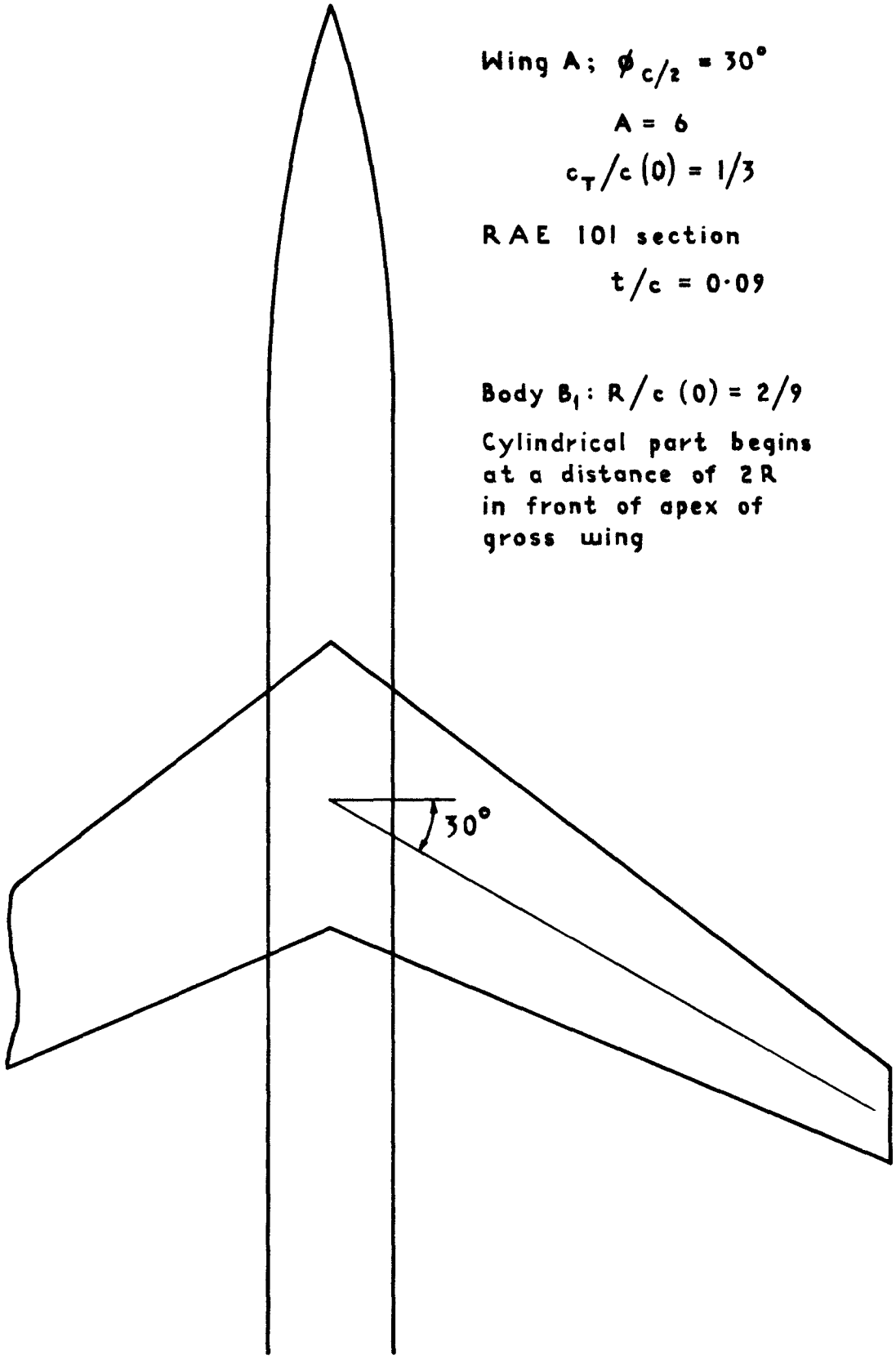

CP1333

Fig. 21 Geometry of wing fuselage combination AB_1

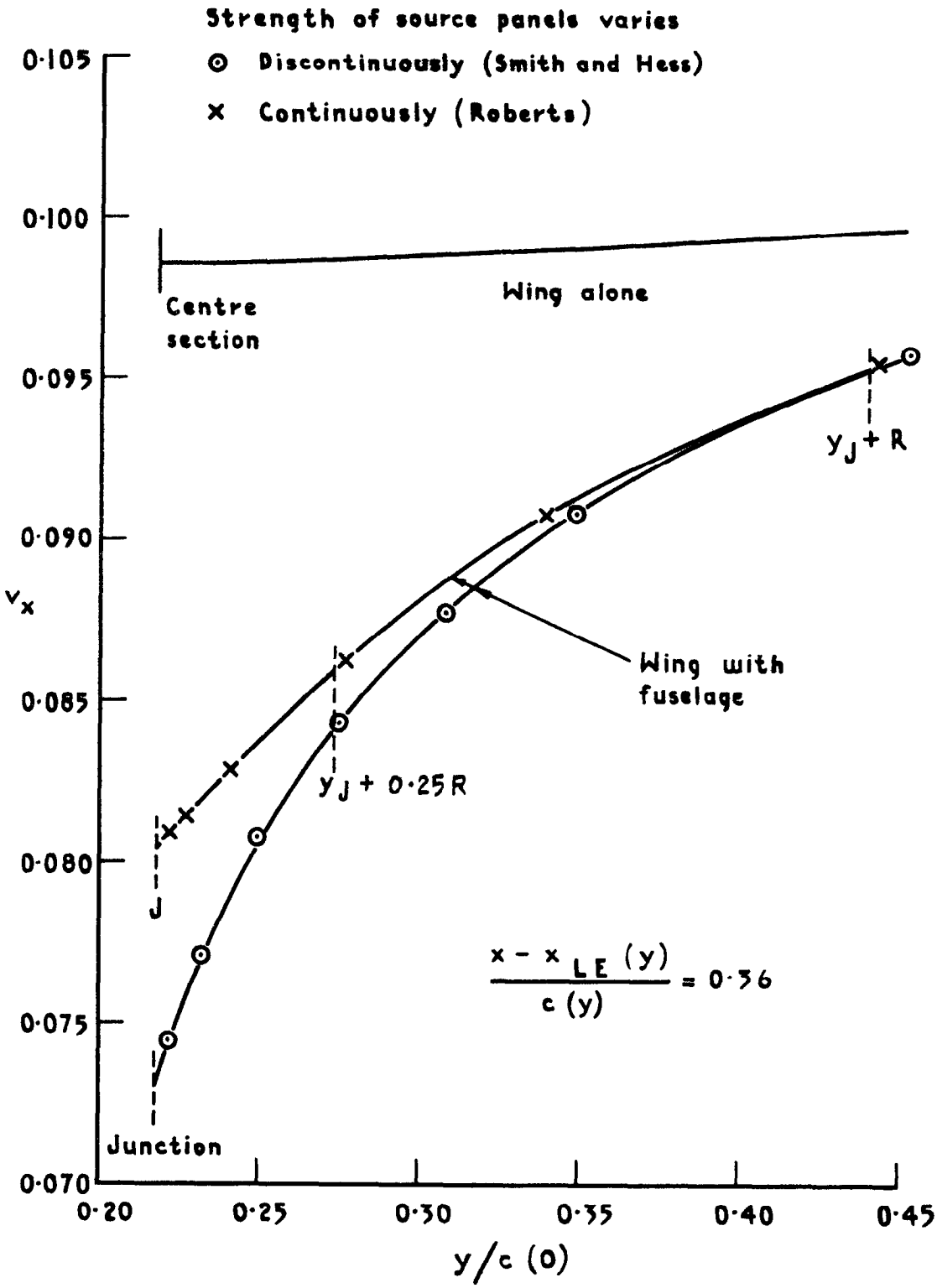

Fig. 22 Streamwise velocity component on the wing-fuselage configuration AB_1 computed by two different panel methods

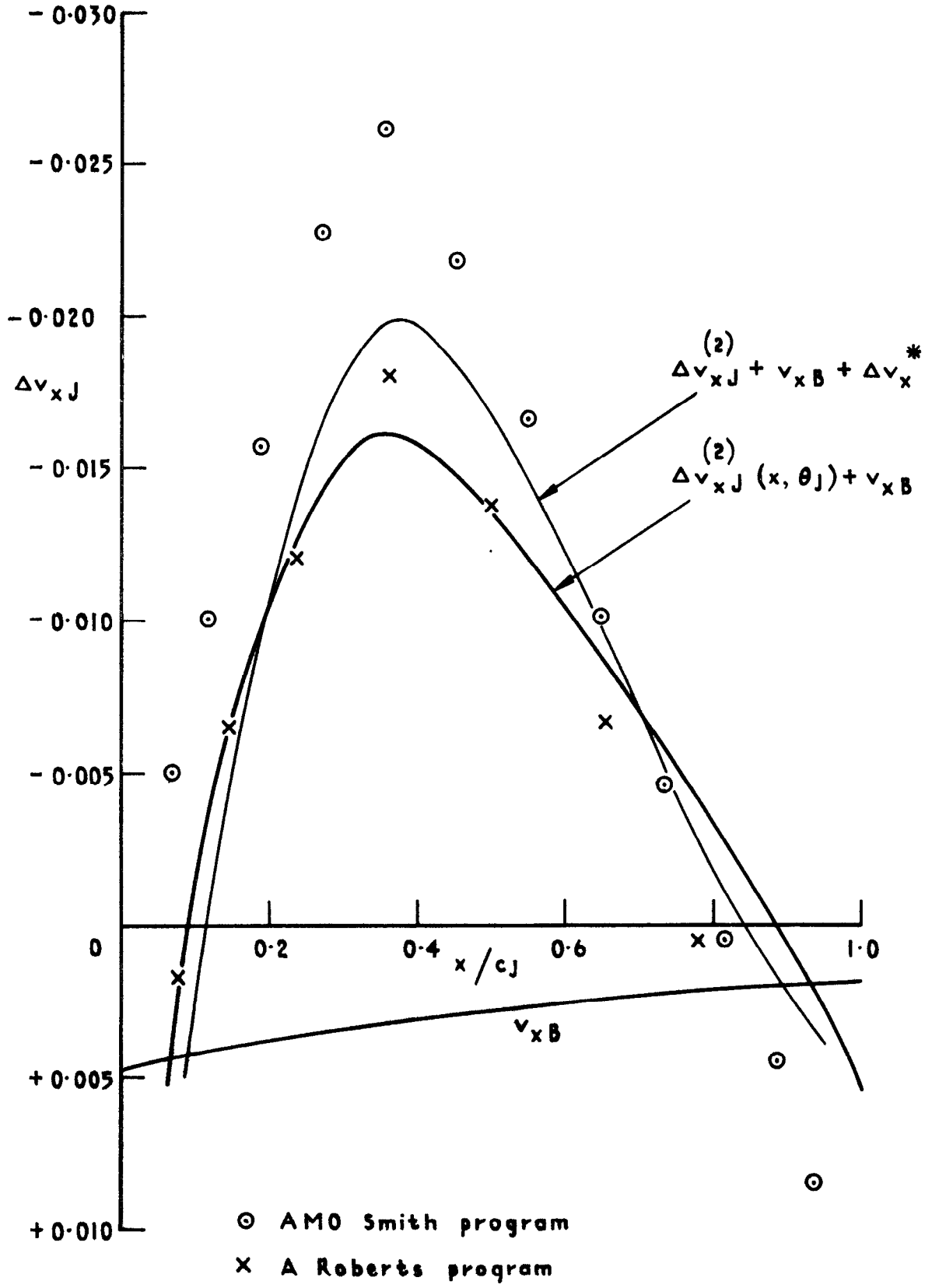

Fig. 23 Interference velocity in the wing-body junction for the configuration AB_1

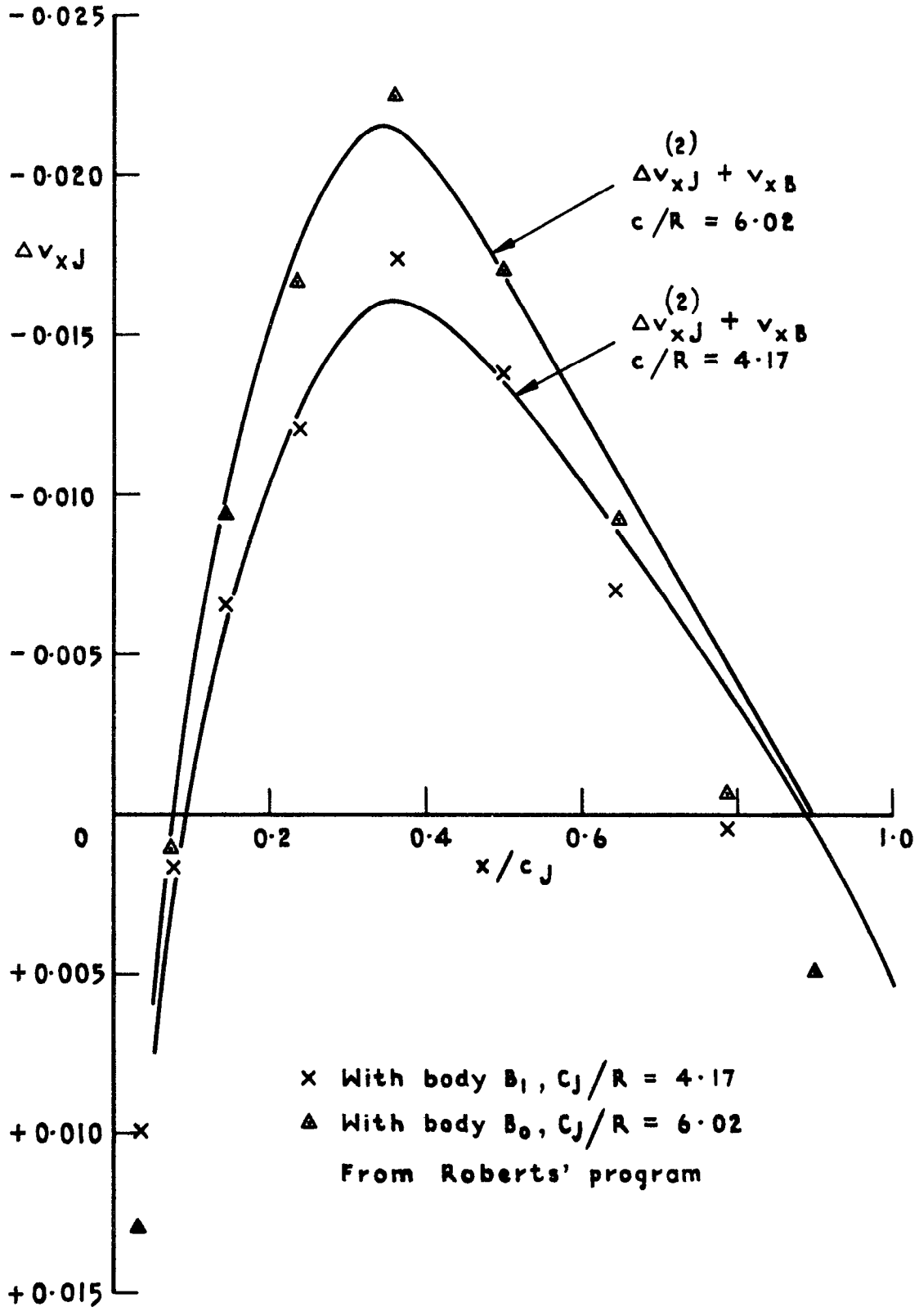

Fig. 24 Interference velocity in the wing-body junction

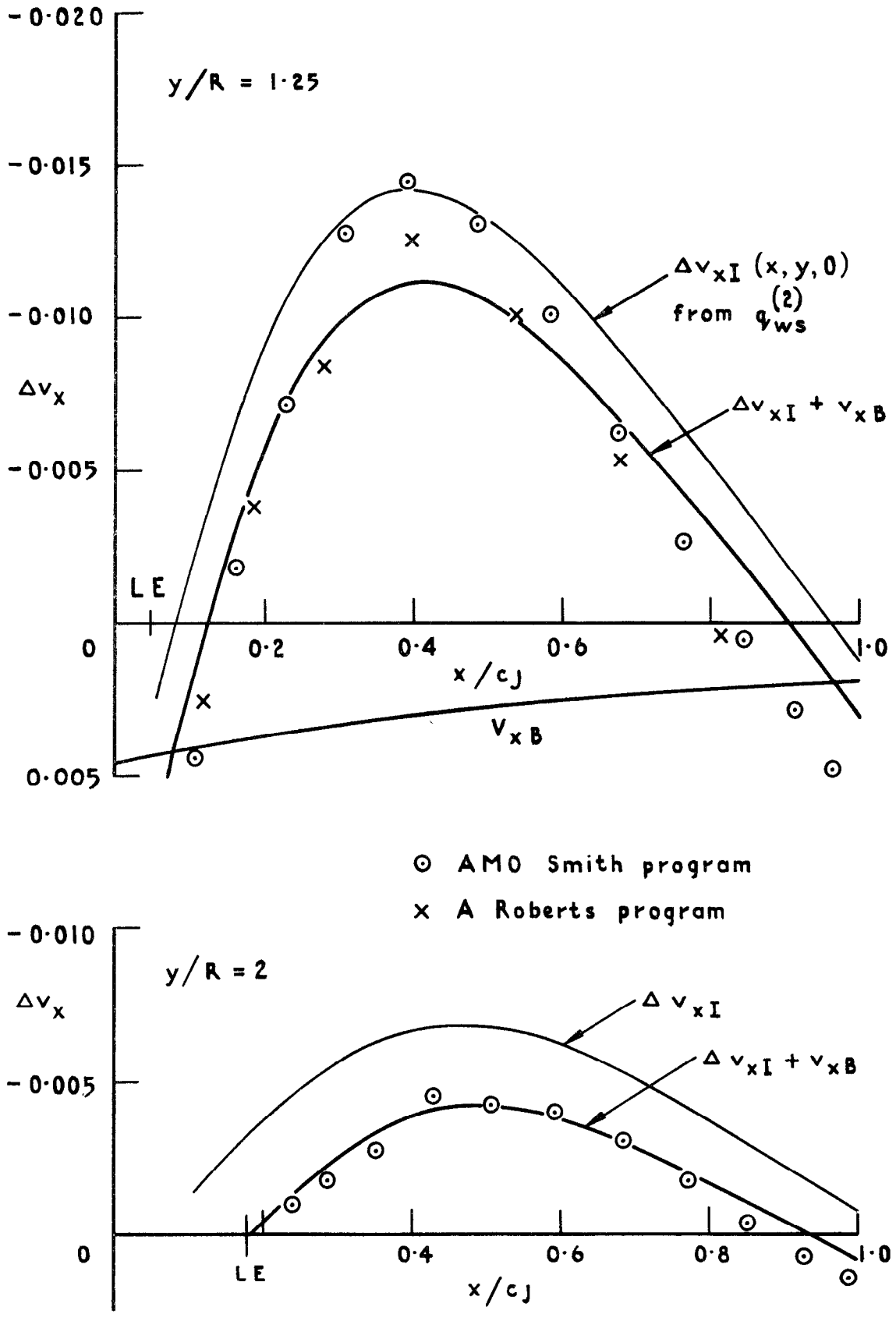

Fig. 25 Interference velocity on wing A with fuselage B_1

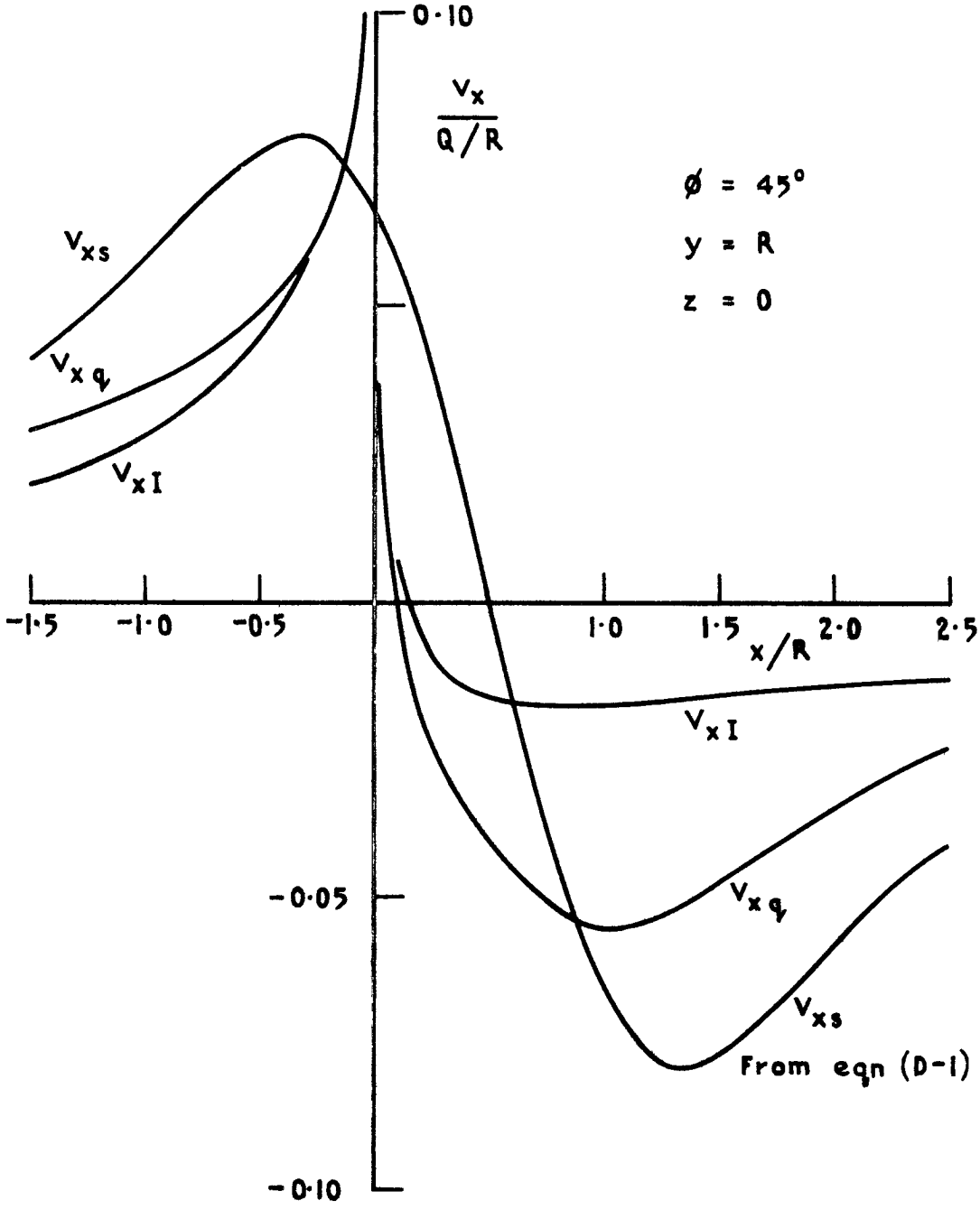

Fig. 26 Additional streamwise velocity in the wing-body junction

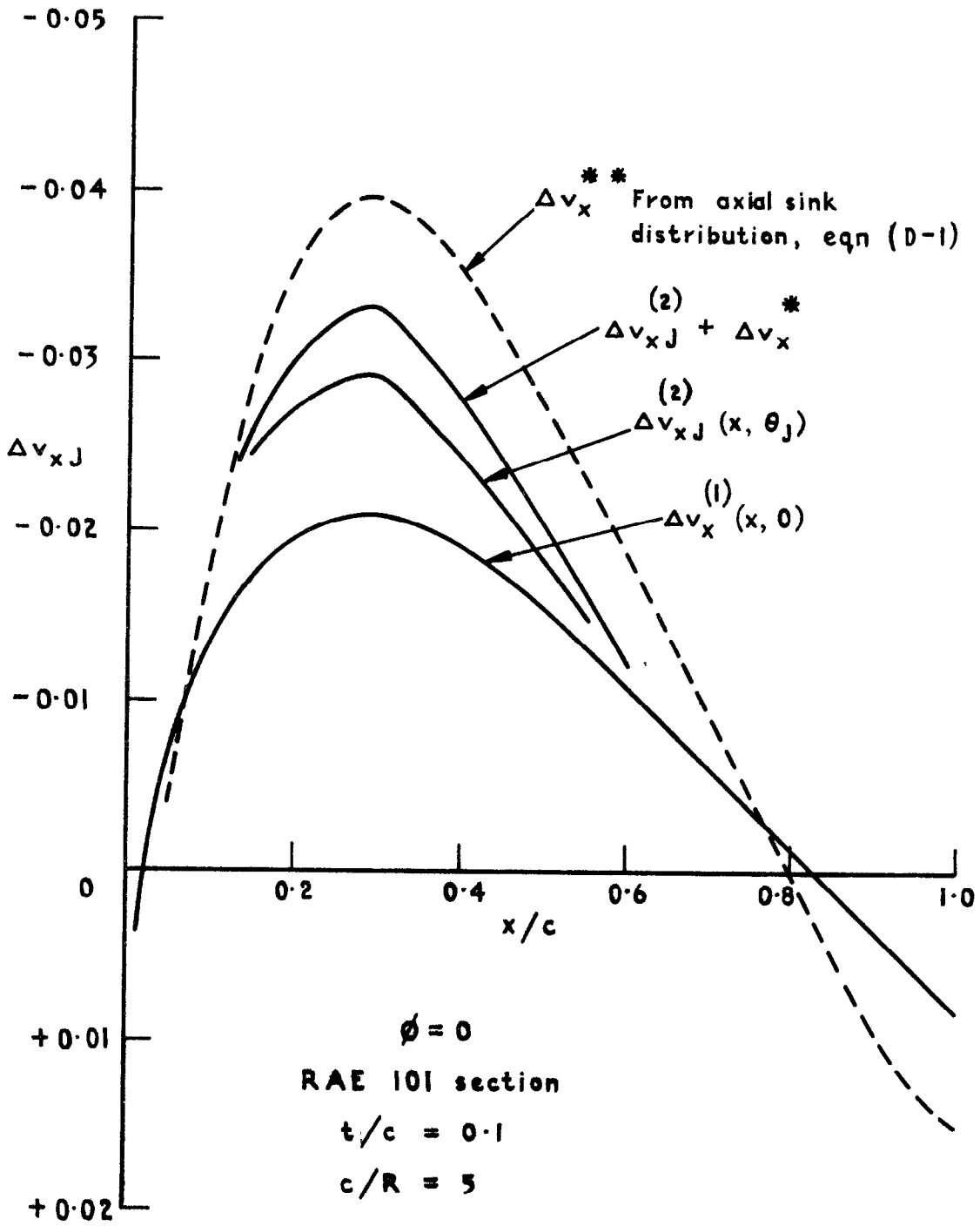

Fig. 27 Interference velocity in the wing-body junction for an unswept wing

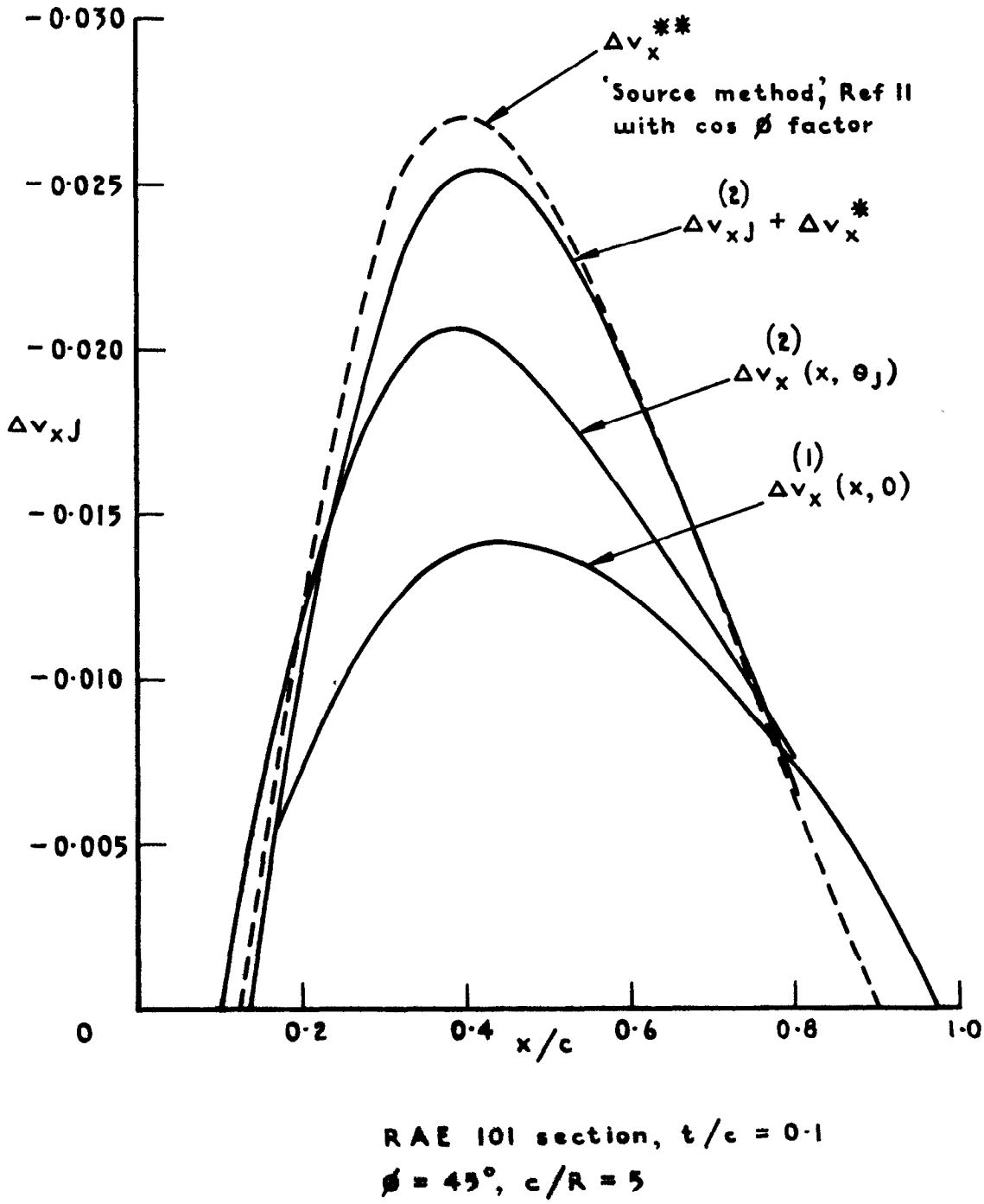

Fig. 28 Interference velocity in the wing-body junction for a swept wing

Printed in England for Her Majesty's Stationery Office by the Royal Aircraft Establishment, Farnborough. Dd. 289030 K5 10/75.

ARC CP No.1333
December 1973

Weber, J.
Joyce, M. Gaynor

533.695.12 :
533.693.1 :
533.6.048.2 :
533.6.011.32

INTERFERENCE PROBLEMS ON WING-FUSELAGE COMBINATIONS. PART III SYMMETRICAL SWEPT WING AT ZERO INCIDENCE ATTACHED TO A CYLINDRICAL FUSELAGE

The interference effect on the incompressible displacement flow past a swept wing attached to a cylindrical fuselage in midwing position is studied It is shown how this varies with the angle of sweep, with the section shape and with the ratio R/c between the body radius and the wing chord

To reduce the amount of computation only wings of constant chord and constant section shape are considered For these wings the results can easily be derived from the velocity field past a single kinked swept source line in the presence of a fuselage. The streamwise velocity component induced in the plane through the source line and the axis of the fuselage and the streamwise and circumferential velocity components induced on the surface of the fuselage have been determined numerically and the values are tabulated It is shown by comparison with results from other methods that,by means of these tables good estimates of the interference velocity can be derived also for tapered wings

ARC CP No.1333
December 1973

Weber, J.
Joyce, M. Gaynor

533.695.12 :
533.693.1
533.6.048.2 :
533.6.011.32

INTERFERENCE PROBLEMS ON WING-FUSELAGE COMBINATIONS. PART III SYMMETRICAL SWEPT WING AT ZERO INCIDENCE ATTACHED TO A CYLINDRICAL FUSELAGE

The interference effect on the incompressible displacement flow past a swept wing attached to a cylindrical fuselage in midwing position is studied It is shown how this varies with the angle of sweep, with the section shape and with the ratio R/c between the body radius and the wing chord.

To reduce the amount of computation only wings of constant chord and constant section shape are considered. For these wings the results can easily be derived from the velocity field past a single kinked swept source line in the presence of a fuselage The streamwise velocity component induced in the plane through the source line and the axis of the fuselage and the streamwise and circumferential velocity components induced on the surface of the fuselage have been determined numerically and the values are tabulated. It is shown by comparison with results from other methods that,by means of these tables good estimates of the interference velocity can be derived also for tapered wings.

Cut here

ARC CP No.1333
December 1973

Weber, J.
Joyce, M. Gaynor

533.695.12 .
533.693.1 :
533.6.048.2 :
533.6.011.32

INTERFERENCE PROBLEMS ON WING-FUSELAGE COMBINATIONS. PART III SYMMETRICAL SWEPT WING AT ZERO INCIDENCE ATTACHED TO A CYLINDRICAL FUSELAGE

The interference effect on the incompressible displacement flow past a swept wing attached to a cylindrical fuselage in midwing position is studied It is shown how this varies with the angle of sweep, with the section shape and with the ratio R/c between the body radius and the wing chord

To reduce the amount of computation only wings of constant chord and constant section shape are considered. For these wings the results can easily be derived from the velocity field past a single kinked swept source line in the presence of a fuselage. The streamwise velocity component induced in the plane through the source line and the axis of the fuselage and the streamwise and circumferential velocity components induced on the surface of the fuselage have been determined numerically and the values are tabulated It is shown by comparison with results from other methods that,by means of these tables good estimates of the interference velocity can be derived also for tapered wings.

Cut here

DETACHABLE ABSTRACT CARDS

DETACHABLE ABSTRACT CARDS

1975

Published by
HER MAJESTY'S STATIONERY OFFICE

Government Bookshops
49 High Holborn, London WC1V 6HB
13a Castle Street, Edinburgh EH2 3AR
41 The Hayes, Cardiff CF1 1JW
Brazennose Street, Manchester M60 8AS
Southey House, Wine Street, Bristol BS1 2BQ
258 Broad Street, Birmingham B1 2HE
80 Chichester Street, Belfast BT1 4JY
Government Publications are also available through booksellers

C.P. No. 1333

ISBN 011 470943 2